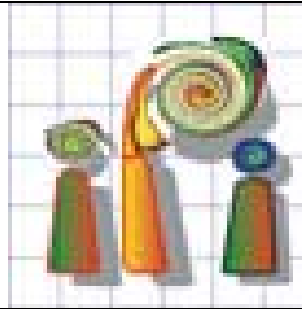




Technical University  
of Civil Engineering of  
Bucharest  
Faculty of Geodesy

Dr.-Ing. F. Zavoianu



Universität Hannover  
Institut für  
Photogrammetrie und  
GeoInformation

Dr.-Ing. K. Jacobsen

# *OPTIMISED GENERATION OF DEMs BASED ON SPOT HRS DATA*

Diploma Thesis

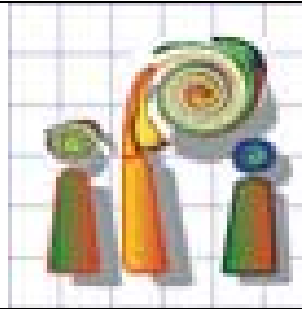
*Student Iulia Dana*

2004



Technical University  
of Civil Engineering of  
Bucharest  
Faculty of Geodesy

Dr.-Ing. F. Zavoianu



Universität Hannover  
Institut für  
Photogrammetrie und  
GeoInformation

Dr.-Ing. K. Jacobsen

# *OPTIMISED GENERATION OF DEMs BASED ON SPOT HRS DATA*

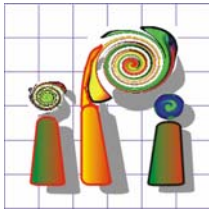
Diploma Thesis

*Student Iulia Dana*

2004

I assure that the present work  
was written independently and  
have not used others than the  
stated sources and aids.

Hannover, 21<sup>th</sup> of May 2004



***Institut für Photogrammetrie und GeoInformation***  
***Universität Hannover***

Nienburger Str. 1

D-30167 Hannover

Tel.: ++49-511/762-2485

Fax: ++49-511/762-2483

e-mail: [jacobsen@ipi.uni-hannover.de](mailto:jacobsen@ipi.uni-hannover.de)

<http://www.ipi.uni-hannover.de>

**Dr.-Ing. Karsten Jacobsen**

---

Hannover, March 2004

## Optimised Generation of DEMs based on SPOT HRS Data

for Iulia Dana

Digital elevation models (DEM) are basic contents of geo information systems. In addition they have to be used for the generation of orthoimages which are becoming more and more important. Very often actual space images are only available as single scenes and a geometric correct use requires the height information. Since few month digital elevation models generated by the Shuttle Radar Topographic Mission (SRTM) are available free of charge in the internet, but only with a spacing of 3 arcseconds.

SPOT 5 includes beside the standard HRG imager with the High Resolution Stereo (HRS) a second combination of two optics for the generation of stereo models taken within the same orbit. Usually the HRS images are not available because SPOT Image likes to distribute only the DEMs based on it, but it made some models available in the frame of the HRS Scientific Assessment Program.

With SPOT HRS models the optimal method in generating a DEM shall be analysed. This includes the required spacing of points for the automatic image matching and as main topic the optimised reduction of Digital Surface Models (DSM), showing the height of the visible surface, to DEMs including only the height of the bare ground. The analysis shall include also the effect of the interpolation of the data sets reduced for points not belonging to the bare ground.

Handing out on: 01.03.2004

Handing in on: 21.05.2004

## **CONTENTS**

	Page no.
Abbreviations	7
Introduction	8
<b>1. Digital Elevation Models (DEMs)</b>	<b>9</b>
1.1. What Is a Digital Elevation Model?	9
1.2. DEM Generation	11
1.3. The Processing Steps of DEM Generation	12
1.4. The Characteristics and Accuracy of DEMs	12
1.5. Fields of Application	15
<b>2. SPOT</b>	<b>18</b>
2.1. The SPOT Series	18
2.2. SPOT 1 – 4 Characteristics	19
2.3. SPOT 5	22
2.4. SPOT 5 HRS	24
2.5. DEM Generation by SPOT 5 HRS	26
<b>3. SRTM INSAR</b>	<b>28</b>
3.1. SRTM Specific Features	28
3.2. SRTM Components	29
3.3. The Principle of INSAR	31
<b>4. TEST AREA</b>	<b>34</b>
4.1. The HRS Scientific Assessment Program	34
4.2. General Description of the Test Area Chiemsee	34
4.3. Prien	38
4.4. Gars	39
4.5. Peterskirchen	40
4.6. Taching	41
4.7. Vilsbiburg	42
4.8. Inzell	43

<b>5. STRATEGY</b>	45
5.1. Used Method	45
5.2. Image orientation: BLASPO	46
5.3. Measurement of the Image Coordinates: DPLX	47
5.4. Image Matching: DPCOR	48
5.5. Computation of ground points: BLPRE→COMSPO	51
5.6. DEM Analysis: DEMANAL	51
5.7. Interpolation: LISA	60
5.8. Filtering of the DSM: RASCOR	61
5.9. Other Programs	62
<b>6. RESULTS</b>	63
6.1. Image Orientation	63
6.2. Image Matching	64
6.3. Prien	69
6.4. Gars	74
6.5. Peterskirchen	79
6.6. Taching	83
6.7. Vilsbiburg	87
6.8. Inzell	93
6.9. Overview of the Results	97
Conclusion	99
Acknowledgements	101
Appendix	102
References	130
List of figures	133
List of tables	138

## **ABBREVIATIONS**

SAP	Scientific Assessment Program
SPOT	Satellite Probatoire pour l'Observation de la Terre
HRS	High Resolution Stereoscopic
DEM	Digital Elevation Model
INSAR	Interferometric Synthetic Aperture Radar
SRTM	Shuttle Radar Topographic Mission
DSM	Digital Surface Model
DHM	Digital Height Model
DTM	Digital Terrain Model
TIN	Triangulated Irregular Network
WGS84	World Geodetic System 1984
3D	Three-Dimensional
ASCII	American Standard Code for Information Interchange
GIS	Geographic Information System
GPS	Global Positioning System
RMSE	Root-Mean-Square Error
USA	United States of America
CE90	Circular Error 90%
CNES	Centre National d'Etudes Spatiales
HRV	High Resolution Visible
PAN	Panchromatic
MONO	Monochromatic
SWIR	Short-Wave InfraRed
HRS	High Resolution Stereoscopic
CCD	Charge Coupled Device
NGA	National Geospatial-Intelligence Agency
NASA	National Aeronautics and Space Administration
SAR	Synthetic Aperture Radar
DLR	German Aerospace Center
LED	Light Emitting Diode
ISPRS	International Society for Photogrammetry and Remote Sensing
IPI	Institute of Photogrammetry and Geoinformation
MOMS	Modular Optoelectrical Multispectral Sensor
IRS	Indian Remote Sensing
ASTER	Advanced Spaceborne Thermal Emission and Reflection Radiometer
TCL	Tool Command Language
RAM	Random Access Memory
BMP	Bitmap
LIDAR	Light Detection And Ranging

## **INTRODUCTION**

A Scientific Assessment Program (SAP) was designed to analyze the performances of the new instrument on board of the SPOT 5 satellite: HRS (High Resolution Stereoscopic). HRS is especially designed for the generation of accurate digital elevation models (DEMs) taking stereo images almost simultaneously in the same orbit. The determination of ground heights is more accurate due to the ground pixel size of 5 meters in orbit direction. The studied images have been made available in the frame of the HRS Scientific Assessment Program. Usually SPOT HRS images are not distributed.

Digital elevation models generated by Interferometric Synthetic Aperture Radar (InSAR) during the Shuttle Radar Topographic Mission (SRTM) are available free of charges on the internet with a spacing of only three arc seconds (approximately 90m). Just in the United States of America the data is available with a spacing of one arc second. There is no reason to spend money for space images if the generated DEM does not have advantages against the free available SRTM data.

In the first chapter the characteristics, accuracy, fields of application and the generation of digital elevation models has been studied. The second chapter contains information about the SPOT family satellites, their technical characteristics, the components and a more detailed description of the SPOT 5 HRS instrument. The next chapter is about SRTM InSAR and the fourth represents a presentation of the test area Chiemsee (Bavaria) in general and a more detailed description of the six test sub areas: Prien, Gars, Peterskirchen, Taching, Vilsbiburg and Inzell. The fifth chapter consists of the strategy and the methods used in order to generate and analyze a DEM. Also, every program that has been used, has a short description about its characteristics and the way it was used during the handling of the data set. The sixth chapter presents the results that have been achieved, comparison studies and results analysis. After this, the final conclusion referring to the optimal generation of DEMs based on SPOT HRS Data and an appendix with the results for test area Prien area presented. The references used for this project are next, also the list of figures and the list of tables.

## 1. DIGITAL ELEVATION MODELS (DEM)

### 1.1. What Is a Digital Elevation Model?

A **Digital Elevation Model (DEM)** is a representation of the topography of the Earth in digital format using the X, Y planimetric coordinates and the altitude Z. This points which are defined by the X, Y, Z coordinates are describing the bare soil.

A **Digital Surface Model (DSM)** contains points located on the visible surface like buildings and vegetation. A digital elevation model is obtained by removing these points which do not belong to the bare ground.

A digital elevation model can be presented in a random form or in a raster form, but usually the last form is more used by representing each point elevation information referenced to the nodes of a rather fine regular grid (figure 1).

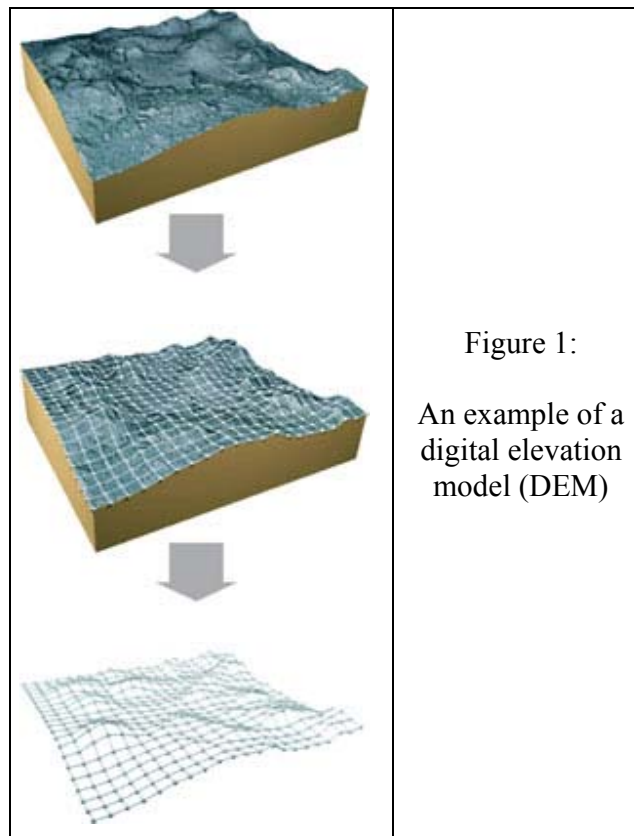


Figure 1:  
An example of a  
digital elevation  
model (DEM)

The term digital height model (DHM) can be used instead of the term DEM.

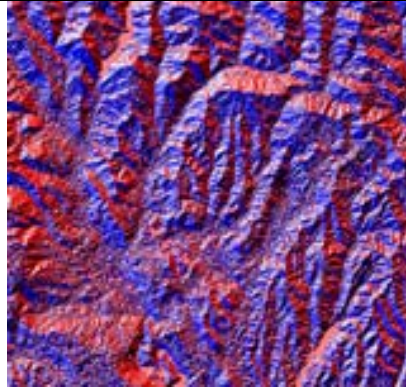
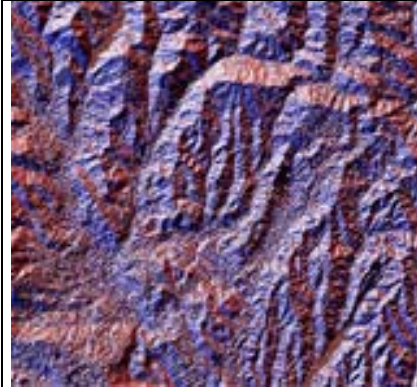
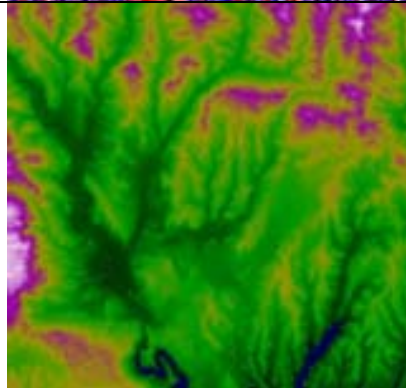
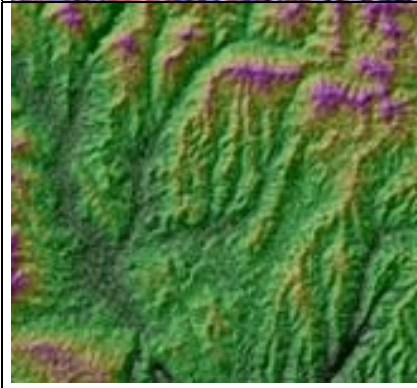
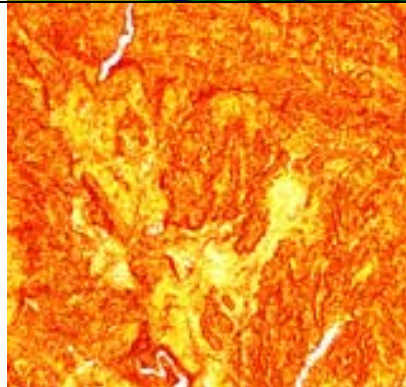
A digital elevation model is the most basic and interesting geographical data type and is usually used to refer to any digital representation of a topographic surface and describes height above sea level being from this point of view the most accurate material

on elevations. A DEM is also considered to be the simplest form of digital representation of topography and the most common.

A more generic term for any digital representation of a topographic surface is the term digital terrain model (DTM), but is not so widely used and it includes also the information about the location of the objects.

A triangulated irregular network (TIN) is another form of a DEM. TINs are a form of DEMs, but they contain points in an irregular pattern that describe the terrain.

The following images represent examples of digital elevation models. The images situated on the left side of the table are colored raster and the ones from the right are enhanced with shaded relief.

	Figure 2: Aspect (Santa Margarita)		Figure 3: Shaded aspect (Santa Margarita)
	Figure 4: Digital elevation model (Santa Margarita)		Figure 5: Hillshaded digital elevation model (Santa Margarita)
	Figure 6: Slope (Santa Margarita)		Figure 7: Slope draped on DEM (Santa Margarita)

## 1.2. DEM Generation

For the creation of a digital elevation model different methods can be used. One of these is the generation of a digital elevation model by means of optical images in a stereo configuration that can be obtained by traditional photogrammetry using aerial photos or using space images. The first method has some disadvantages because some photos are classified and not available and the second one is more economic.

A digital elevation model can also be generated using the Interferometric Synthetic Aperture Radar (InSAR) and the airborne laser scanning, which is expensive but has the advantage of producing detailed and accurate information.

For the generation of a digital elevation model based on space images most of the data acquisition has to be made by automatic image matching since the manual measurement is too time consuming. But the model which is generated is not a digital elevation model, but a digital surface model (DSM) because it contains points located on the visible surface like buildings and vegetation. For obtaining a digital elevation model the points that don't belong to the bare ground must be removed.

When optical images are used for the generation of a digital elevation model it is necessary to have two or more images of the interest area shown from two different directions (figure 8). It is also required to know the coordinates of the projection center in a specified object coordinate system and the view direction.

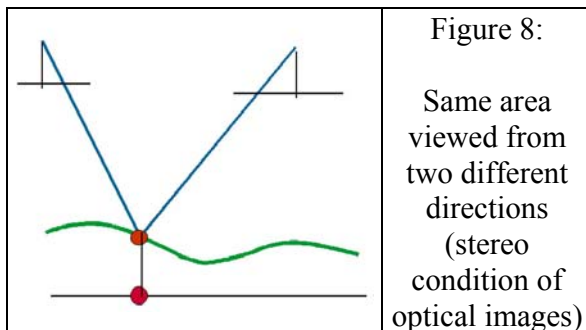


Figure 8:  
Same area viewed from two different directions (stereo condition of optical images)

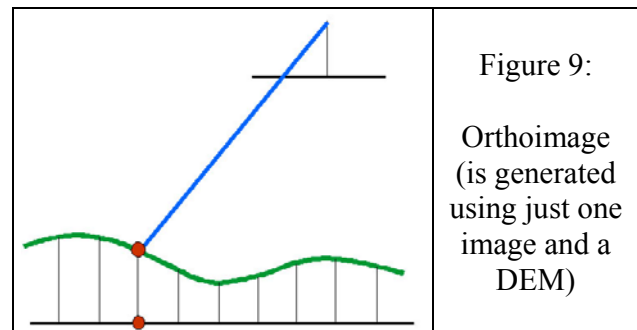


Figure 9:  
Orthoimage (is generated using just one image and a DEM)

The most important and the most often used photogrammetric product are orthoimages which can be achieved using only one image and a digital elevation model. That means a correct geolocation is possible based just on these two items (figure 9). When an orthoimage is created the digital elevation model must contain heights which are in the same reference system like the control points.

For the computing of the discrepancies in the horizontal position  $dl$  caused by a discrepancy in the vertical position  $dh$  of a digital elevation model, formula 1 can be used (figure 10):

$$dl = dh \cdot \tan \nu \quad (1)$$

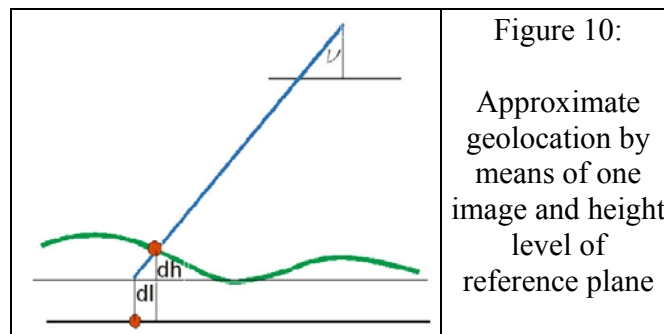


Figure 10:

Approximate geolocation by means of one image and height level of reference plane

### 1.3. The Processing Steps of DEM Generation

DEM generation implies the sequence of six processing steps. This routine is used for the generation of a digital elevation model based on stereo images. These steps are only summarized:

- Acquisition and pre-processing of the remote sensing data (images and meta data) to determine an approximate value for each parameter of 3D physical model for the two images.
- Collection of ground control points (GCPs).
- Computation of the 3D stereo model.
- Image matching.
- Computation of X,Y,Z cartographic coordinates from determined corresponding image coordinates.
- Generation of regular grid spacing with interpolation of mismatched areas. Elimination of points not belonging to the bare ground.

### 1.4. The Characteristics and Accuracy of DEMs

A digital elevation model is considered to be reliable if it accomplishes four major requirements: it must be available, it must have the required accuracy and resolution and it should not have gaps in important areas.

A digital elevation model is an ASCII or binary file that contains spatial elevation data in a regular gridded pattern or in a random form in raster format. A very important parameter for describing a digital elevation model is the resolution or the distance between adjacent grid points. The higher the density of elevation points recorded the

more accurate is the description of the actual terrain. Using 3-D modeling software a dense grid of points is created by means of interpolation algorithms which gives the impression of a continuous three-dimensional surface. That means for displaying and analyzing a digital elevation model the computer software is very important.

DEMs can be integrated in GIS software for special analysis. The 3-D modeling is very useful in many different applications. For obtaining a more complete 3-D view of the landscape other layers of information like hydrography or land cover can be overlaid onto a DEM. Another type of layers can be also overlaid onto a digital elevation model: satellite imagery or digital orthophotos.

A very important problem in the creation of a digital elevation model is the number of the selected points. This number is depending upon the type of the landscape. Although is better to know as many elevations as possible sometimes a big number of Z coordinates can conduce to some disadvantages like time consuming operations. In flat areas there is no need of having a large number of elevations, but over an irregular terrain a very dense network of elevations is necessary to represent the best the variations in the land surface.

Coverages of the entire globe (figure 11), including the ocean floor (figure 12), can be obtained at various resolutions. But the accuracy of these DEMs is not always sufficient. Using the Shuttle Radar Topographic Mission (SRTM) C-band digital elevation models with satisfying accuracy could be created but only for areas which are not above  $60^{\circ}$  north and  $58^{\circ}$  south geographic latitude. But the achieved DSM has only a spacing of 3'' corresponding to approximately 90m and some gaps exists in some very steep areas. Not for every purpose the accuracy and details are sufficient.

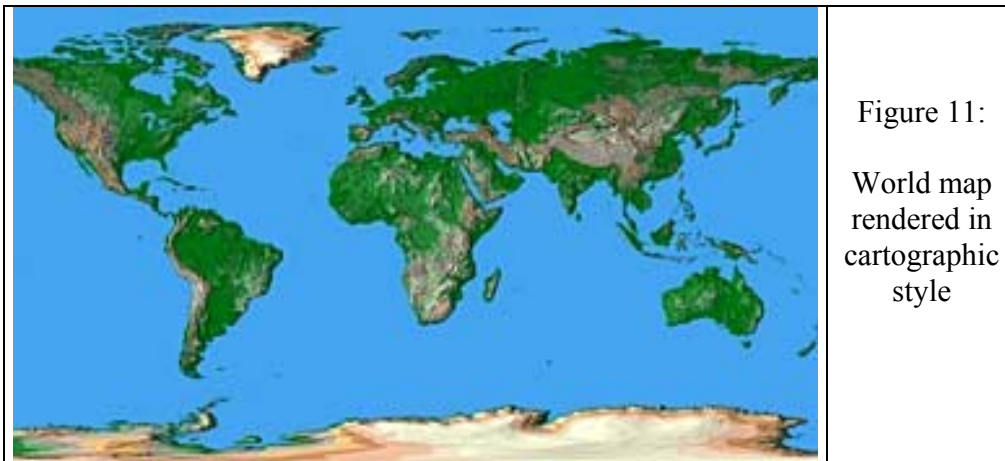
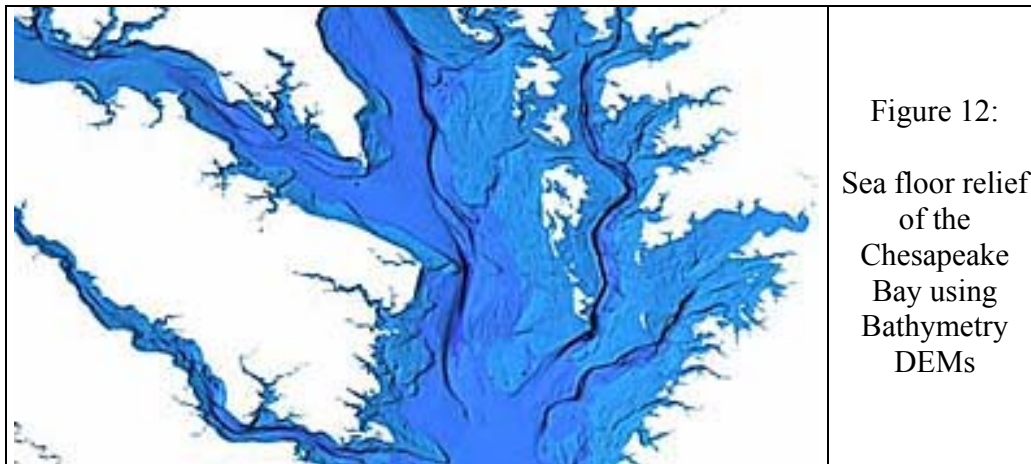


Figure 11:  
World map  
rendered in  
cartographic  
style



Elevations may be obtained using traditional surveying methods including photogrammetric data acquisition or the Global Positioning System (GPS), but often elevations are computed from contour lines on pre-existing maps.

Another parameter which can be used for describing the accuracy of a digital elevation model is the root-mean-square error (RMSE) as a measure of how closely a data set matches the actual world. Digital elevation model should be tested in order to check the accuracy of the available points. This test establishes whether the obtained digital elevation model is accurate in comparison to the reference model. The digital elevation model which is considered to be the reference model should have a higher accuracy like the tested DEM.

In the case of DEMs acquired by means of space images the accuracy is mostly depending upon the image resolution (ground pixel size), the height-to-base relation and the image contrast (radiometric quality). A difference between a relative and an absolute accuracy can be noticed when systematic image errors have not be respected and the orientation quality is limited.

The standard deviation can be used as well for describing the accuracy of a DEM. This parameter is defined on a probability level of 68%. Especially in the USA also the circular error on the 90% probability level CE90 is used. It has a fixed relation of 2.1 to the standard deviation of X and Y coordinates. The vertical accuracy (the accuracy of a height) is depending upon the accuracy of the x-parallax  $S_{px}$  and the height to base relation of the imaging configuration.

$$SZ = image\_scale\_number \cdot h/b \cdot S_{px} \quad (2)$$

$$SZ = pixel\_on\_ground \cdot a \cdot h/b \quad (3)$$

Formula (3) is used for computing the standard deviation in the case of digital space images. The value of the parameter “a” which is a multiplication factor is usually below 1 and the accuracy of the x-parallax  $S_{px}$  is depending upon the contrast and is also usually below one pixel.

Another way to express the height to base relation is to use the nadir angles in the base direction. The same result is obtained when the inverse sum of the tangent of the nadir angles is used instead of the height to base relation.

When using radar images the advantage is that they are independent upon the cloud conditions, but the disadvantages are important: the object recognition is poor and the geometric situation in mountainous area is difficult.

## 1.5. Fields of Application

Digital Elevation Models are often used in:

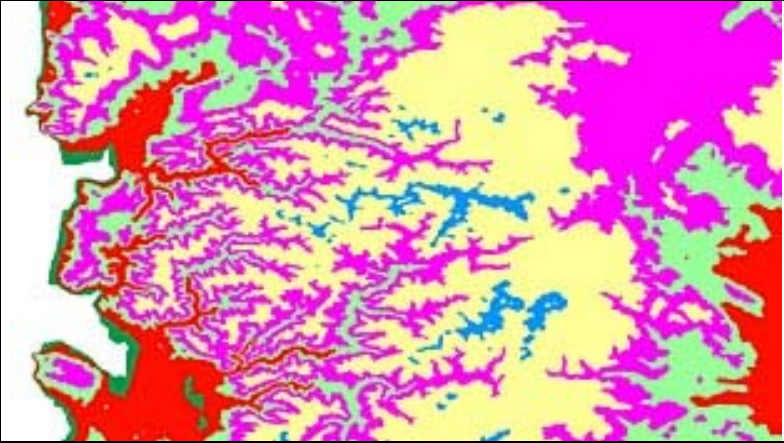
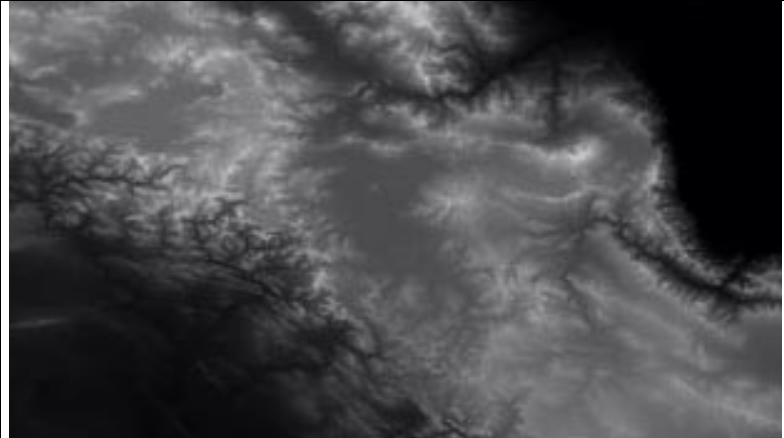
- geographic information systems (GIS).

DEMs are a very considerable matter in mapping (figure 13, 14). The most important photogrammetric product are very high resolution orthoimages that can be generated using a single image and a digital elevation model.

	<p>Figure 13:</p> <p>World 1,000 meter resolution land relief merged with world sea relief at 10,000 meter resolution for a map of the Mediterranean Sea, Northern Africa, and Central Europe</p>
	<p>Figure 14:</p> <p>The map was digitally rendered in a painted look to create terrain images in a soft watercolor style</p>

The knowing of the digital description of the three-dimensional surface can be used in various applications like:

- flood planning
- erosion control
- agriculture
- generation of contour lines (figure 15)
- visibility check, 3-D views (figure 17)

	<p>Figure 15:</p> <p>Contour maps with selective elevation banding that may be used to identify elevation ranges for technical, cartographic or scientific purposes</p>
	<p>Figure 16:</p> <p>North-Western Afghanistan as grey value coded DEM. The lowest altitudes are black pixels and the highest peaks are white - the elevation is graded into a range of 255 grayscale shades</p>

DEMs are commonly used in:

- environmental analysis (figure 17)
- civil applications
- telecommunication modeling
- simulation and training – military, aviation
- urban planning
- cartography.



Using a DEM it is possible to simulate for example TV and radio reception areas or cellular phone signal coverage. Mass calculations for excavation and infill areas can be estimated, the inclination and profiles can also be calculated easily.

A digital elevation model can also be used for determining the attributes of the terrain such as elevation at any point, slope and aspect, for finding features on the terrain, such as drainage basins and watersheds, drainage networks and channels, peaks and pits and other landforms or for modeling of hydrologic functions, energy flux and forest fire.

## 2. SPOT

### 2.1. The SPOT Series

SPOT (Satellite Probatoire pour l'Observation de la Terre) is designed by CNES (Centre National d'Etudes Spatiales) and developed by France in cooperation with Belgium and Sweden. The SPOT Mission Center is located in Toulouse, France and a second command center is in Kiruna, Sweden. Apart from these two stations which are in the possession of SPOT Image, the company which runs SPOT marketing, there are another ground stations which collect real-time images located in different part of the world like Canada, India, Spain, Brazil, Thailand, Japan, Pakistan, Saudi Arabia, South Africa, Australia, and Equador.

The SPOT system includes a series of spacecraft and associated ground facilities for satellite control, acquisition, programming, data reception and imagery production.

SPOT system is operational since 1986, when SPOT 1, the first SPOT satellite, was launched on the 22<sup>nd</sup> of February by the French Government Agency aboard an Ariane 1. This was followed in 1988 on the 22<sup>nd</sup> of January by SPOT 2, in 1993 on the 26<sup>th</sup> of September by SPOT 3 and on the 24<sup>th</sup> of March 1998 by SPOT 4. SPOT 3 ended his mission in November 1996.

SPOT 5 was launched on the 4<sup>th</sup> of May 2002 and it has increased resolution and spectral capabilities (figure 18). Today the SPOT system includes two operational in-orbit satellites: SPOT 4 and SPOT 5.



Figure 18:  
Satellites of the  
SPOT series

## 2.2. SPOT 1 – 4 Characteristics

The most important characteristics of the SPOT imagery are the high geometric accuracy and the radiometric quality. Each SPOT satellite has two identical sensors or scanners HRV (high resolution visible) that can operate in the panchromatic and multi-spectral mode and a moveable mirror that allows off-nadir viewing and stereoscopic imaging.

The panchromatic system consists of a high resolution (10 meter) single channel and is primarily used for applications which require geometric detail. The multispectral system has three channels (green, red and near infrared) of a coarse resolution which are used for interpreting vegetation and other types of land-cover.

In the figure 19 is presented a multispectral image which shows the areas covered with fresh vegetation (such as grass) in deep red colour. This information can not be seen in the panchromatic image (figure 20) although the resolution is better.



Figure 19: Multispectral image from SPOT  
(pixel size: 20 x 20m)



Figure 20: Panchromatic image from SPOT  
(pixel size: 10 x 10m)

The SPOT satellites are placed into a sun synchronous circular orbit at 98.7° inclination and an altitude of 822 km. SPOT satellites were the first to use “pushbroom” along track sensor technology.

The repeat cycle of the SPOT satellites is of 26 days but because of their sensors which can be tilted to view areas that are under different orbital tracks the same areas of the earth can be seen with a 5-10 day frequency. SPOT has the ability to point the sensors up to  $27^\circ$  from nadir and this allows the satellite to view within 950 km swath (figure 21).

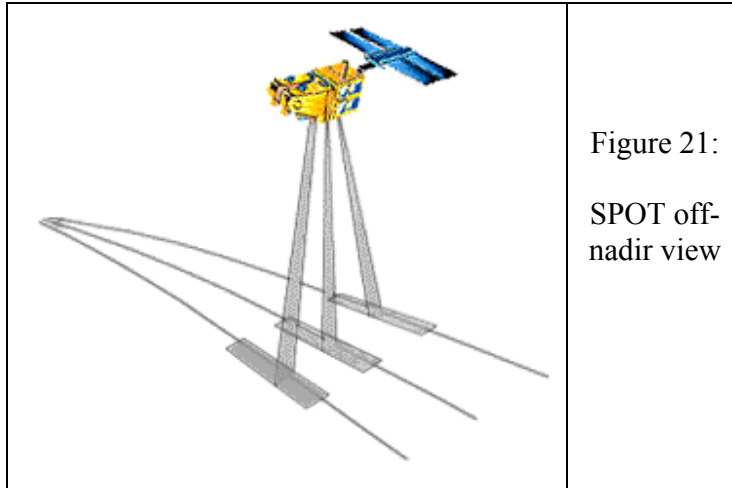


Figure 21:  
SPOT off-nadir view

The SPOT satellites can acquire data in each and every part of the world and they have the capability of acquiring imagery for stereoscopic coverage. The stereopairs can be achieved at different viewing angles during separate passes.

The swath width of the recorded area is approximately 60 km and SPOT satellites are capable to acquire simultaneously coloured and panchromatic data. The panchromatic system consists of 6000 detectors each imaging a 10m wide portion of the landscape. Then the both HRV are functioning the swath width is of 117 km including a 3 km overlap (figure22).

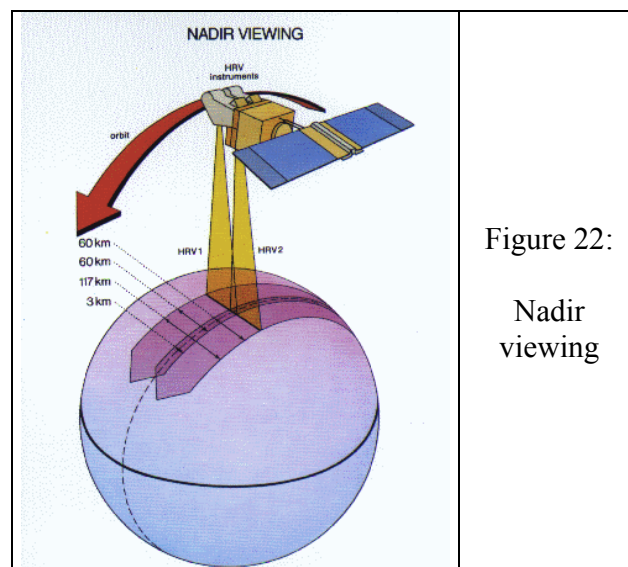


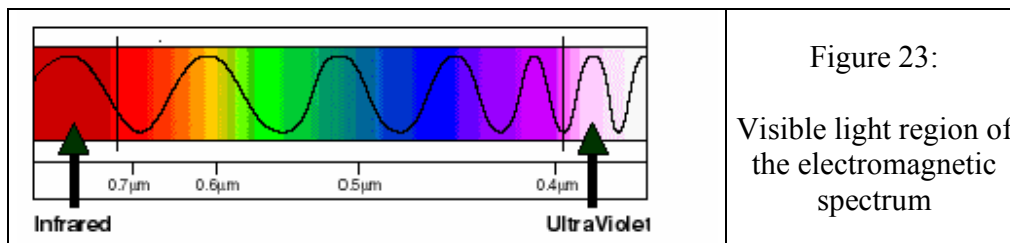
Figure 22:  
Nadir viewing

The SPOT 1-4 satellites' multi-spectral mode has a pixel size of 20m and the PAN and MONO a pixel size of 10m, compared to the 20m to 10m multi-spectral and 10m, 5m and 2.5m panchromatic of SPOT 5.

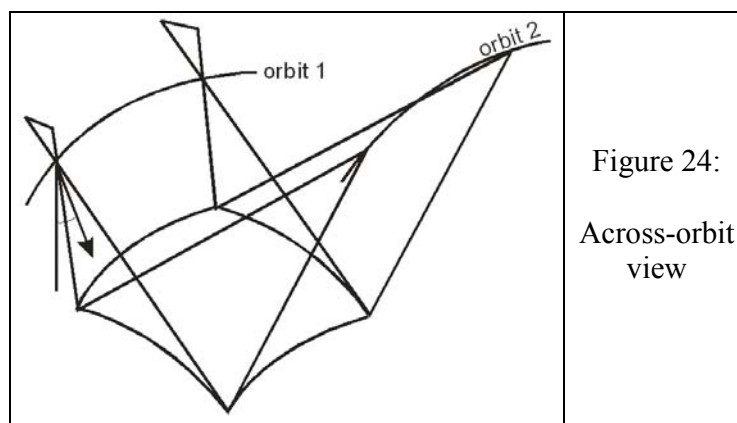
The characteristics of the bands used by SPOT satellites are presented in Table 1:

SPOT satellite	Band no.	Spectral range ( $\mu\text{m}$ )	Spectral region
SPOT 1-5	B1	0.50 to 0.59	Visible green
SPOT 1-5	B2	0.61 to 0.68	Visible red
SPOT 1-5	B3	0.79 to 0.89	Near infrared
SPOT 4-5	SWIR	1.58 to 1.75	Short-wave infrared
SPOT 1-3-5	PAN	1.550 to 1.750	Visible
SPOT 4-5	MONO	0.61 to 0.68	Visible

The human eyes visible wavelength is shown in the following graphic (figure 23):



SPOT is viewing across the orbit (figure 24). So the images are taken from different orbit with a time interval of at least few days between. The main disadvantage is that the characteristics of the object may change in this time or the weather conditions might not permit the imaging. This can lead to a very difficult or impossible automatic image matching because the grey values in the two images can be very different.



The vertical accuracy in a stereo model is depending upon the terrain type and upon the height to base relation. If the characteristics of the object are not changing in the time interval between imaging both scenes, a vertical accuracy of 5 to 10m is possible in open and more flat areas with sufficient contrast. This problem of time delay concerns all the system which are using viewing just across orbit, but SPOT 5 succeeded to solve it by using the HRS instrument.

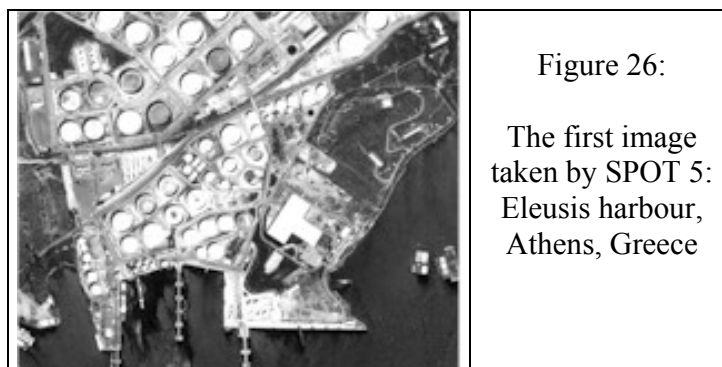
### 2.3. SPOT 5

On the 4<sup>th</sup> of May 2002 SPOT 5, the earth observation satellite from CNES, was launched from French Guiana Space Centre aboard an Ariane 42P spacecraft. SPOT 5 is on the same orbital plan like SPOT 2 and 4.



SPOT 5, in comparison with the satellites from this series, has new and improved technical characteristics and bright performances which are suitable for high resolution spatial imagery and stereoscopy. Spot 5 is designed to be in use until 2007, at least.

The first images taken by SPOT 5 satellite equipped with the High Resolution Geometric (HRG) instrument were obtained on the 7<sup>th</sup> of May. The images were received in Toulouse SPOT Mission Center and they show the city of Athens in Greece (figure 26).



These images are acquired in panchromatic mode and their quality matches the expected technical specifications. Using the staggered CCD-line of HRG at a physical resolution of 5 meters sampled according to the Supermode technique an image with a resolution of 2.5 meters can be obtained.

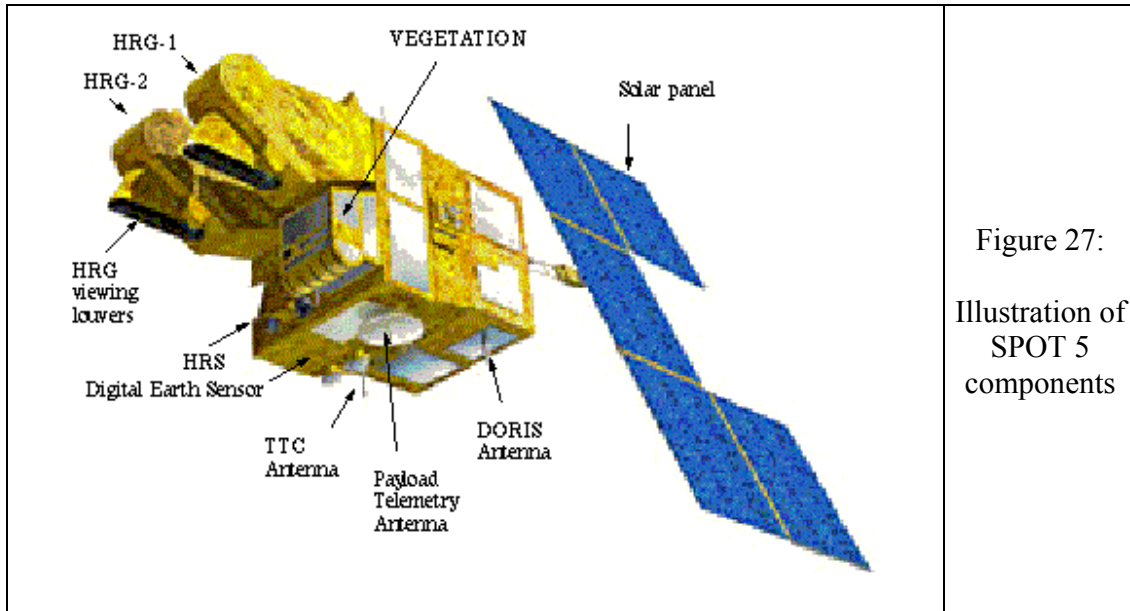


Figure 27:  
Illustration of  
SPOT 5  
components

SPOT 5 preserves the same characteristics like the previous satellites:

- A circular, polar, sun synchronous, phased orbit;
- The altitude is 822 km;
- The time when it passes by the equator is 10:30 local time;
- The swath width of 60 km along the satellite track;
- The ability of lateral viewing up to 27° from nadir;
- Spectral bands: B1, B2, B3, SWIR and P.

SPOT 5 is an improved satellite system and major developments were made to increase its performances. Among these there are:

- The resolution of the SPOT 5 images is: 10 meters in multispectral mode, 5 meters in panchromatic mode and 2.5 meters in the Supermode;
- A new instrument named High Resolution Stereoscopic (HRS) which is designed to take stereoscopic images and to generate digital elevation models (figure 27);
- The absolute precision of the planimetric location is better than 50 meters without using ground control points;
- The ability to obtain at the same time 120 kilometers width products instead of 60 km like SPOT 4;

- The instrument Vegetation 2 (figure 27) which is an improved version of Vegetation 1 (SPOT 4) is a planet observation system and it can cover almost all of the globe's land masses in one day. The characteristics of this instrument are: 2250 km wide-swath, 1 km spatial resolution, four spectral bands (red, near infrared, mean infrared and one blue band for atmospheric corrections).

SPOT 5 is equipped with two identical High Resolution Geometric (HRG) instruments (figure 27) which can operate individually or simultaneously. These instruments are able to acquire data at four resolution levels: images in the SWIR band with the resolution of 20 meters, images taken in the multispectral mode with the resolution of 10 m, panchromatic images with the resolution of 5 meters and Supermode images of the resolution of 2.5 meters.

The Supermode is a technique which uses two panchromatic scenes taken with staggered CCD-lines of 5 meters physical resolution together with an oversampling in the orbit direction for generating one image sampled at 2.5 meters. This technique is using a detector constituted in two linear array of CCD (Charge Coupled Device) sensors with 12000 detectors shifted in the focal plan. The size of a single detector is 6.5  $\mu\text{m}$  square and they convert the incoming light into electrical signals. Each linear array is obtaining a image which has the resolution of 5 meters. These two images are shifted 2.5 meters one to another and the acquired image has an improved resolution because twice more pixels are collected from the ground. By theory this is an image information corresponding to the contents of a 3m physical pixel size.

SPOT 5 is offering two types of images: Level 1A and Level 1B. Level 1A means original images and Level 1B is referring to images that represent projection to a plane with constant height. The results achieved using Level 1A or Level 1B images are almost the same.

The most important characteristics of the SPOT 5 satellite are: the resolution, the wide swath and the stereoscopy.

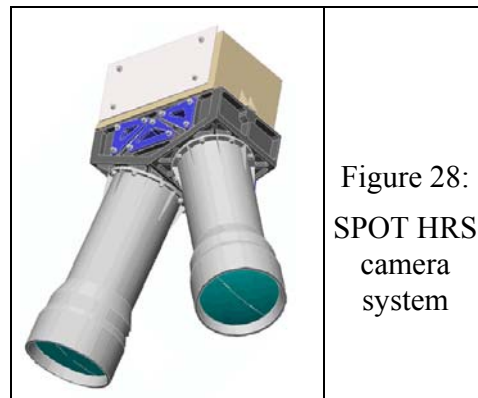
The information obtained from the satellite data can be used in many and different domains such as cartography, topography, land use, agriculture of precision, forest, natural hazard management, urban planning, disaster monitoring, environmental studies, surveillance, defence, telecommunications. The satellite images provide accurate information about any place of the world in a quick and regular manner.

## 2.4. SPOT 5 HRS

Today only a small part of the world is covered with accurate digital elevation models (DEMs), mainly few highly developed countries have the possibility to possess this type of data. The demand for large-scale digital elevation models with sufficient accuracy

and resolution able to be used in geographic information systems (GIS) is spread all over the world and the SPOT 5 HRS may improve the situation.

The HRS (High Resolution Stereoscopic) instrument on board of the satellite SPOT 5 is especially designed for the generation of Digital Elevation Models from along-track stereo imagery. The stereoscopic imaging of this system has the height to base relation of 1.2 and just 90 seconds time interval. This instrument is able to acquire two images simultaneously from the same orbit using forward and backward looking sensors (figure 28).



The time period between acquisition of the stereo pairs is very short so the images are taken almost instantaneous. By this reason there is reliable guarantee that there are the same illumination conditions, no change of the object and the same atmospheric situation. This represents a very important advantage of this system because the two images have perfect radiometric resemblance which eases the automatic correlation process.

At the time of the same passage of the satellite the forward-looking sensor acquires images of the ground at a viewing angle of  $20^\circ$  ahead of the vertical and after one minute and a half the backward-looking sensor achieves images of the same portion of the ground at an angle of  $20^\circ$  behind the vertical (figure 29). The nadir angle of  $20^\circ$  corresponds to  $22.5^\circ$  incidence angle on account of the earth curvature. That means the height to base relation has the optimal value of 1.2 for generating digital elevation models. The height to base relation represents the angle between the intersecting rays and the achieved vertical accuracy is depending upon this parameter. Theoretically a value of 1.0 is better for the determination of the coordinates of the ground points but the disadvantage is that the automatic image matching has not good results. But the optimal base to height relation is depending upon the area itself – for an open and flat area the relation 1.0 is optimal, for more undulated areas with buildings and vegetation the factor 1.6 may lead to better results (Börner et al 1997).

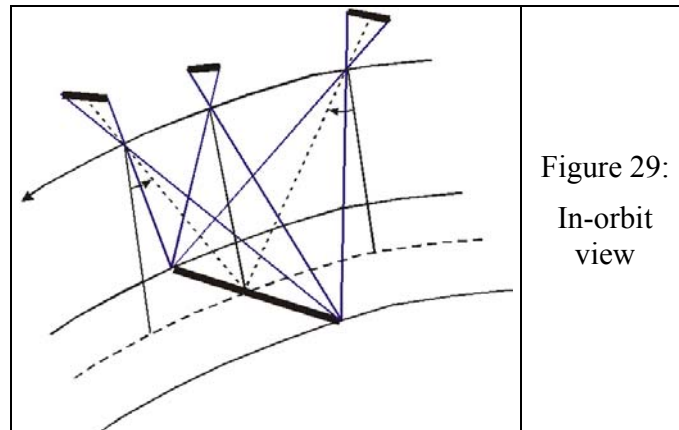


Figure 29:  
In-orbit  
view

The HRS camera system includes two combined CCD-line cameras. Each CCD-line has 12000 pixels and the pixel size on the ground is of 5m in orbit and 10m across the orbit. The height determination is better because it depends upon the pixel size in orbit direction. The standard scene size covered by this stereoscopic arrangement has the size of 120 km x 60 km. The spectral domain of the HRS is the panchromatic band (0.49-0.69 $\mu$ m).

## 2.5. DEM Generation by SPOT 5 HRS

A digital elevation model generated by automatic correlation of SPOT 5 HRS stereopairs is a uniform grid of terrain elevation values of an area of interest (figure 30). The sampling step of such a DEM generated by SPOT Image is 1 second of arc, that means almost 30m at the equator, but this value is varying according to latitude.

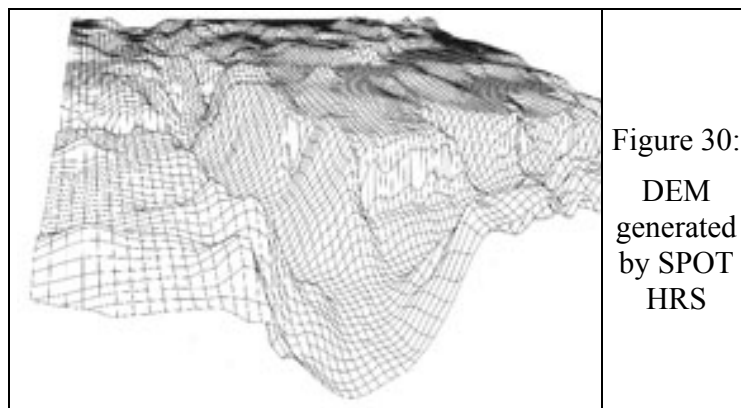
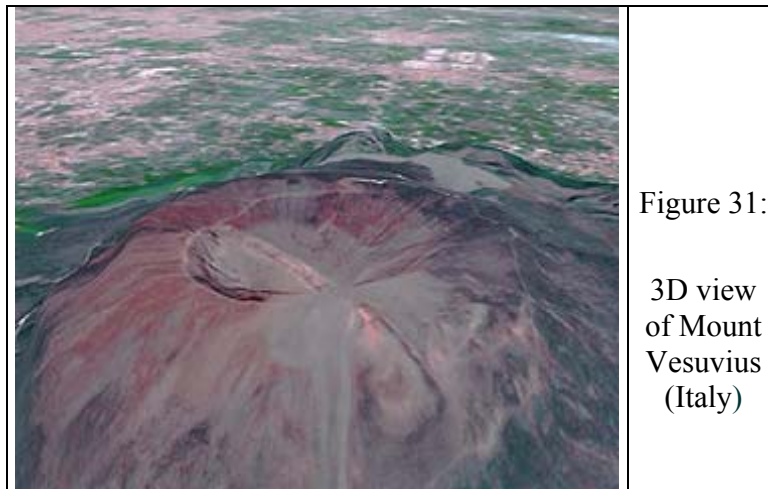


Figure 30:  
DEM  
generated  
by SPOT  
HRS

On the 15<sup>th</sup> of May 2002 the first digital elevation model was produced from a pair of stereoscopic images acquired by HRS. The stereopair of images was taken in Naples, Italy and represent a 3-D view of the Mount Vesuvius (figure 31).



The absolute elevation accuracy is from 10m to 20m depending on the slope and the absolute planimetric accuracy is from 15m to 30m without using ground control points.

DEMs obtained from HRS stereo pair imagery are useful in many civil applications like natural disaster management, flood monitoring, agriculture, forestry, geology, transportation and urban development, mobile telephone network planning, environmental impact studies and mapping as well for military requirements. DEMs are usually used for a 3-D view of the landscape in order to simulate for example natural phenomenon or future structure projects.

### 3. SRTM INSAR

#### 3.1. SRTM Specific Features

The Shuttle Radar Topography Mission (SRTM) is an international project supported by the National Geospatial-Intelligence Agency (NGA), the National Aeronautics and Space Administration (NASA) and the German and Italian agencies to map the world in three dimensions.

SRTM consists of a specially modified Synthetic Aperture Radar (SAR) system that flew onboard the Space Shuttle Endeavour (figure 32) which was launched into space on the 11<sup>th</sup> of February 2000. During an 11-day mission SRTM had the goal to obtain data in order to generate the most complete high-resolution digital topographic database of the Earth. The final product is the most accurate and detailed digital elevation model of Earth's surface that has ever been produced.



The Shuttle Radar Topography Mission (SRTM) which uses the technique called interferometric SAR was launched into an orbit with an inclination of  $57^\circ$  and it collected data over Earth's land surface that lies between  $60^\circ$  north and  $56^\circ$  south latitude during this single, 11 days mission. SRTM orbited Earth 16 times each day and during the entire mission it completed 182 orbits with the velocity of 7.5 km/sec and the distance between equator crossing of about 220 kilometers.

All of the acquired radar data is processed to the same specifications and all the SRTM generated topographic maps have the same characteristics.

The SAR systems used during the SRTM mission in February 2000 were utilized before in two shuttle missions that took place in April and October of 1994 to obtain data about Earth's environment.

For obtaining information about altitude in order to generate digital elevation models regular optical cameras on board of aircrafts or satellites can be used but they have the disadvantage of depending on a cloud free view. In addition the sun angle should not be below approximately  $25^\circ$  to avoid long shadows. For this application, radar is a better option because it can operate day and night and it can penetrate clouds. However the radar does not see through thick vegetation canopies, but it penetrates a little in not so dense canopies. SAR images are used especially for mapping in areas with cloud coverage and they are very efficient in the generation of digital elevation models.

The information achieved by using SRTM can be used in many fields of application which require accurate knowledge of the shape and height of the land such as improved water drainage modeling, more realistic flight simulations, safety navigation, better location for cell phone towers, military, flood control, soil conservation, reforestation, volcano monitoring, earthquake research, glacier movement monitoring.

### 3.2. SRTM Components

SRTM is equipped with two SAR systems, each with two antennas (the main radar antenna and the outboard radar antenna) and a mast (figure 33).

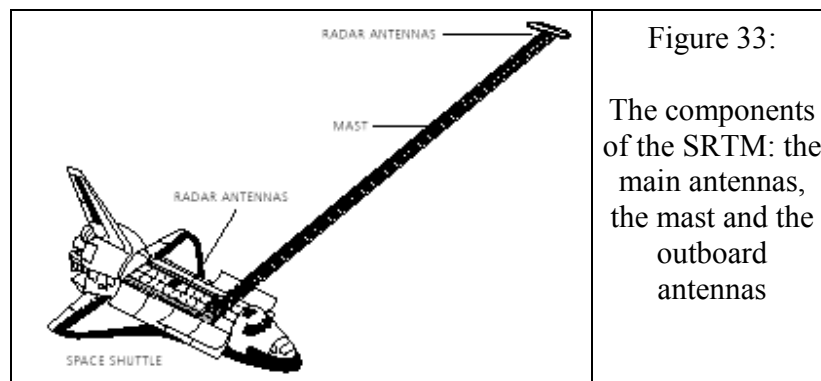


Figure 33:

The components of the SRTM: the main antennas, the mast and the outboard antennas

The main antennas are located in the payload bay of the shuttle and the outboard antennas are attached to the end of a 60 meter mast. The mast is extended from the payload bay when the shuttle is in space and it represents the longest rigid structure ever flown in space. The use of these two times two additional antennas is a major innovation because the system is capable to obtain accurate elevation data from a single pass without time difference between image acquisition. The Doppler method is used to separate and average the mixed signals. Using the principle of interferometry the SRTM instruments were designed to capture one radar signal using two different antennas.

The main radar antennas transmit the radar pulse and it has special panels that can receive the returned radar pulse after the interaction with the surface of the Earth. These antennas are mounted into a structure which is fixed into the payload bay of the space shuttle. SRTM used C-band and the X-band SAR (figure 34). The C-band antenna is able to emit and receive radar wavelengths that are 5.6 centimeters long. The swath width of the C-band radar is 225 kilometers and this radar band covered almost 94.6% of the land mass twice and approximate 50% three times. The X-band radar antenna transmits and receives radar wavelengths that are 3 centimeters long. The swath width of the X-band is 45 kilometers. This band is able to produce maps at a higher resolution but it does not have a global coverage. The X-band data are processed and distributed by the German Aerospace Center (DLR). By theory, the accuracy of the X-band is better than the one of the C-band because the wavelength is shorter, but the multiple coverage of the C-band improved the accuracy.

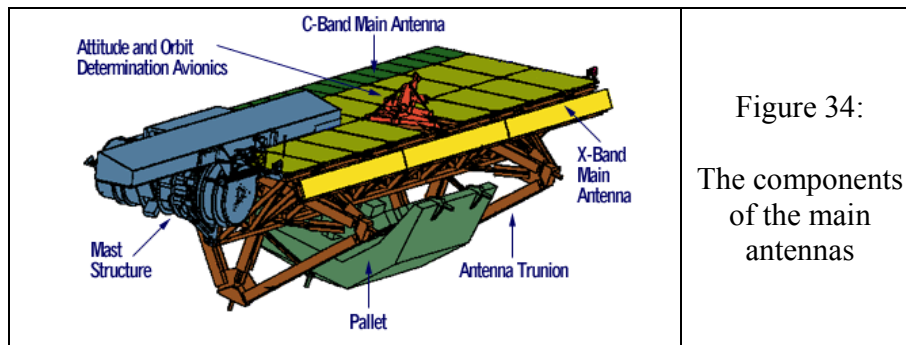


Figure 34:  
The components  
of the main  
antennas

The mast is folded up and put inside a canister that is attached to the side of the main antenna and when the shuttle is in space it is emerging from the canister and extends out to 60 meters. This mast represents the baseline distance between the main antenna and the outboard antenna.

The outboard antennas are located at the end of the mast and are receiving the same returned pulse as the main antenna. These antennas have only the possibility of receiving, not transmitting, radar signals (figure 35). The C-band and the X-band can operate simultaneously or independently, but during the mission they operated mostly at the same time.

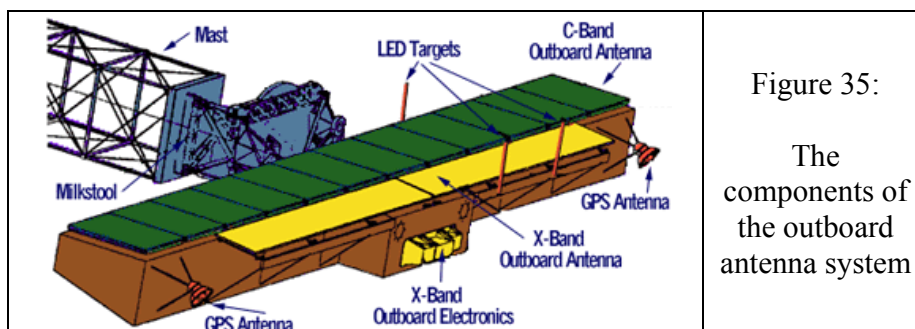
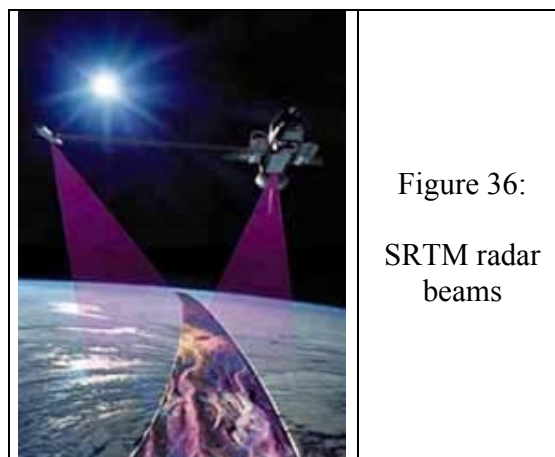


Figure 35:  
The  
components of  
the outboard  
antenna system

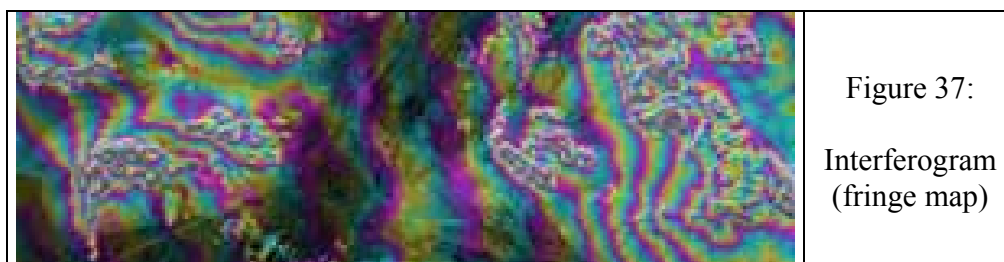
Besides these two times two antennas there are two GPS (Global Positioning System) antennas, Light Emitting Diode (LED) targets and a corner-cube reflector. The GPS antennas are used for an accurate determination of the space shuttle position. The LED targets are measuring the position of the outboard antenna relative to the main antenna and the corner-cube reflector is measuring the length of the mast within 3 millimeters. Although the mast represents a rigid structure its length must be very accurate measured because during the flight the space shuttle is going in and out of the sunlight and some thermal distortions can appear. An error in the mast length knowledge of only 3 millimeters produces a height error of 9 meters.

### 3.3. The Principle of INSAR

InSAR is using two radar systems with different wavelengths. One is the C-band radar system which is operated by the USA and has the wavelength  $\lambda=5.6\text{cm}$  and the other is the X-band radar system with  $\lambda=3\text{cm}$  operated by Germany and Italy. The radar interferometry technique implies the acquirement of two radar images from slightly different locations in order to calculate the surface elevation.



Radar interferometry is a technique that can be used for the generation of three dimensional images of the Earth's surface (figure 36). Interferometry is the study of interference patterns accomplished by combining two sets of signals. The result of this combination is called an interferogram or a fringe map (figure 37).



The two antenna systems of the SRTM which are separated by a fixed distance of 60 meters (the mast) are collecting two radar data sets. The main antenna is considered to be both active and passive because it transmits and also receives signals while the outboard antenna is just passive. One radar data set is collected by the main antenna and the other by the outboard antenna. The C-band radar is using two polarizations to form two beams. One beam uses HH polarization (horizontally transmitted, horizontally received) and the other VV polarization (vertically transmitted, vertically received). The X-band radar is using only a single beam with VV polarization. The main antenna illuminates a portion of the Earth's surface with a pulse of 1/10 of a microsecond using a beam of radar waves. This beam of radar waves hits the surface of the Earth and the rays that are scattered in different directions are collected by the two antennas (figure 38).

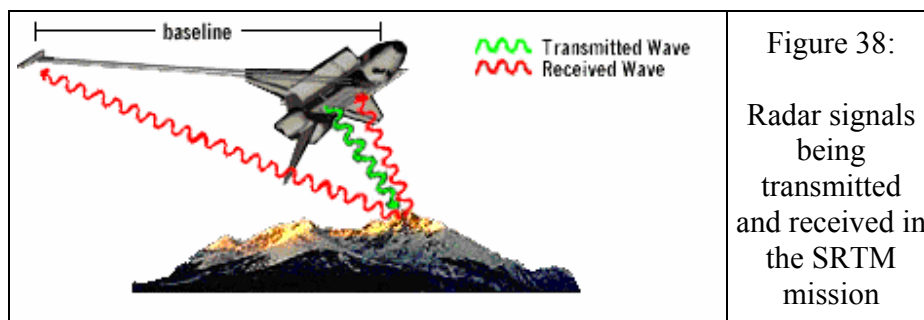


Figure 38:  
Radar signals being transmitted and received in the SRTM mission

The length of the mast has the same value all during the time of the measurements and this value is known very accurately. The length of the mast is not changing, the radar wavelength is also not changing so this means that the only parameter who is different is the distance between the Earth's surface and the two antennas. Accurate elevation of the Earth's surface can be calculated using the information about the baseline and the differences in the reflected radar wave signals. Combining both radar images – one from the main antenna and one from the outboard antenna – a single 3-D image is achieved.

The disadvantages of the SAR-images are foreshortening, layover and shadows in the mountains (figure 39).

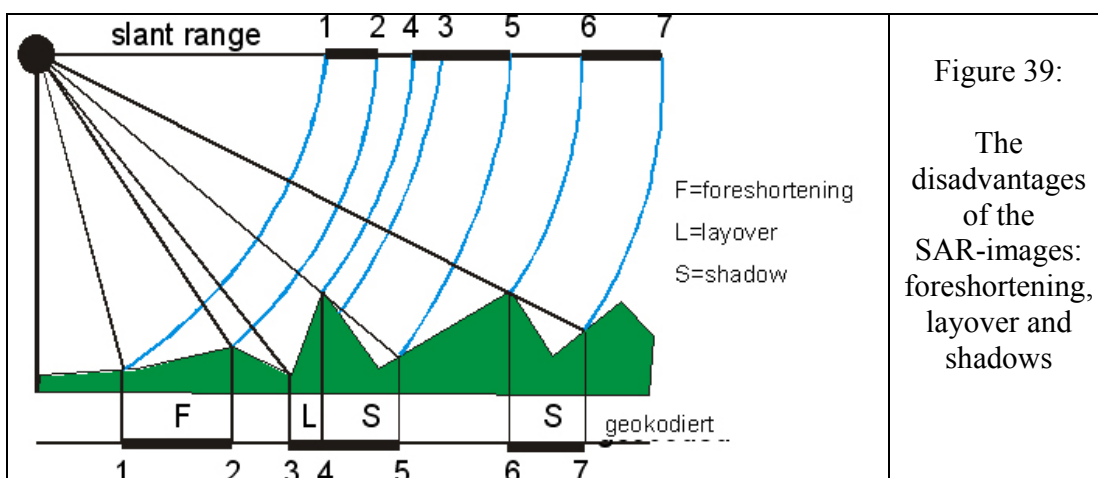


Figure 39:  
The disadvantages of the SAR-images: foreshortening, layover and shadows

The C-band SAR has an incidence angle between  $31^{\circ}$  and  $61^{\circ}$  while the X-band is limited to  $50^{\circ}$  and  $54^{\circ}$ . Corresponding to this the radar layover where the returned signal cannot be separated depending upon the location is in the range of a terrain slope across the view direction of the same value (Jacobsen, 2004). In very steep areas both C-band and X-band cannot operate properly because it is not possible to separate the reflected pulse. A comparison between the C-band elevation models accuracy and the X-band elevation models accuracy reveals the fact that the results are similar. The X-band is more advantageous to use because the data are available with the spacing of 1 arc second (approximately 30m) while the C-band data are available with a spacing of only 3 arc seconds (approximately 90m).

## 4. TEST AREA

### 4.1. The HRS Scientific Assessment Program

Few months after the launch of SPOT 5 CNES (Centre National d'Études Spatiales) invited ISPRS (International Society for Photogrammetry and Remote Sensing) to join an initiative for assessing the new HRS (High Resolution Stereoscopic) instrument and the quality and accuracy of the DEM derived from the HRS stereo pairs. The name of this program is HRS Scientific Assessment Program (HRS-SAP) and the organisation which is dealing with it, is HRS Study Team. This program is designed to help CNES to improve its future Earth Observation systems and to inform the users about the accuracy and quality of the HRS instrument and the derived DEM.

In the frame of the HRS-SAP nine test areas have been selected and analyzed. The selected sites are well diversified regarding the climate, relief and landscape in order to be representative of most situations in the world. Three test areas are located in France: Manosque, Aix-en-Provence and Montmirail, three in Europe (outside France): Chiemsee (Bavaria - Germany), Liege (Belgium), Barcelona (Catalonia- Spain) and three in other parts of the world: Merowe (Sudan -Africa), Melbourne (Australia) and Rasht (Iran). No sites could be selected in America.

### 4.2. General Description of the Test Area Chiemsee

Test area Chiemsee is located in south-east of Germany in the federal state Bavaria, small parts of Austria are also included (figure 40).

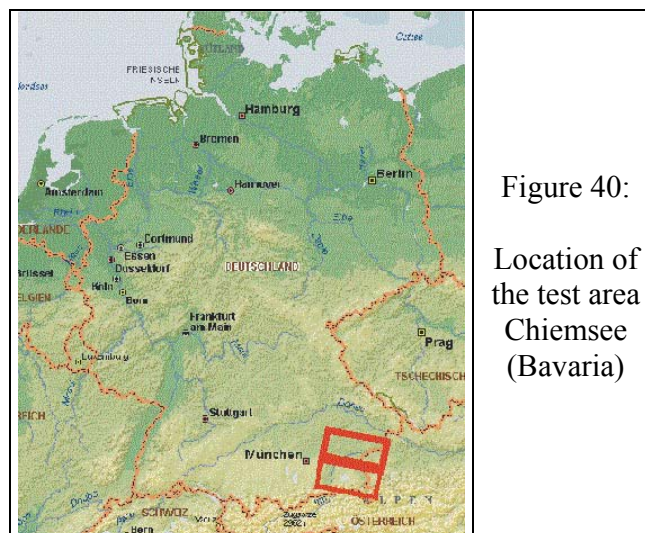


Figure 40:  
Location of  
the test area  
Chiemsee  
(Bavaria)

The two slightly overlapping SPOT 5 HRS-models are covering each an area of 120km x 60km. The test area consists of 6 reference sub-areas: Prien, Gars, Peterskirchen, Taching, Inzell and Vilsbiburg (figure 41 and figure 42).

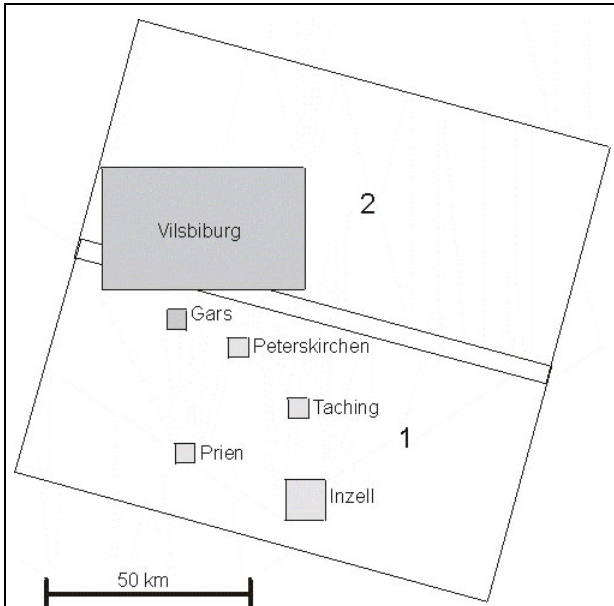


Figure 41: Overlapping SPOT HRS-models with the reference areas

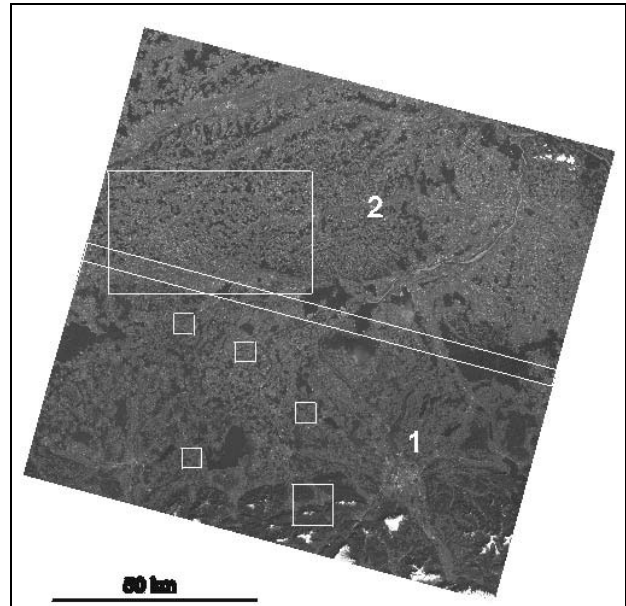


Figure 42: Overlapping SPOT HRS-models with the reference areas

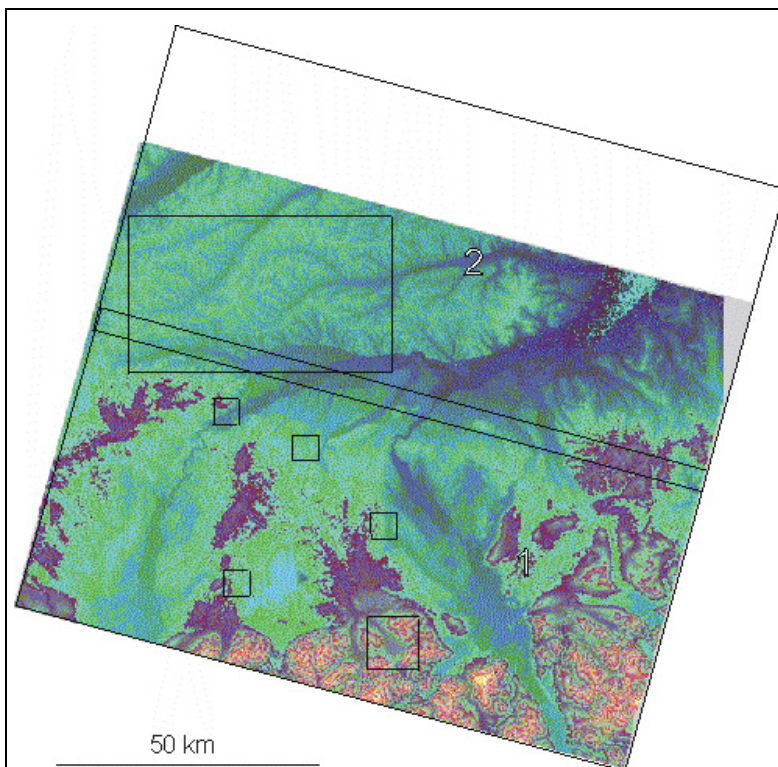
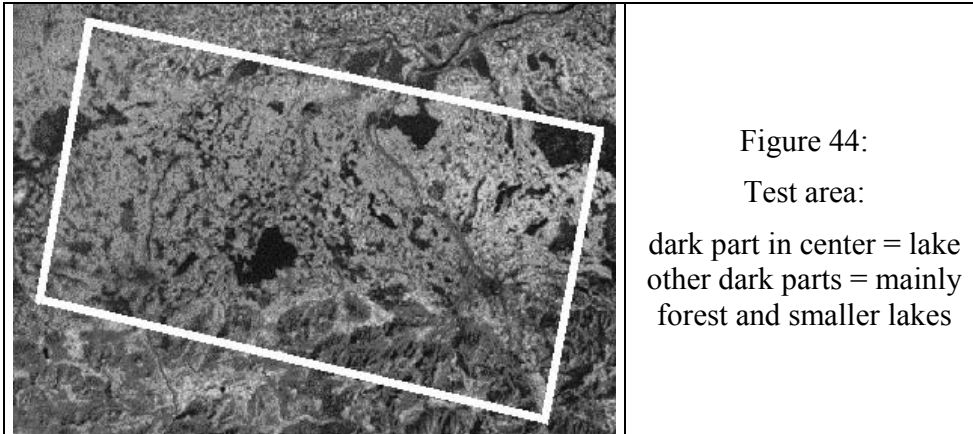


Figure 43:  
Colour coded  
DEM  
generated  
with the  
SPOT HRS  
data

The considered test area has mainly flat up to rolling relief and just a mountainous small part which includes the Alps (figure 43). The height of the test area is ranging from 270m up to 1850 above the sea level. This region is covered almost 20% by a mixture of smaller and larger forests and also some lake are included (figure 44).



The Survey Administration of the federal state Bavaria has made available the reference data organised by the German Aerospace Center (DLR) in order that the digital elevation model generated by the HRS instrument could be analysed. The reference data for four sub-areas (Prien, Gars, Peterskirchen, Taching) is from airborne laser scanner with a vertical accuracy better than 0.5m and for the other two (Inzell, Vilsbiburg) it is from topographic map. As control points trigonometric points are given.

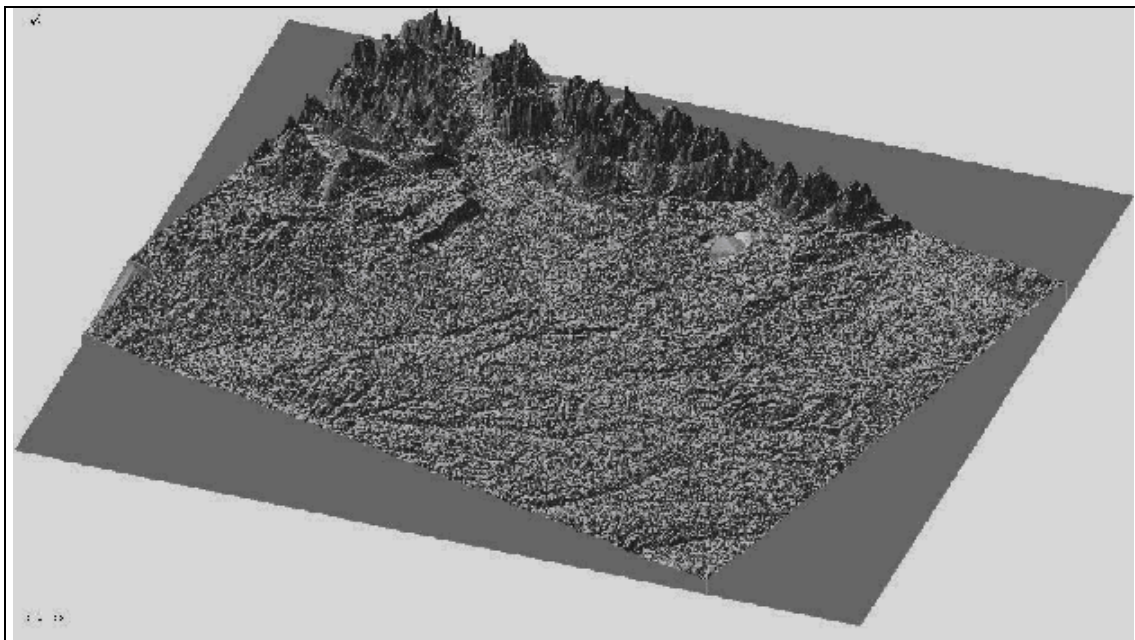


Figure 45: 3D-view to the DEM generated by HRS images (view direction: south)

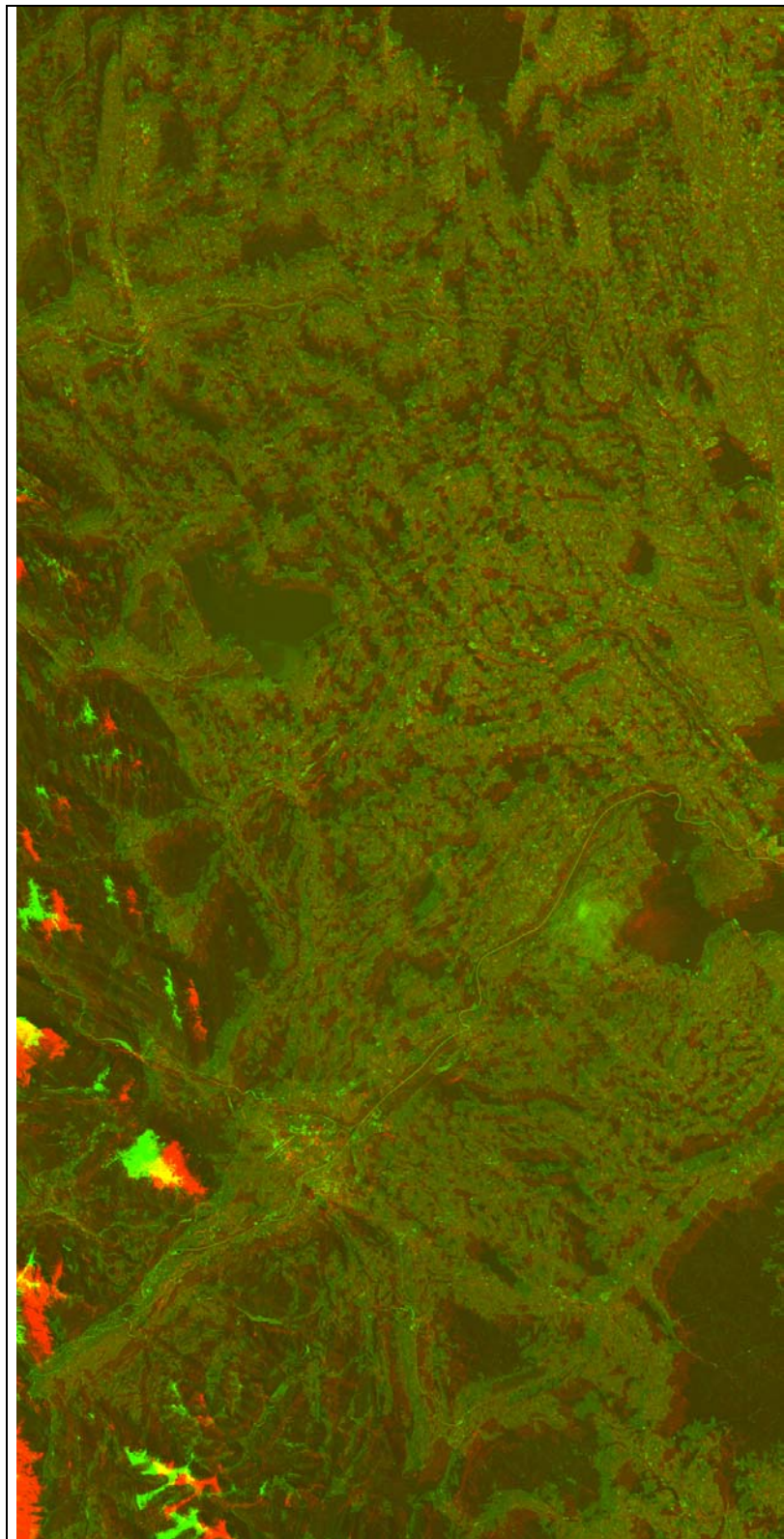


Figure 46: Anaglyph of the HRS model

### 4.3. Prien

Test sub-area Prien (figure 47) has a size of 5km x 5km and its relief is flat up to rolling with heights ranging from 471m to 691m. The area is covered approximately 23% with forest (figure 48). The reference data (figure 49) is from airborne laser scanner and it is available with the spacing of 5m both in X and in Y direction. The limits of the test area Prien are shown below:

	X [m]	Y [m]	Z [m]
Minimum	522000.000	5301000.000	471.000
Maximum	527000.000	5306000.000	691.000

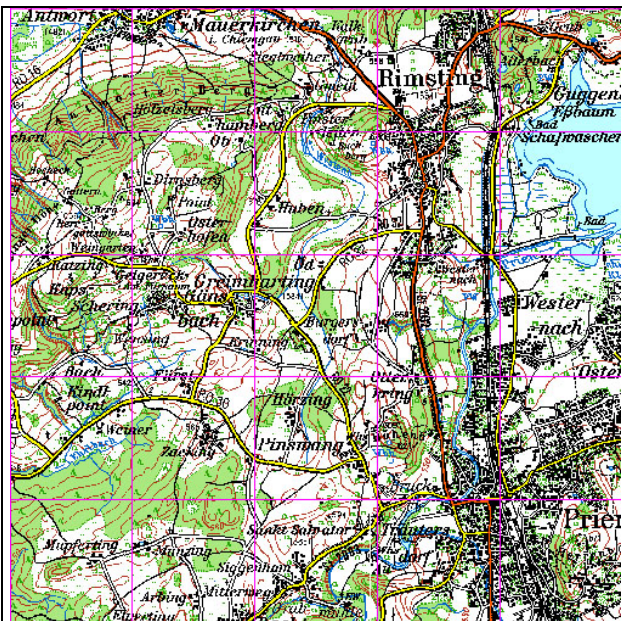


Figure 47: Topographic map of test area Prien



Figure 48: Forest layer of test area Prien

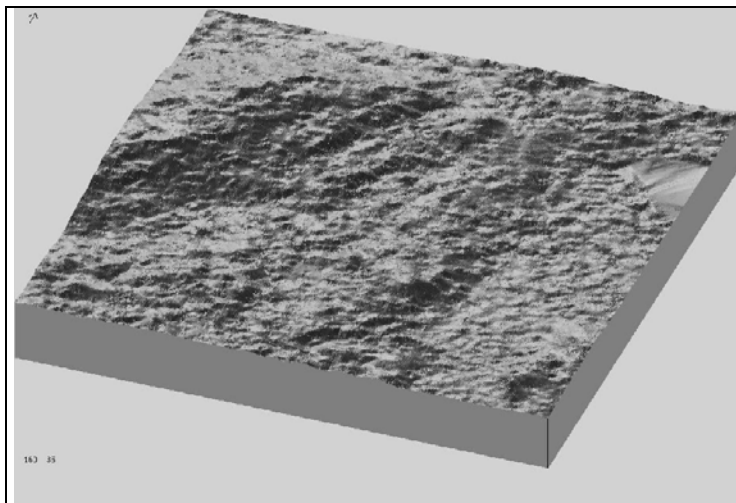


Figure 49:  
3-D view of the reference DEM in test area Prien

### 4.4. Gars

The second test sub-area Gars (figure 50) has a size of 5km x 5km and its relief is also flat up to rolling with heights between 397m and 597m. Gars is covered approximately 21% with forest (figure 51). The reference data (figure 52) is from airborne laser scanner and it is available with the spacing of 5m both in X and in Y direction. The limits of the test area Gars are shown below:

	X [m]	Y [m]	Z [m]
Minimum	520000.000	5333990.000	397.000
Maximum	525000.000	5339010.000	597.000



Figure 50: Topographic map of test area Gars



Figure 51: Forest layer of test area Gars

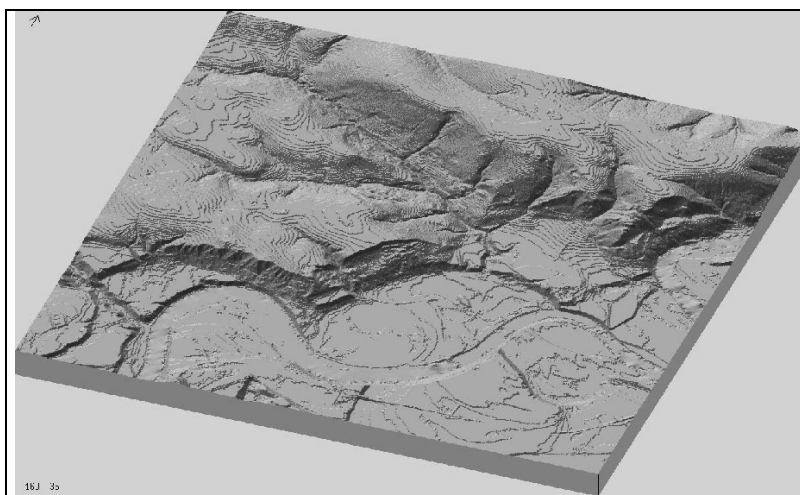


Figure 52:  
3-D view of the reference DEM in test area Gars

### 4.5. Peterskirchen

The size of the test sub-area Peterskirchen (figure 53) is 5km x 5km. The heights in this area are between 461m and 534m and the relief is flat up to rolling with. Approximately 16% of the area is covered with forest (figure 54). The reference data (figure 55) is from airborne laser scanner and it is available with the spacing of 5m both in X and in Y direction. The limits of the test area Peterskirchen are shown below:

	X [m]	Y [m]	Z [m]
Minimum	534990.000	5327000.000	461.000
Maximum	540000.000	5332000.000	534.000

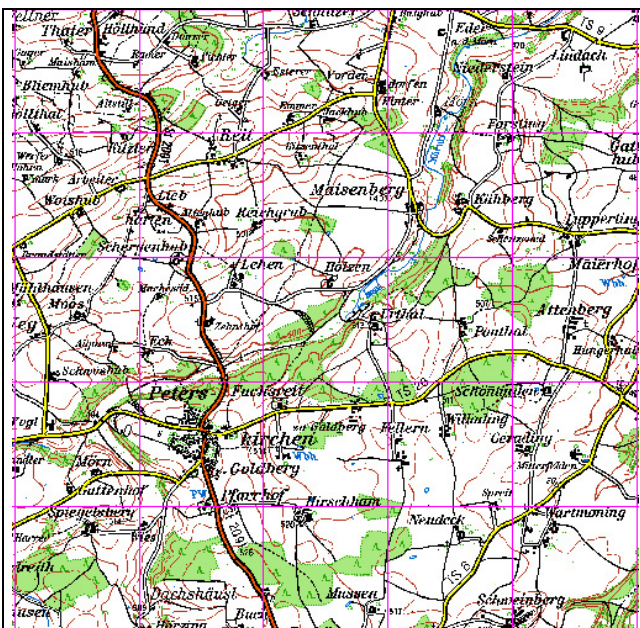


Figure 53: Topographic map of test area Peterskirchen



Figure 54: Forest layer of test area Peterskirchen

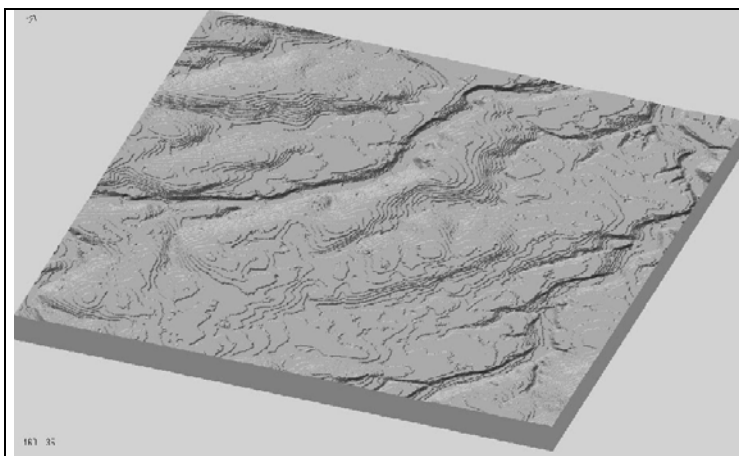


Figure 55:  
3-D view of the reference DEM in test area Peterskirchen

### 4.6. Taching

Test sub-area Taching (figure 56) has the same characteristics like the areas mentioned before: the size of 5km x 5km, the heights between 441m and 604m, the relief is flat up to rolling with, approximately 24% of the area is covered with forest (figure 57) and the reference data (figure 58) is from airborne laser scanner and it is available with the spacing of 5m both in X and in Y direction. The limits of the test area Taching are shown below:

	X [m]	Y [m]	Z [m]
Minimum	550000.000	5312000.000	441.000
Maximum	555000.000	5317000.000	604.000

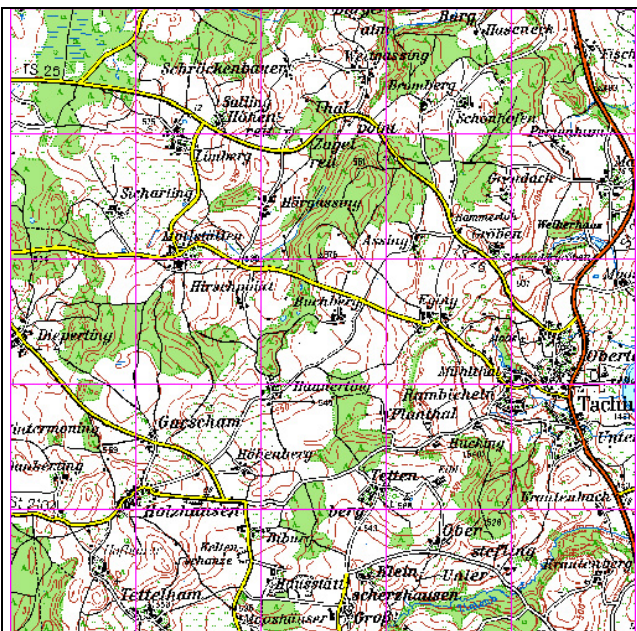


Figure 56: Topographic map of test area Taching



Figure 57: Forest layer of test area Taching

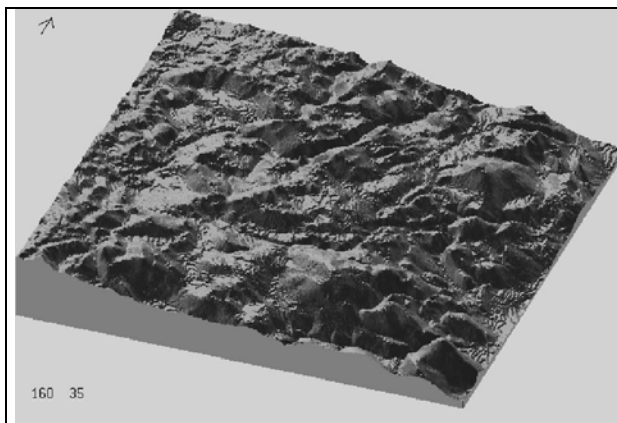


Figure 58:  
3-D view of the  
reference DEM  
in test area  
Taching

### 4.7. Vilsbiburg

Vilsbiburg (figure 59) has the size of 30km x 50km. This area is located mainly in the northern model, but also partially in the southern model. For this reason the analysis of the DEM has been made separately for both models. The relief is flat up to rolling with the heights between 362m and 569m; approximately 14% of the area is covered with forest (figure 60) and the forest areas are small. The reference DEM (figure 61) is from topographic map and it is available with the spacing of 50m both in X and in Y direction and with a limited vertical accuracy of 2m. The limits of the test area Vilsbiburg are shown below:

	X [m]	Y [m]	Z [m]
Minimum	504000.000	5344000.000	362.000
Maximum	554000.000	5374000.000	569.000



Figure 59:  
Topographic  
map of test  
area  
Vilsbiburg

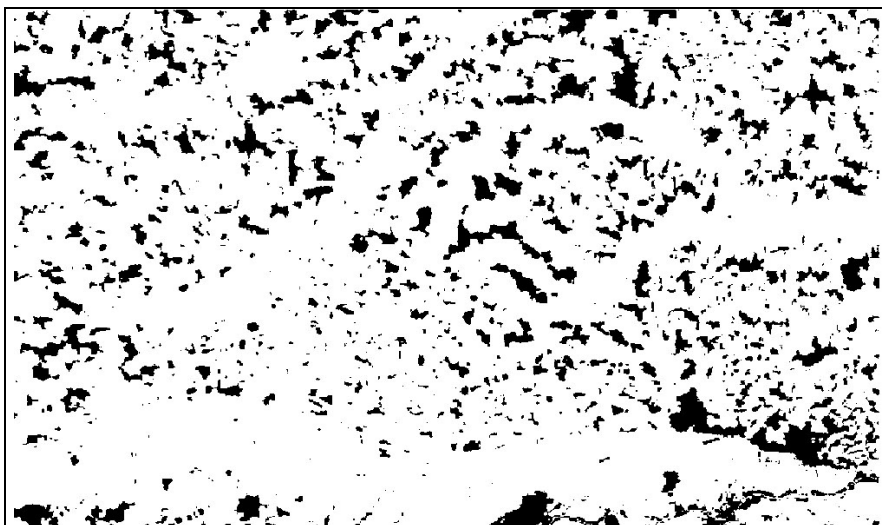


Figure 60:  
Forest layer  
of test area  
Vilsbiburg

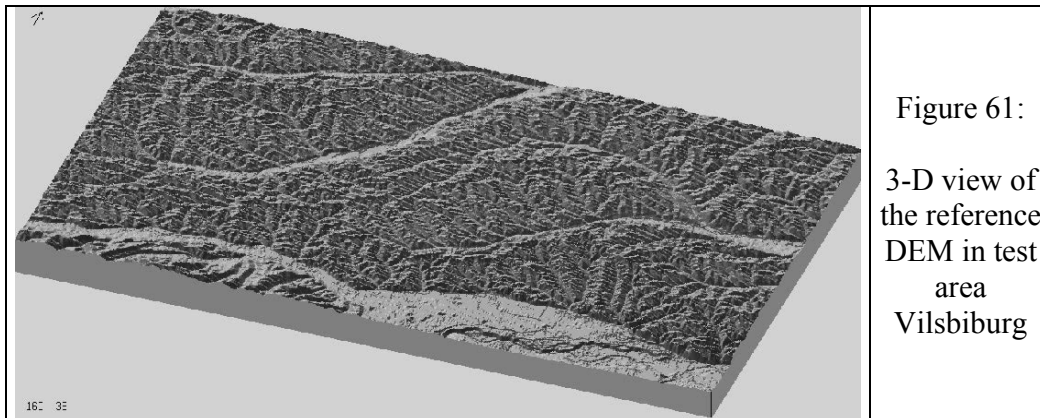


Figure 61:  
3-D view of  
the reference  
DEM in test  
area  
Vilsbiburg

#### 4.8. Inzell

Test sub-area Inzell (figure 62) is different from all the other test sub-areas. The size of the area is 10km x 10km. The region has a mountainous relief that includes steep parts of the Alps which are covered by forest. The heights are in the range from 610m up to 1681m. The forest coverage is approximately 68% (figure 63). The reference DEM (figure 64) is in the moderate northern part (13%) from laser scanner with a vertical accuracy better than 0.5m and in the mountainous southern part (87%) from digitised contour lines from maps 1:10 000 with a vertical accuracy of only 5m. The spacing is 25m both in X and in Y direction. The limits of the test area Inzell are below.

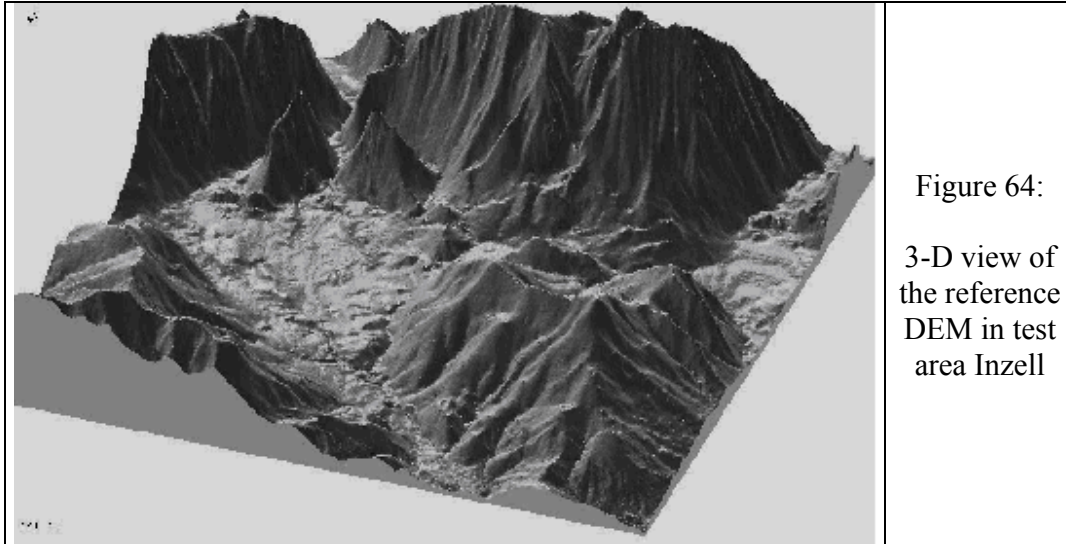


Figure 62: Topographic map of test area Inzell



Figure 63: Forest layer of test area Inzell

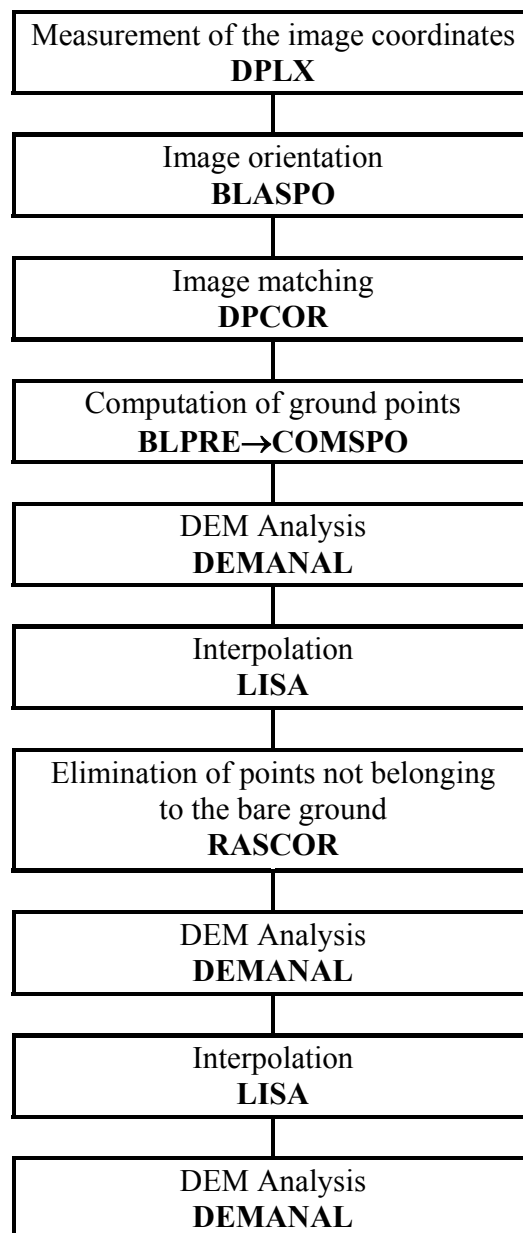
	X [m]	Y [m]	Z [m]
Minimum	549000.000	5287000.000	610.000
Maximum	559000.000	5297000.000	1681.000



## 5. STRATEGY

### 5.1. Used Method

In order to generate and analyze a digital elevation model for the test area Bavaria a sequence of programs was used. These programs are part of the Program System BLUH, created at the Institute of Photogrammetry and Geoinformation (IPI) in Hannover, Germany. The strategy and the sequence of programs are presented below:



All the six test sub-areas (Prien, Gars, Peterskirchen, Taching, Vilsbiburg, Inzell) included in the investigated area Chiemsee (Bavaria) were used for the analysis of the digital elevation model achieved by means of SPOT HRS images.

The orientation of the SPOT HRS images was made using the program BLASPO. The image positions of the control points and of some seed points used for the image matching were measured manually handling the program DPLX. The image matching was accomplished with the program DPCOR. The program COMSPO was applied for the computation of the ground point coordinates and for the transformation of these coordinates to the map projection in order that the heights and the reference points to be in the same national coordinate system. LISA was used for acquiring a raster arrangement of the not totally regular distributed ground points.

DEMANAL is used for comparing a digital elevation model with another, usually with the reference DEM. In this sequence of programs DEMANAL was first used to compare the height model achieved after the image matching, the manipulation with COMSPO and the arrangement in a raster form with the reference DEM. This height model is a digital surface model (DSM) because it includes the visible surface of the objects and not just the bare ground which represents the definition of a digital elevation model. The program RASCOR removes all the points that don't belong to the bare ground in order to create a DEM which will be compared with the reference DEM managing the program DEMANAL again. RASCOR is eliminating points. For the finally generated DEM these values have to be interpolated which was done again with LISA. The final data set was analyzed again with DEMANAL.

For comparison of the digital elevation model accuracy obtained by handling SPOT HRS images, data from INSAR by SRTM were used in case of two test sub-areas (Prien and Inzell).

## 5.2. Image orientation: BLASPO

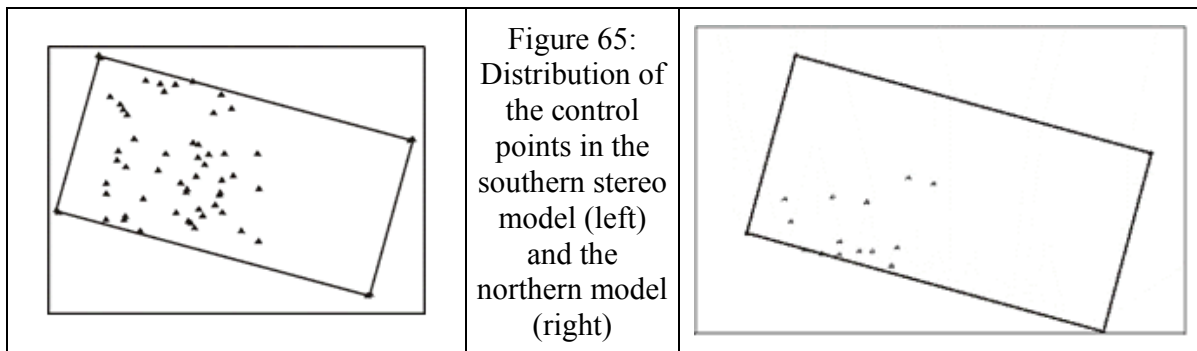
BLASPO (bundle block adjustment) is created for the bundle adjustment of satellite line scanner images like SPOT, MOMS, IRS-1C/1D, QuickBird Basic Imagery and ASTER that have perspective geometry only in the sensor line. In the direction of the orbit it is close to a parallel projection.

For the image orientation BLASPO needs control points and general information about the view direction and the orbit (inclination and ellipse specification). The data about the orbit is important because any line has a separate exterior orientation and the connection of the different lines is based on this information. The orientations of the neighbored lines or even in the whole scene are highly correlated because no rapid angular movements are happening.

The computation of the orbit parameters can be done with two methods: based on the ephemeris or using standard orbit data together with a transformation of the image

coordinates to the control points coordinates using the sensor orientations. The minimal number of the control points is three, but for a reliable mapping at least four should be used. These two methods lead to the same results.

In this project the image orientation has been made before. The program BLASPO effectuated the orientation in a tangential coordinate system to avoid the negative influence of the map projection. The control points used for the image orientation were usually located closely to road crossings in order to ease their identification. For the orientation four unknowns have to be determined together with some additional parameters and at least one additional parameter has to be used for respecting the yaw control. The image orientation was made using 46 control points in the southern model and 14 in the northern model (figure 65). The part of the models which includes a fragment of Austria doesn't contain any control point.



### 5.3. Measurement of the Image Coordinates: DPLX

DPLX (computer supported digital photogrammetric determination of image coordinates) was developed for the precise determination of image coordinates in digital images. It is based on the script language TCL/TK. Large images cannot be handled on usual PC's directly; this is too time consuming and requires a large RAM. By this reason the original images are divided into sub-images which can be handled fast enough without problems. Raw images, \*.ima and BMP-files are accepted (Jacobsen 2003).

DPLX was used for the measurement of the image positions of the control points for the image orientation. It was also handled for measuring some seed points for the image matching. These operations were done manually. The program DPLX uses overview images for handling large images more quickly and zoom windows for a more accurate positioning in a point measurement (figure 66).

The manual measurement of the point location (pixel address which can be transformed into image coordinates) implies the next operations: selection of the area where a point or points have to be measured using a window of the overview images, specification of the image points in the menu below the original sub-images on the right, specification of the point number of the point which will be measured (the next available

point number is shown below the original images on the left), generation of zoom windows by clicking the right mouse button in the sub-image of the original images in order to execute a more accurate positioning for measuring the image coordinates of the points. The measured coordinates of the points are stored immediately and they can be viewed, renamed or deleted.

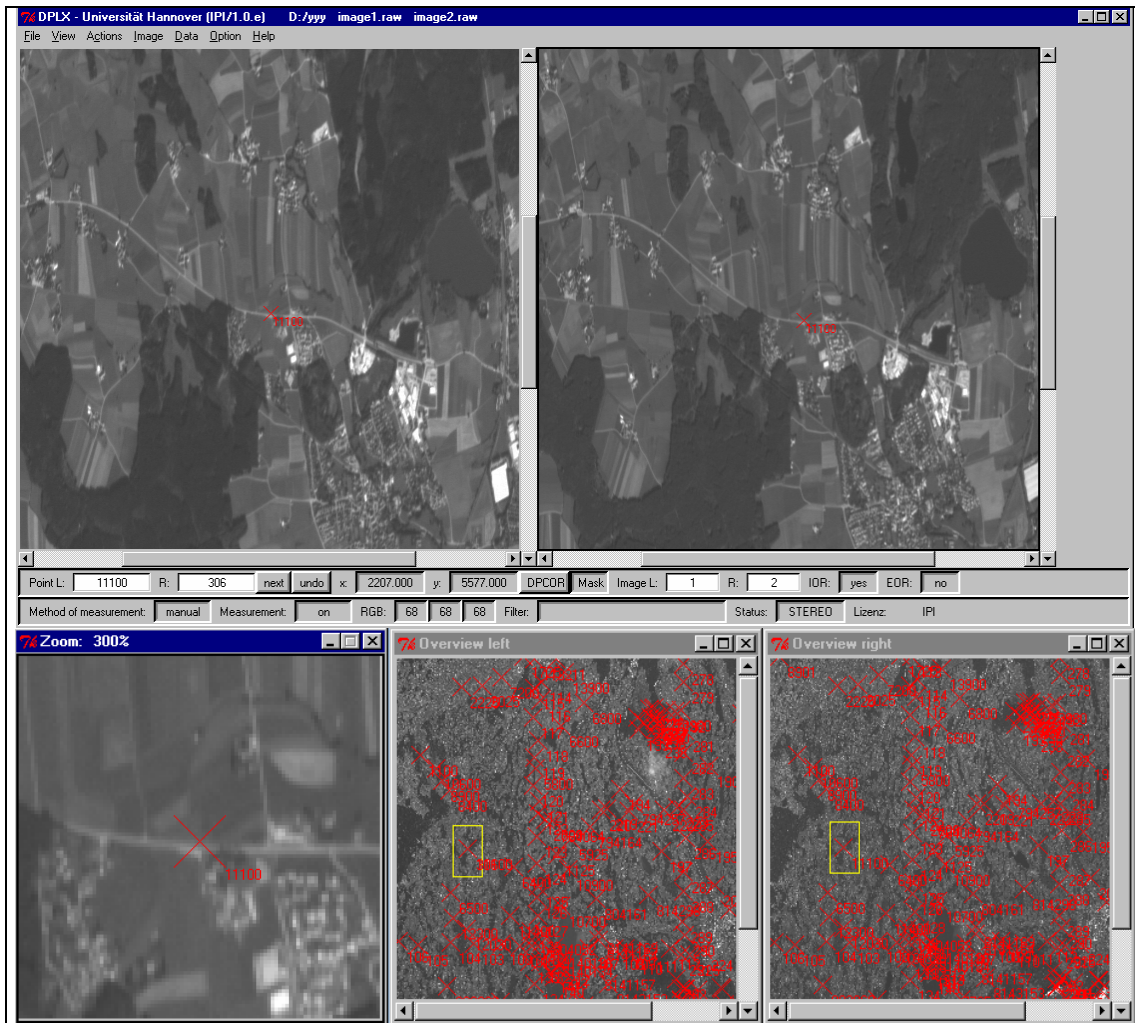


Figure 66: DPLX – original images (above), overview images (lower right) and zoom window (lower left)

#### 5.4. Image Matching: DPCOR

The image matching was made automatically using the program DPCOR. This program identifies corresponding image points in a model of two digital images without any information about the orientation. DPCOR is using a least squares matching method in the image space with region growing. This method represents the most accurate possibility of image matching with advantages especially in inclined areas. The automatic matching in

the image space requires at least one start point with the corresponding positions in the both images (seed point), but also control points can be used as seed points. The neighbored points of this seed start point are determined by matching and they become seed points for the next points that are matched. This method is based on the image contrast. In areas with sufficient contrast the matching leads to good results, but in areas without any contrast such as water surface or with limited grey value variations like forest areas the matching has problems or it is impossible to be done.

DPCOR can be combined with DPLX in the case when the start points necessary for the automatic image matching with DPCOR have to be manually measured using DPLX. The results of the image matching are pixel coordinates. The pixel coordinate system used by DPCOR has the rows from top to bottom and the columns from left to right. That means the first pixel is located in the upper left corner of the digital image and its coordinates 1.0/1.0 (figure 67).

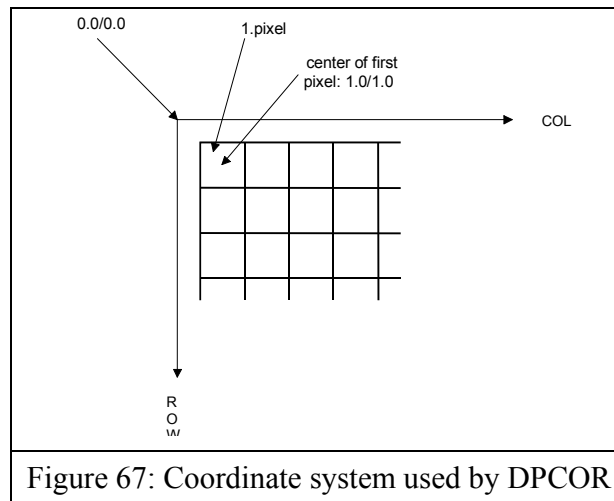


Figure 67: Coordinate system used by DPCOR

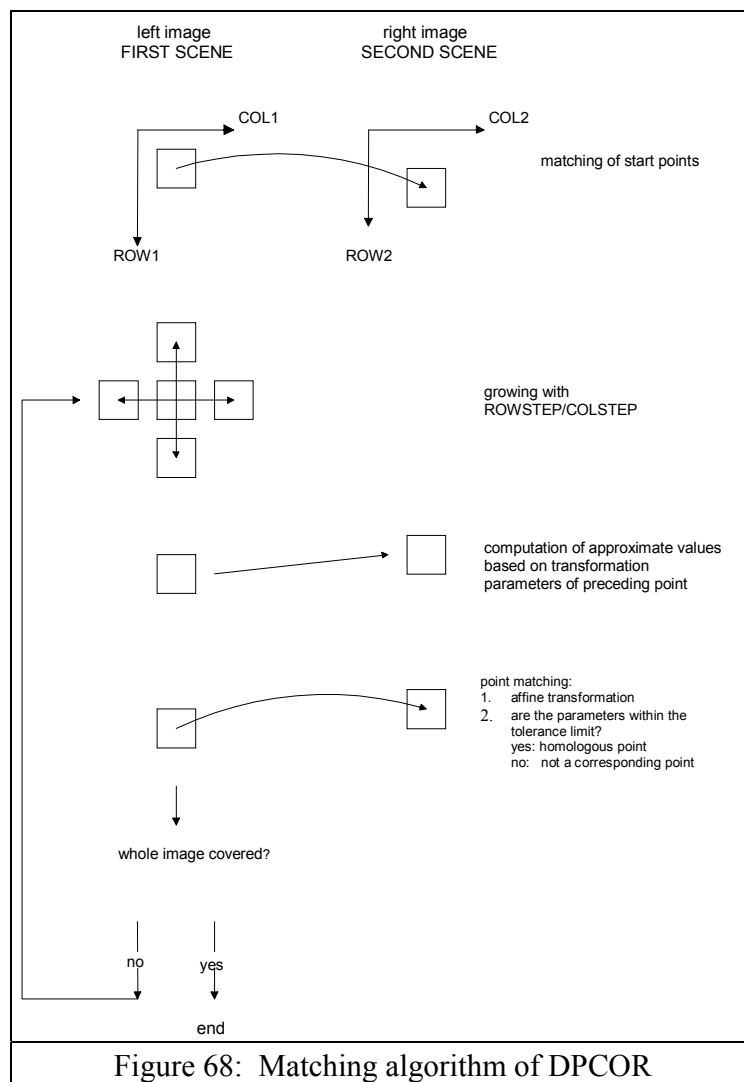
The matching algorithm used by the program DPCOR is: the points from the left image are fixed and their corresponding points in the right scene are searched. Points located in the left and the right image are corresponding if the gray values in the close neighborhood are similar and identical. The size of the pixel-window can be defined and the searched point is in the middle of the window. The value of correspondence is described as correlation coefficient. For an optimal fit of the sub-windows for image matching, the affine transformation is used (formula 4a and 4b):

$$ROW_{right} = a_0 + a_1 ROW_{left} + a_2 COL_{left} \quad (4a)$$

$$COL_{right} = b_0 + b_1 ROW_{left} + b_2 COL_{left} \quad (4b)$$

$ROW_{left}$  and  $COL_{left}$  are known, at first they are identical to the start points, later they are defined by the growing with row step or column step in relation to the start points.  $ROW_{right}$  and  $COL_{right}$  are also at first defined by the start points, later by the

approximate computation based on  $ROW_{left}$  and  $COL_{left}$  and the transformation parameters of the next neighbored homologous point  $ROW_{right}$  and  $COL_{right}$ . For each pixel in the corresponding windows of both images the difference of the gray values are computed. A radiometric correction can be done based on an equalization of the histograms of the right image in relation to the left image. The correlation coefficients are computed using the affine transformation. If the center of the actual windows in both images are corresponding and all the parameters satisfy the tolerance conditions the two points are homologous. In this way the whole image will be covered using the growing method. The matching algorithm is presented in the picture below (figure 68):



The automatic matching has been done in two ways.

1. automatic matching for every third pixel with a window size of 10 pixels x 10 pixels for the whole area of test; with this method were achieved sufficient independent ground points in a raster of approximately 15m x

30m (15m in the orbit and 30m across the orbit direction). The grey value variation for both scenes is not optimal, but sufficient with the exception of some parts in the forest. Usually in the forest areas, in steep parts of the model, in areas covered by snow or in the case of water surfaces the matching was very difficult or impossible. In these areas where the contrast is limited the correlation coefficient is very low and sometimes below the tolerance value of 0.6. The y-parallax of the intersection can be used as quality indicator. The matching has been done independently for both models.

2. automatic matching of every pixel with a window size of 10 pixels x 10 pixels for two test sub-areas (Prien and Gars); with this method the achieved ground points are in a raster form of 5m x 10m (5m in the orbit and 10m across the orbit direction).

### 5.5. Computation of ground points: BLPRE→COMSPO

The result of the image matching is a file that contains pixels coordinates of the points matched successfully. Using the program BLPRE (preparation of photo coordinates) the pixel coordinates are transformed in image coordinates.

Then the image coordinates are transformed in ground point coordinates handling the program COMSPO (computation of correction grids and ground coordinates in national coordinate system). This program computes the ground coordinates directly in the national coordinate system. In total, approximately 27 million points have been determined in the southern model where the whole area of 12000 x 12000 pixels has been used and the northern model where only 12 000 x 8000 pixels were included.

### 5.6. DEM Analysis: DEMANAL

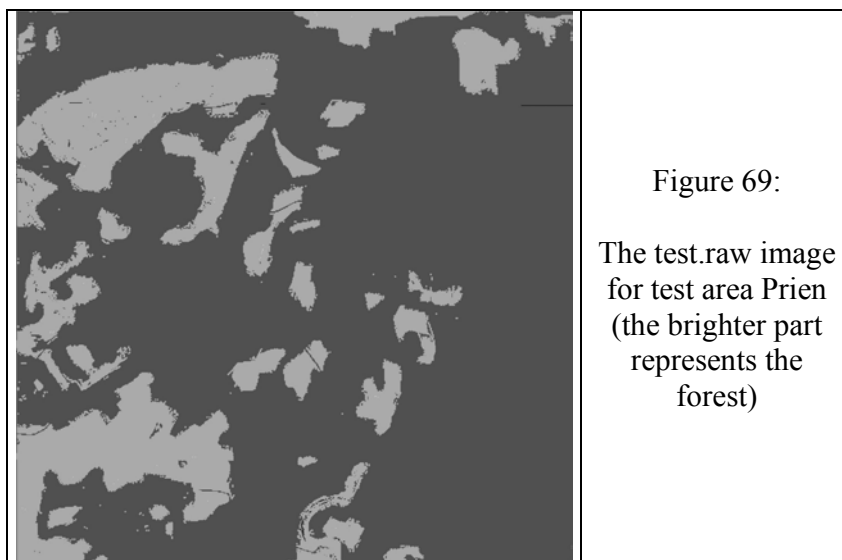
DEMANAL (analysis of digital elevation models) is a program that evaluates the accuracy and accuracy characteristics of a DEM against a reference DEM. The analysis of a DEM is made separate for distinct land classes (for example forest) because the accuracy and the accuracy characteristics may be different from case to case. DEMANAL uses geocoded layer images for each land class. The program investigates in detail the discrepancies between the both DEM and also the dependency against the terrain inclination and the height level. It is possible to define tolerance limits for the terrain inclination and the discrepancies of the DEM-points. The influence of a vertical scale difference can be respected iteratively.

The reference DEM must be available as ASCII-file in raster arrangement (equal point spacing) and it may have some data gaps. The DEM for analysis has to be also in

ASCII-form, but it may have a random point distribution or a regular point distribution (ASCII-raster form). The results of the analysis are stored by default in the file demanal.lst.

In the investigation of test area Chiemsee the program DEMANAL has been used in three situations. First, DEMANAL was used for the analysis of the height model achieved from the image matching. In fact this was an evaluation of the digital surface model because it contained points located on the visible surface and not on the bare ground. The second time DEMANAL was used for the analysis of the DEM obtained handling the program RASCOR. The DEM for analysis had a random point distribution. In the third situation, DEMANAL was handled for the evaluation of the DEM with the points eliminated by RASCOR and interpolated by LISA. In all three cases, DEMANAL made the investigation of the DEM using two geo-referenced layer images: one for open areas and one for forest. The forest layers have been extracted from the topographic maps 1: 50000.

An example of handling the program DEMANAL is shown below for the case of test area Prien. The reference DTM data is contained in prien.dat, which is an ASCII-raster file (the points are arranged in a regular distribution). The file with the analysed DEM data is prienr4.dat and is an ASCII file, but not in a regular point distribution arrangement. In this case DEMANAL is comparing the reference DEM with the DEM acquired by filtering the DSM with RASCOR using two iterations and considering that the type of terrain is flat and has the same characteristics. The analysis is made for the forest areas. That means that the forest layer is used and the raster file with the area for investigation is forst.raw. When this file is specified the program is searching for a file which has instead of the extension raw the extension tfw. In a tfw file some information about the layer are specified: the pixel size in X-direction, rotation information, negative pixel size in Y-direction, the Easting and northing of the upper left image corner. The Z-interval for grouping DZ is 1.00m, the tolerance limit for the accepted height discrepancies is 50.00m and the maximal accepted tangent (slope) is 1.0000. The results of the analysis are shown in a raw-image called test.raw (figure 69). The listing of the results is short and the analysis is made using one iteration.



## DEMANAL.1 Dialogue

```

=====
PROGRAM DEMANAL          UNIVERSITY OF HANNOVER    FEB 2004
ANALYSIS OF DIGITAL ELEVATION MODEL

          INSTITUTE FOR PHOTOGRAMMETRY AND GEOINFORMATION

DATE : 14.05.2004    09:47:38
=====

VERSION NUR FUER LEHRE   IPI UNIVERSITAET HANNOVER

OUTPUT UNIT FOR LISTING = ? T/F    T = TERMINAL
F = FILE demanal.lst = DEFAULT

TYPE ONE LINE TEXT
DEFAULT=

FILE NAMES AND OPTIONS
CODE  FILE / FUNCTION                NAME
  1  INPUT FILE WITH RASTER DEM      prien.dat
  2  INPUT FILE WITH POINT NAMES ? Y/N  Y
  3  INPUT FILE FOR COMPARISON        prienr4.dat.
  4  INPUT FILE WITH POINT NAMES ? Y/N  N
  5  RASTER FILE WITH SPECIAL AREA    forst.raw
  6  Z-INTERVAL FOR GROUPING DZ        1.00
  7  MAXIMAL ACCEPTED DZ               50.00
  8  MAXIMAL ACCEPTED TANGENT(SLOPE)   1.0000
  9  OUPUT FILE RASTER OVERVIEW (*.raw) test.raw
10  LISTING    S / V / L              S
11  ITERATIONS 1 / 2                  1
FILE NAME = BLANK = NO CREATION OF FILE
TYPE CODE AND FILE NAME IN ONE LINE    DEFAULT = NEXT INPUT

```

Code 1: input file with the reference DEM, which must be in ASCII-form and in a raster arrangement.

Code 2: specify if the reference DEM includes point numbers or not. If the file name under code 1 will be specified, the first lines will be read and shown on the screen. DEMANAL identifies automatic if a point number is available or not and sets the correct code. Only if no point name is available, but the Z-value will be followed by some more information, this specification has to be made manually.

Code 3: input file with DEM for analysis – this file must be in ASCII-form and may have any distribution and size.

Code 4: usually the program specifies this value automatic – it corresponds to code 2

Code 5: a raster file which includes the information of special areas or an area may be used for the separation of the input data. Only raw-images with 8bit and 1 channel are accepted. This file may be the result of an classification. Different layers may be included with different gray values. A class will be identified by the same gray value.

Code 6: The discrepancies are grouped by a multiple of this value for the generation of a histogram and for detailed analysis. 100 groups are used, so the interval for grouping should have a size corresponding to the largest important height discrepancies divided by 100.

Code 7: The accepted height discrepancies may be limited by a tolerance limit

Code 8: The maximal accepted slope of the reference DEM may be limited by a slope limit. Points in these locations are not respected

Code 9: The results of the analysis, including the area of the reference DEM, the used layer and not respected points may be shown in a raw-image with 8bit and 1 channel.

Code 10: The listing may be short (S), very long (V) or long (L) including different details

Code 11: An analysis for a vertical shift and vertical scale difference between both DEMs will be made. In a second iteration the analysis can be repeated using a correction for shift and scale.

TFW DATA FROM: forst.tfw

255 = open area

0 = forest

```
SPECIFY IMAGE SIZE AND GEOCODING FOR *.raw-FILE
CODE  FUNCTION          VALUE
 1  NUMBER OF COLUMNS (WIDTH)      1000
 2  NUMBER OF ROWS (HEIGHT)         1000
 3  X LEFT UPPER CORNER             522000.00
 4  Y LEFT UPPER CORNER             5306000.00
 5  PIXEL SIZE IN X-DIRECTION        5.00
 6  PIXEL SIZE IN Y-DIRECTION        5.00
 7  GRAY VALUE FOR AREA TO BE USED   0
TYPE CODE AND VALUE IN ONE LINE   DEFAULT = NEXT INPUT  B=BACK
```

If a raster file with layer information has been specified, the geo-reference (code 3 – 6) is required. If a 'tfw'-file is available the values coming from this file are shown.

Code 1 and 2: The image size has to be specified

**Code 7: The layer with this gray value will be used for the analysis – only points located inside the layer are respected**

```
GRAY VALUES FOR OUTPUT RASTER FILE
CODE  FUNCTION          RANGE: 0 - 255
 1  BACKGROUND          0
 2  INPUT DEM           80
 3  SPECIAL LAYER       170
 4  EXCLUDED POINTS     255
 5  EXCLUDED SLOPE      40
 6  LOCATION OF SLOPE GROUP 1
 7  SLOPE GROUP         255
 8  0=ONLY SLOPE GROUP 1=ALL ABOVE 0
TYPE CODE AND VALUE IN ONE LINE   DEFAULT = NEXT INPUT  B=BACK
```

If a raster output image has been specified (first dialogue, code 9), the gray values to be used in this file have to be specified. The shown default values can be used.

```
SPACING IN X:      5.00000000    IN Y:      5.00000000    1001877 POINTS
      1001 LINES IN X-DIRECTION    1001 LINES IN Y-DIRECTION    ( 1002101)
```

```
SPECIFICATION OF WINDOW
CODE  MEANING          VALUE
 1  X-MINIMUM          522000.000 (ACTUAL DATA SET: 522000.000)
 2  X-MAXIMUM          527000.000 (ACTUAL DATA SET: 527000.000)
 3  Y-MINIMUM          5301000.000 (ACTUAL DATA SET: 5301000.000)
 4  Y-MAXIMUM          5306000.000 (ACTUAL DATA SET: 5306000.000)
 5  Z-MINIMUM          469.000 (ACTUAL DATA SET: 469.000)
 6  Z-MAXIMUM          691.000 (ACTUAL DATA SET: 691.000)
TYPE CODE AND VALUE IN ONE LINE   JUST RETURN = NEXT INPUT
"C" = CHANGE TO ACTUAL LIMITS OF DATA SET
```

A window of the input files may be used – only points located inside the specification will be respected for the analysis

## DEMANAL.2 Listing

```
=====
PROGRAM DEMANAL          UNIVERSITY OF HANNOVER    FEB 2004

ANALYSIS OF DIGITAL ELEVATION MODEL

      VERSION NUR FUER LEHRE AN DER UNIVERSITÄT HANNOVER

DATE : 14.05.2004    14:14:20
=====
MEAN HEIGHT:  558.23  RMS +/- 40.904          58.882
```

FOR WHOLE DATA SET:

```
DISTRIBUTION OF HEIGHT 1001877 POINTS
< 483.31 2.01 % 2.01 % **
483.31 - 497.61 1.08 % 3.10 % *
497.61 - 511.92 1.18 % 4.28 % *
511.92 - 526.23 17.61 % 21.89 % *****
526.23 - 540.53 14.25 % 36.13 % *****
540.53 - 554.84 12.92 % 49.06 % *****
554.84 - 569.15 19.46 % 68.52 % *****
569.15 - 583.45 13.63 % 82.15 % *****
583.45 - 597.76 5.32 % 87.46 % *****
597.76 - 612.07 2.48 % 89.94 % ***
612.07 - 626.37 1.59 % 91.53 % **
626.37 - 640.68 2.27 % 93.80 % **
640.68 - 654.99 1.45 % 95.25 % *
654.99 - 669.29 2.09 % 97.35 % **
> 669.29 2.65 % ***
```

height distribution of the reference image

```
226334 REFERENCE POINTS FROM prien.dat
775543 POINTS REMOVED - NOT BELONGING TO SPECIAL AREA = 77.41 %
```

```
MEAN SLOPE IN X-DIRECTION: .1189 MAXIMUM: .8000
```

```
MEAN SLOPE IN Y-DIRECTION: .1349 MAXIMUM: .8000
```

```
780 VALUES REMOVED BECAUSE EXCEEDING SLOPE 1.0000
```

```
SLOPE % FREQUENCY DISTRIBUTION OF SLOPE
.00 69.718 *****
.03 .000
.05 .000
.08 .000
.10 .000
.13 .000
.15 .000
.17 .000
.20 .000
.22 .000
.25 .000
.28 .000
.30 .000
.32 .000
.35 .000
.38 .000
.40 28.857 *****
.43 .000
.45 .000
.47 .000
.50 .000
.52 .000
.55 .000
.57 .000
.60 .000
.63 .000
.65 .000
.68 .000
.70 .000
.73 .000
.75 .000
.77 .000
.80 1.425 *
.82 .000
.85 .000
.88 .000
.90 .000
.93 .000
.95 .000
.98 .000
```

38710 POINTS IN FILE FOR COMPARISON      3947 POINTS IN AREA  
 DZ ACCEPTED UP TO:      50.00      0 VALUES NOT ACCEPTED =      .00 %

=====  
 RMSZ:      16.47      MEAN DZ:      -13.51  
 RMSZ WITHOUT SYSTEMATIC PART:      9.42  
 =====

SLOPE	N	% USED	RMSZ AS FUNCTION OF SLOPE
.00	1986	100.0	15.51 *****
.03	0	100.0	.00
.05	0	100.0	.00
.08	0	100.0	.00
.10	0	100.0	.00
.13	0	100.0	.00
.15	0	100.0	.00
.17	0	100.0	.00
.20	1166	100.0	18.40 *****
.22	0	100.0	.00
.25	0	100.0	.00
.28	0	100.0	.00
.30	0	100.0	.00
.32	0	100.0	.00
.35	0	100.0	.00
.38	0	100.0	.00
.40	280	100.0	20.53 *****
.43	0	100.0	.00
.45	0	100.0	.00
.47	0	100.0	.00
.50	0	100.0	.00
.52	0	100.0	.00
.55	0	100.0	.00
.57	0	100.0	.00
.60	18	100.0	29.72 *****
.63	0	100.0	.00
.65	0	100.0	.00
.68	0	100.0	.00
.70	0	100.0	.00
.73	0	100.0	.00
.75	0	100.0	.00
.77	0	100.0	.00
.80	4	100.0	21.28
.82	0	100.0	.00
.85	0	100.0	.00
.88	0	100.0	.00
.90	0	100.0	.00
.93	0	100.0	.00
.95	0	100.0	.00
.98	0	100.0	.00

Root mean square differences of both DEMs depending upon the mean terrain inclination in X- and Y-direction of the reference DEM and the percentage of used points (below DZ = 50m in this case). Only points with 4 neighbored Z-values are respected for this.

The RMS-values for slope groups with less than 6 values are not displayed with asterisks (\*)

$$SZ = 15.52 + 7.041 * \text{TAN}(\text{SLOPE})$$

=====

WITHOUT FIRST GROUP:

$$SZ = 16.21 + 5.469 * \text{TAN}(\text{SLOPE})$$

Sometimes the first slope group (nearly horizontal) shows a different characteristics, especially in mountainous areas where especially buildings are located in the flat part.

SLOPE	N	SYST P.	RMSZ WITHOUT SYSTEMATIC PART
.00	1986	-13.03	8.40 *****
.03	0	.00	.00

.05	0	.00	.00	
.08	0	.00	.00	
.10	0	.00	.00	
.13	0	.00	.00	
.15	0	.00	.00	
.17	0	.00	.00	
.20	1166	-15.51	9.90	*****
.22	0	.00	.00	
.25	0	.00	.00	
.28	0	.00	.00	
.30	0	.00	.00	
.32	0	.00	.00	
.35	0	.00	.00	
.38	0	.00	.00	
.40	280	-17.07	11.41	*****
.43	0	.00	.00	
.45	0	.00	.00	
.47	0	.00	.00	
.50	0	.00	.00	
.52	0	.00	.00	
.55	0	.00	.00	
.57	0	.00	.00	
.60	18	-28.02	9.90	*****
.63	0	.00	.00	
.65	0	.00	.00	
.68	0	.00	.00	
.70	0	.00	.00	
.73	0	.00	.00	
.75	0	.00	.00	
.77	0	.00	.00	
.80	4	-19.41	8.73	
.82	0	.00	.00	
.85	0	.00	.00	
.88	0	.00	.00	
.90	0	.00	.00	
.93	0	.00	.00	
.95	0	.00	.00	
.98	0	.00	.00	

WITHOUT SYSTEMATIC PART:  
 SZ = 8.40 + 3.745 \* TAN(SLOPE)

FREQUENCY DISTRIBUTION OF DZ AS F(DZ)

-48.00	1	
-46.00	2	
-44.00	0	
-42.00	2	
-40.00	5	
-38.00	13	*
-36.00	24	**
-34.00	42	****
-32.00	54	*****
-30.00	107	*****
-28.00	149	*****
-26.00	170	*****
-24.00	206	*****
-22.00	170	*****
-20.00	170	*****
-18.00	186	*****
-16.00	230	*****
-14.00	247	*****
-12.00	287	*****
-10.00	377	*****
-8.00	423	*****
-6.00	416	*****
-4.00	332	*****
-2.00	151	*****
.00	67	*****
2.00	40	****
4.00	35	****

6.00	17	**
8.00	5	
10.00	3	
12.00	3	
14.00	3	
16.00	3	
18.00	1	
20.00	1	
22.00	0	
24.00	1	
26.00	1	
28.00	1	
30.00	0	
32.00	0	
34.00	1	
36.00	1	
38.00	0	
40.00	0	
42.00	0	
44.00	0	
46.00	0	
48.00	0	
50.00	0	

Z	SZ	N	MAX	MEAN	SZ WITHOUT SYST
469.00	8.47	116	13.21	-8.06	2.62
483.31	3.72	8	8.18	-2.78	2.47
497.61	12.28	361	30.20	-10.88	5.69
511.92	17.06	568	46.34	-14.15	9.53
526.23	19.12	593	48.80	-15.94	10.57
540.53	15.00	720	38.09	-11.86	9.17
554.84	16.18	621	37.12	-13.32	9.19
569.15	19.37	211	37.59	-16.56	10.04
583.45	21.13	182	35.87	-18.97	9.30
597.76	18.91	132	33.64	-16.17	9.81
612.07	16.94	93	34.58	-13.62	10.07
626.37	17.74	61	32.95	-15.22	9.11
640.68	10.51	120	35.40	-7.03	7.81
654.99	15.44	129	29.94	-13.46	7.57
669.29	10.51	32	18.50	-8.70	5.90

root mean square discrepancies depending upon the terrain height of the reference DEM, number in the height group, largest discrepancy including also the not accepted points which have not been respected for the other computations, linear mean of the discrepancies in the different height groups and root mean square after respecting the linear mean

Z	MEAN
469.00	-8.06
483.31	-2.78
497.61	-10.88
511.92	-14.15
526.23	-15.94
540.53	-11.86
554.84	-13.32
569.15	-16.56
583.45	-18.97
597.76	-16.17
612.07	-13.62
626.37	-15.22
640.68	-7.03
654.99	-13.46
669.29	-8.70

systematic discrepancies for the different height groups

$$Z^* = -11.18 + -.00433 * Z$$

systematic discrepancy between both DEMs depending upon Z - in this case there is a scale difference between both of 4.33 per mille. The adjusted vales do respect the different number of observations (column

"N") in the different height groups. If negative height groups are available, they are respected only with the weight factor 1.

SYSTEMATIC HEIGHT ERROR				
Z	ORIGINAL	IMPROVEMENT	RESIDUAL	
1	469.000	-8.059	-13.210	5.151
2	483.307	-2.785	-13.272	10.487
3	497.613	-10.878	-13.334	2.456
4	511.920	-14.149	-13.396	-.754
5	526.227	-15.936	-13.458	-2.478
6	540.533	-11.865	-13.520	1.655
7	554.840	-13.318	-13.582	.263
8	569.147	-16.559	-13.644	-2.916
9	583.453	-18.974	-13.706	-5.269
10	597.760	-16.169	-13.767	-2.401
11	612.067	-13.623	-13.829	.206
12	626.373	-15.222	-13.891	-1.330
13	640.680	-7.032	-13.953	6.921
14	654.987	-13.458	-14.015	.557
15	669.293	-8.697	-14.077	5.380

ROOT MEAN SQUARE OF SYSTEMATIC HEIGHT ERROR AS F(Z)  
 BEFORE 14.779 AFTER FITTING 2.786

Z	N	SIZE OF SZ AS F(Z)
469.00	116	*****
483.31	8	*****
497.61	361	*****
511.92	568	*****
526.23	593	*****
540.53	720	*****
554.84	621	*****
569.15	211	*****
583.45	182	*****
597.76	132	*****
612.07	93	*****
626.37	61	*****
640.68	120	*****
654.99	129	*****
669.29	32	*****

Z	N	SIZE OF SZ WITHOUT SYSTEMATIC PART AS F(Z)
469.00	116	*****
483.31	8	*****
497.61	361	*****
511.92	568	*****
526.23	593	*****
540.53	720	*****
554.84	621	*****
569.15	211	*****
583.45	182	*****
597.76	132	*****
612.07	93	*****
626.37	61	*****
640.68	120	*****
654.99	129	*****
669.29	32	*****

SITUATION PLOT STORED AS RAW IMAGE WITH 1001 WIDTH 1001 HEIGHT  
 IN: test.raw

-----  
 LAYER FROM: forst.raw  
 GRAY VALUE FOR AREA TO BE USED 0  
 77.41 % NOT BELONGING TO USED AREA  
 INPUT DATA FROM: prien.dat  
 INPUT DATA FROM: prienr4.dat

-----  
 41 INPUT POINTS (100 %) SPACING: 5.00000000 5.00000000  
 14.05.2004 14:46:50

END OF PROGRAM DEMANAL

### 5.7. Interpolation: LISA

The program LISA was used for the interpolation of the points which are in an irregular distribution in order to obtain a regular grid of points without gaps. The spacing of the grid is very important. For the investigation of test area Chiemsee usually a grid with a spacing of 15m was used. LISA was used for the interpolation of the data obtained from the image matching in order that program RASCOR could be used (RASCOR uses only raster-form data). Then LISA was handled for the interpolation of the data acquired after using RASCOR.

The interpolation was made using the option Triangulation from the program menu. This option is preferable when the reference points are fairly well distributed but relatively widely scattered. This method uses triangles to create the terrain surface. No filter was used for interpolation. The program was handled also for converting a raster-form into a vector format or vice versa and for graphical evaluation of the achieved DEMs (figures 64 and figure 65). Using the option Base image – Shading and then Block image – Raster image 3D a three-dimensional situation overview of the investigated area can be obtained. The exaggeration factor and the view direction can be chosen.

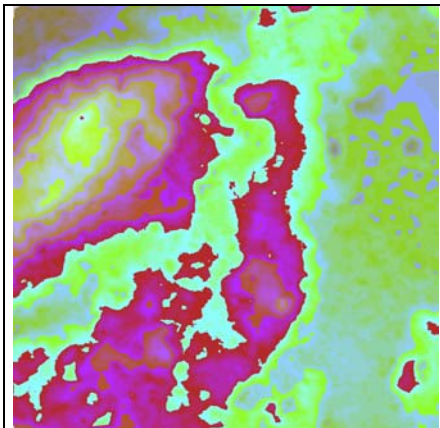


Figure 70: Colour coded DSM for test area Prien

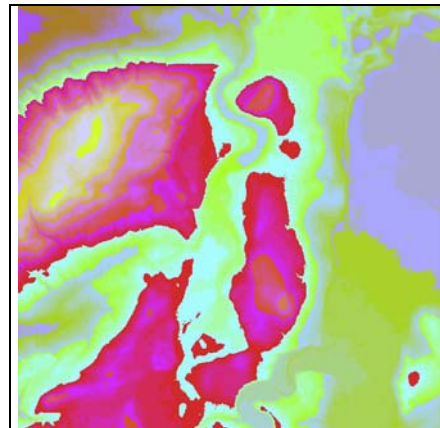


Figure 71: Colour coded DEM for test area Prien

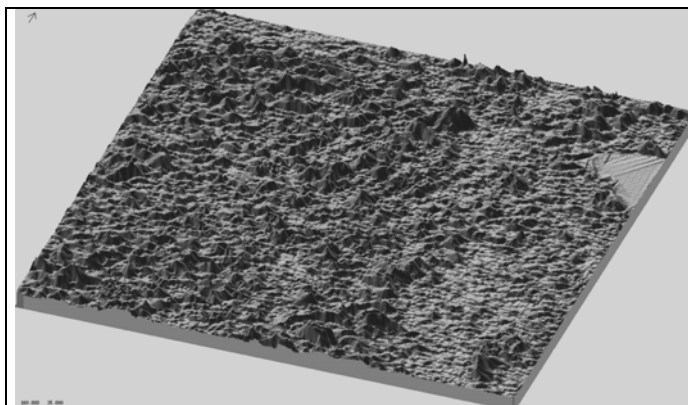


Figure 72:  
Differential DTM for test area Prien  
(difference between DSM and DEM,  
exaggeration factor: 3 times)

## 5.8. Filtering of the DSM: RASCOR

The program RASCOR (analysis, correction and plot of a DEM) can analyze, improve, smooth and interpolate a digital elevation model which may be created by automatic image matching or laser scanning (LIDAR) in an equal spacing arrangement.

RASCOR is eliminating the points which don't belong to the bare ground generating a digital elevation model. It is using a sequence of different methods for the filtering of a DSM in a raster form. The identification of points not located on the solid ground but in top of buildings or vegetation is possible by a minimal and maximal height in the area, by maximal height differences between neighbored points, by a sudden change of the height level, by a linear or polynomial interpolation in X- and Y-direction, by a minimal and maximal height difference against a local tilted plane or polynomial surface and a local prediction (least squares interpolation) based on the tilted plane or polynomial surface. The final results can be filtered (smoothened) in relation to a rotated plane or polynomial surface fitted to the neighbored. An overview of the filtering is stored in a file named situ.raw that shows the location of the remaining points.

Based on the analysis of the DSM RASCOR is establishing the procedure and the tolerance limits without user interaction. In the case of small objects or boundary of larger elements located in flat areas RASCOR is analyzing the height distribution and the height differences of neighbored points. It identifies the upper and lower limit of the accepted heights based on height distribution and the accepted limit of neighbored points depending upon the slopes and the random errors. In the case of larger buildings this method can also be used with the condition that there is no vegetation beside the buildings and the data are coming from laser scanning. Larger buildings can be identified using a moving local profile analysis.

RASCOR is using two characterizations of the area. First characterization is regarding the homogenous aspect of the area. That means an area is considered to be homogenous if the whole area has almost the same type of relief. The second characterization is referring to the type of terrain: flat, rolling or mountainous. This information is useful because the program is using specific methods depending on the terrain type.

A filtered DEM has type I errors (points belonging to the bare terrain and removed) and type II errors (points not belonging to the terrain but kept). These errors appear regardless of the type of terrain, terrain cover, photo scale, grid size. Filtered DEMs of flat terrains with high point density do have a negligible number of type I and type II errors.

RASCOR was used for the digital surface model filtering of the test area Chiemsee. Five of the six test sub-areas (Prien, Gars, Peterskirchen, Taching, Vilsbiburg) have flat up to rolling type of terrain and one has mountainous relief (Inzell). Each of the mentioned five areas was tested using four iterations in the following cases considering:

1. the terrain is rolling and has a homogenous character (rolling, same type of terrain);
2. the terrain is rolling and it has not a homogenous character because a part of it is flat (rolling, varying type of terrain);
3. the terrain is flat and has a homogenous character (flat, same type of terrain);
4. the terrain is flat and it has not a homogenous character because a part of it is rolling (flat, varying type of terrain),

Test area Inzell was tested in two cases: in one it is considered to have a uniform mountainous type of terrain (mountainous, same type of terrain) and in the other a not homogenous character (mountainous, varying type of terrain). For the analysis also four iterations were used.

### 5.9. Other Programs

Other programs had been used during the analysis process of the digital elevation model. IMASK (creation image mask and quality map overlay of image and image points, representation of correlation coefficient as gray value) was used for creating an overview image of the image matching situation. Managing this program, quality maps were made for the image matching at every first pixel for test areas Prien and Gars.

A height model can be shifted or it might have a difference in scale compared to the reference DEM. Program MANI (manipulation of object coordinates, image orientations, pixel addresses) was used for an approximately shift of the achieved digital elevation model against the reference DEM. The program was handled for the test areas Prien and Gars in the case of the image matching at every first pixel. A precise shift was achieved using the program DEMSHIFT.

BLTRA (transformation of national net, geographic and geocentric coordinates or image orientation) was used in different situations like, for example, transformation from geographic coordinates to Gauss-Krueger coordinates using the WGS84 ellipsoid in the case of handling INSAR-SRTM data.

## 6. RESULTS

### 6.1. Image Orientation

The image orientation has been done before and is not part of this project. The results below are published in the paper “DEM Generation by SPOT HRS” by K. Jacobsen 2004, Institute of Photogrammetry and Geoinformation, University of Hannover, Germany.

The root mean square discrepancies (figure 73 and figure 74) at the control points after the image orientation are presented in Table 2. The results are similar in the two models.

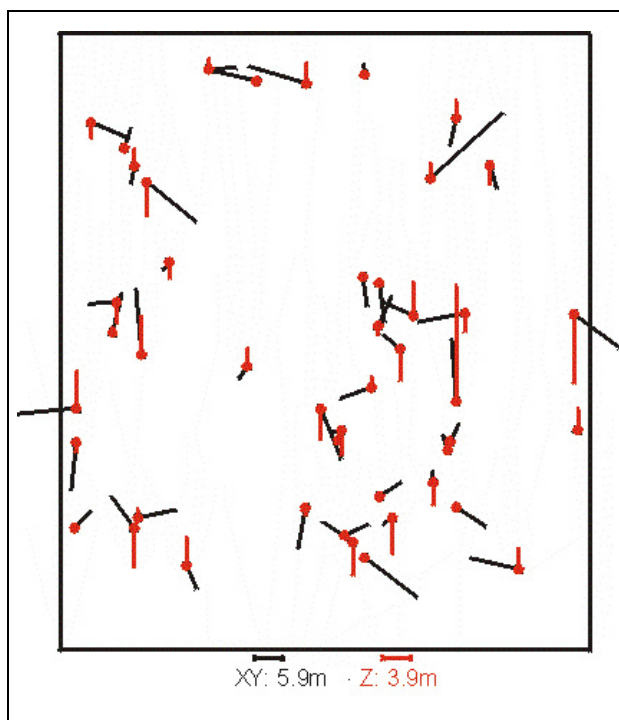


Figure 73: Discrepancies at control points, vertical vectors (red) = DZ (southern model)

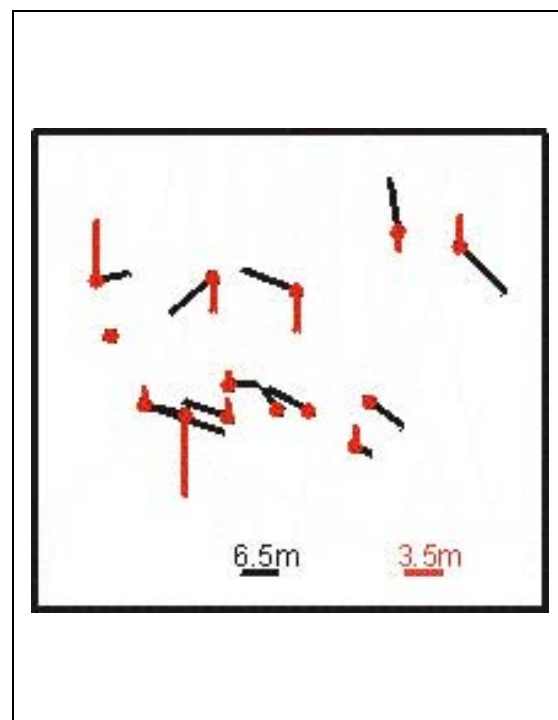


Figure 74: Discrepancies at control points, vertical vectors = DZ (northern model)

	SX [m]	SY [m]	SZ [m]
Southern model	6.0	5.8	3.9
Northern model	7.7	5.0	3.5

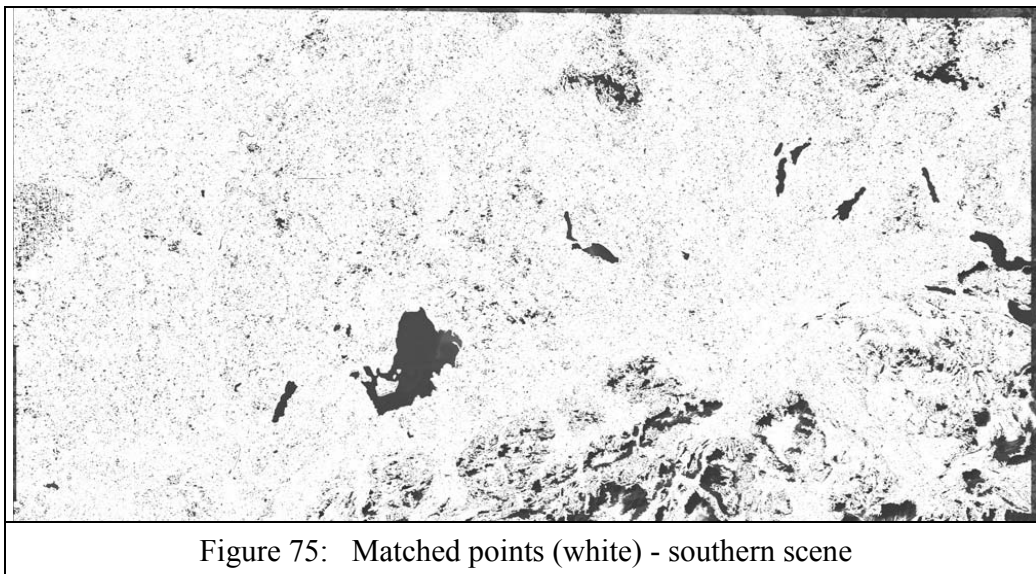
Table 2: Discrepancies at the control points (southern and northern model)

The results of the image orientation are considered to be sufficient whereas the identification of the control points was made manually. The discrepancies in X and Y are influenced by problems of the point identification in the images. In the case of heights, the

results are better and demonstrate that the HRS system has a higher accuracy potential. The vertical accuracy corresponds to a standard deviation of the x-parallax of 0.6 pixels.

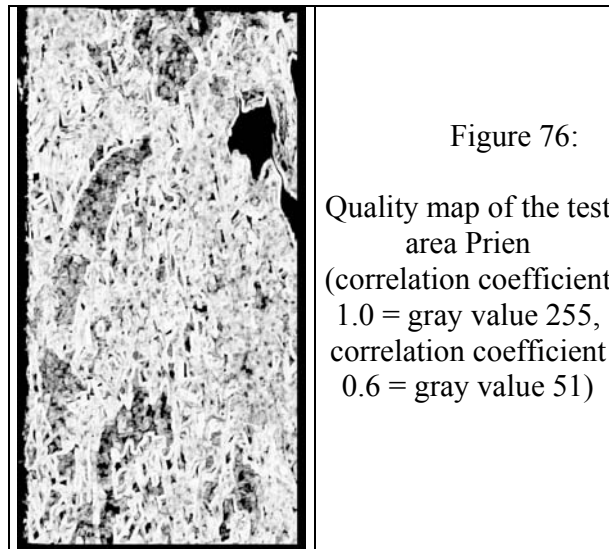
## 6.2. Image Matching

1. In the southern model 85% to 90% of the possible points have been matched with a correlation coefficient exceeding 0.6 (figure 75). The quality map of the image matching shows that distribution of matched points and the gaps in the image matching. In the figure below the dark spot from the center represents the lake Chiemsee and the other dark parts are also lakes or forests.



The root mean square y-parallax error has values between 4.67m and 7.11m with a mean value of 6.0m corresponding to 0.6 pixel (pixel size in y-direction is 10m).

2. In the test area Prien for approximately 7% of the points the matching was not possible (almost 2.5% are points not matched and 4.5% are points matched incorrectly). In the test area Prien 94% of the possible points have been matched with a correlation coefficient exceeding 0.6 (figure 70). In the figure below the dark spot from the upper right represents a lake and the other dark parts are forests areas. In the case of test area Gars for approximately 10% of the points the matching was not possible (almost 4% are points not matched and 6% are points matched incorrectly). In the test area Gars the same percentage of 94% possible points have been matched with a correlation coefficient exceeding 0.6.



The results obtained in these two cases were analyzed. A comparative study regarding the accuracy of the DEM achieved by using image matching at every third pixel and at every pixel is presented below. The analyzed test areas are Prien (figure 77) and Gars (figure 78) and the analysis was made separately for open area and forest. An overview of the results is shown in figure 79. Then a comparison between Prien and Gars was made (figure 80). The results of analysis in the case of interpolated data with LISA using 2 iterations from RASCOR (case 27) are shown in Table 3.

Test area	Layer	RMSZ		MEAN DZ		RMSZ WITHOUT SYST. PART		SZ				Z*			
								a		b		m		n	
		3 Pixels	1 Pixel	3 Pixels	1 Pixel	3 Pixels	1 Pixel	3 Pixels	1 Pixel	3 Pixels	1 Pixel	3 Pixels	1 Pixel		
Prien	open area	4.83	5.68	-1.01	-0.85	4.72	5.62	4.58	1.990	5.38	2.450	-1.09	0.00031	-1.52	0.00135
	forest	9.51	9.99	-0.99	-0.64	9.46	9.97	8.53	4.625	9.11	4.447	-3.20	0.00464	-3.07	0.00479
Gars	open area	5.84	6.47	-0.35	-0.36	5.83	6.46	5.34	2.110	6.04	1.885	0.43	-0.00158	0.21	-0.0008
	forest	10.15	10.69	0.07	0.25	10.15	10.69	8.97	3.344	9.19	4.560	-1.01	0.00227	2.68	-0.0046

Table 3: Results of height model analysis in the case of test areas Prien and Gars using every third pixel and every pixel for image matching

In Table 3 the discrepancies SZ are calculated using formula (5) and Z\* using formula (6) where m represents the shift and n the scale of the height model.

$$SZ = a + b \cdot \tan \alpha \quad (5)$$

$$Z^* = m + n \cdot Z \quad (6)$$

- 1 reference data and matched points (DSM)
- 2-5 reference data and 1-4 iterations data from RASCOR (same type of terrain: rolling)
- 6-9 reference data and 1-4 iterations data from RASCOR (varying type of terrain: rolling)
- 10-13 reference data and 1-4 iterations data from RASCOR (same type of terrain: flat)
- 14-17 reference data and 1-4 iterations data from RASCOR (varying type of terrain: flat)
- 18-21 reference data and interpolated data with Lisa using 1-4 iterations from RASCOR (same type of terrain: rolling)
- 22-25 reference data and interpolated data with LISA using 1-4 iterations from RASCOR

- (varying type of terrain: rolling)
- 26–29 reference data and interpolated data with LISA using 1-4 iterations from RASCOR (same type of terrain: flat)
- 30–33 reference data and interpolated data with LISA using 1-4 iterations from RASCOR (varying type of terrain: flat)

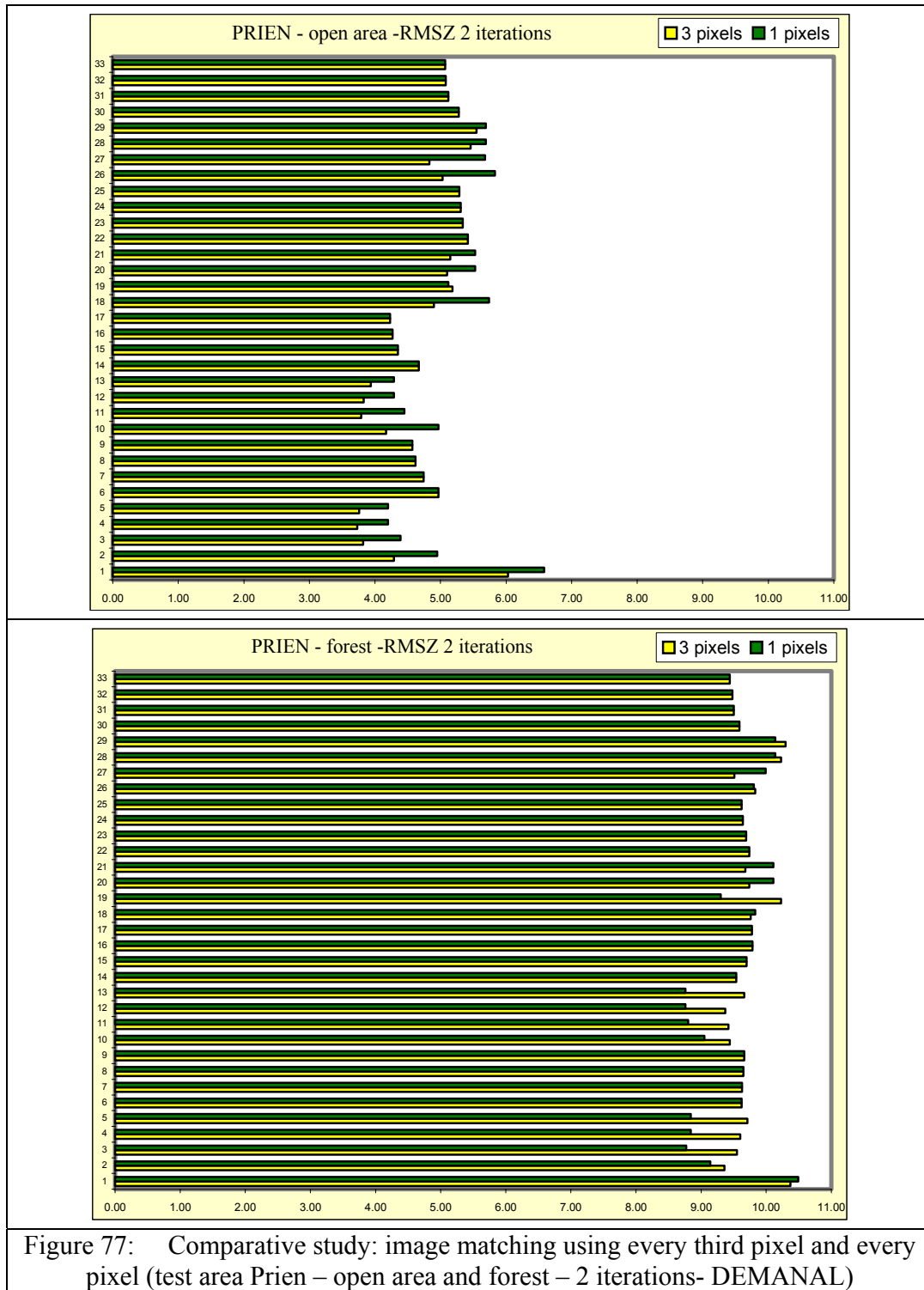


Figure 77: Comparative study: image matching using every third pixel and every pixel (test area Prien – open area and forest – 2 iterations- DEMANAL)

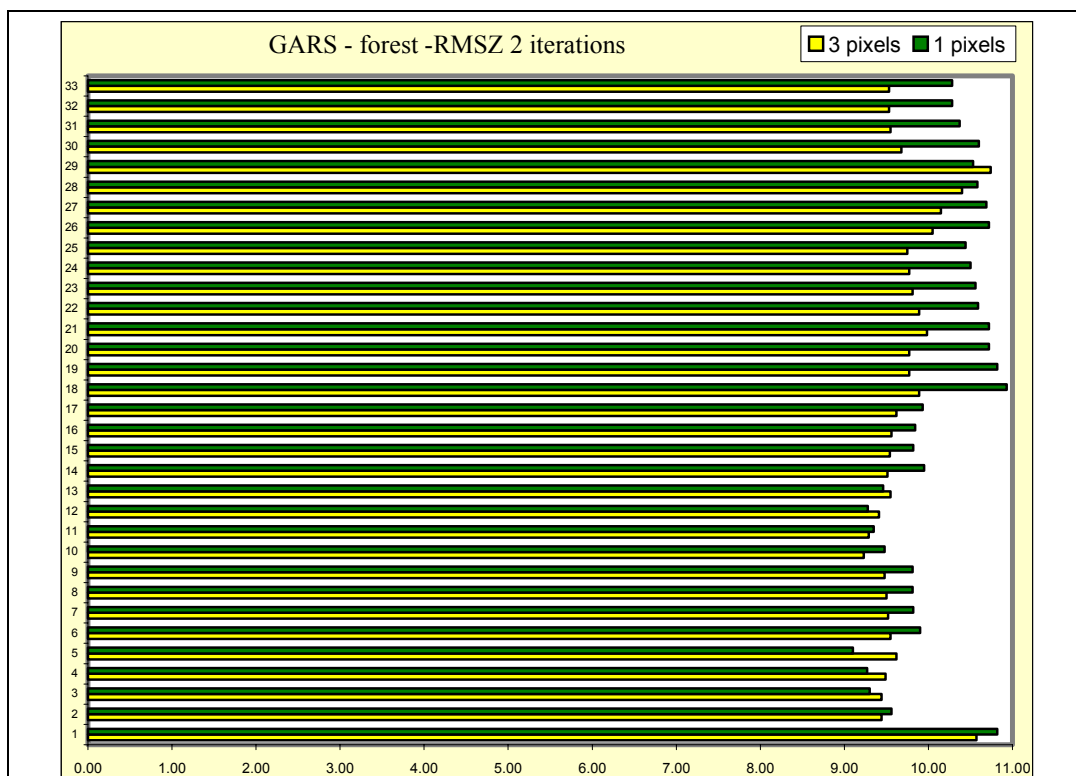
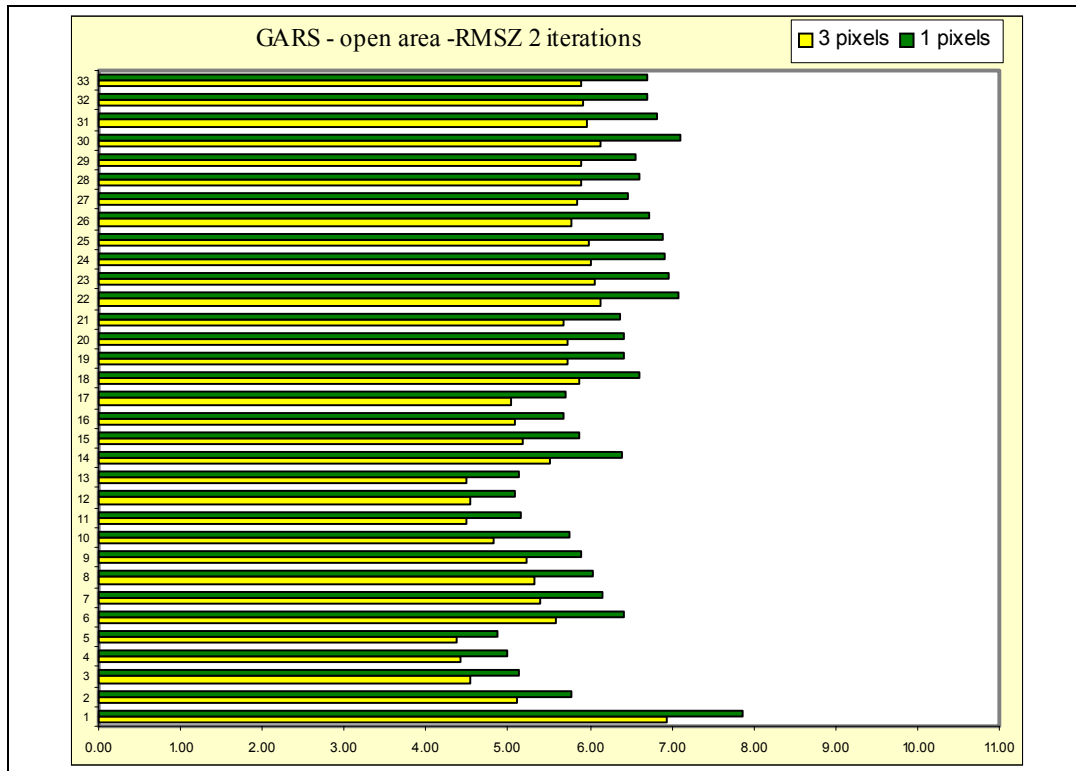


Figure 78: Comparative study: image matching using every third pixel and every pixel (test area Gars – open area and forest – 2 iterations - DEMANAL)

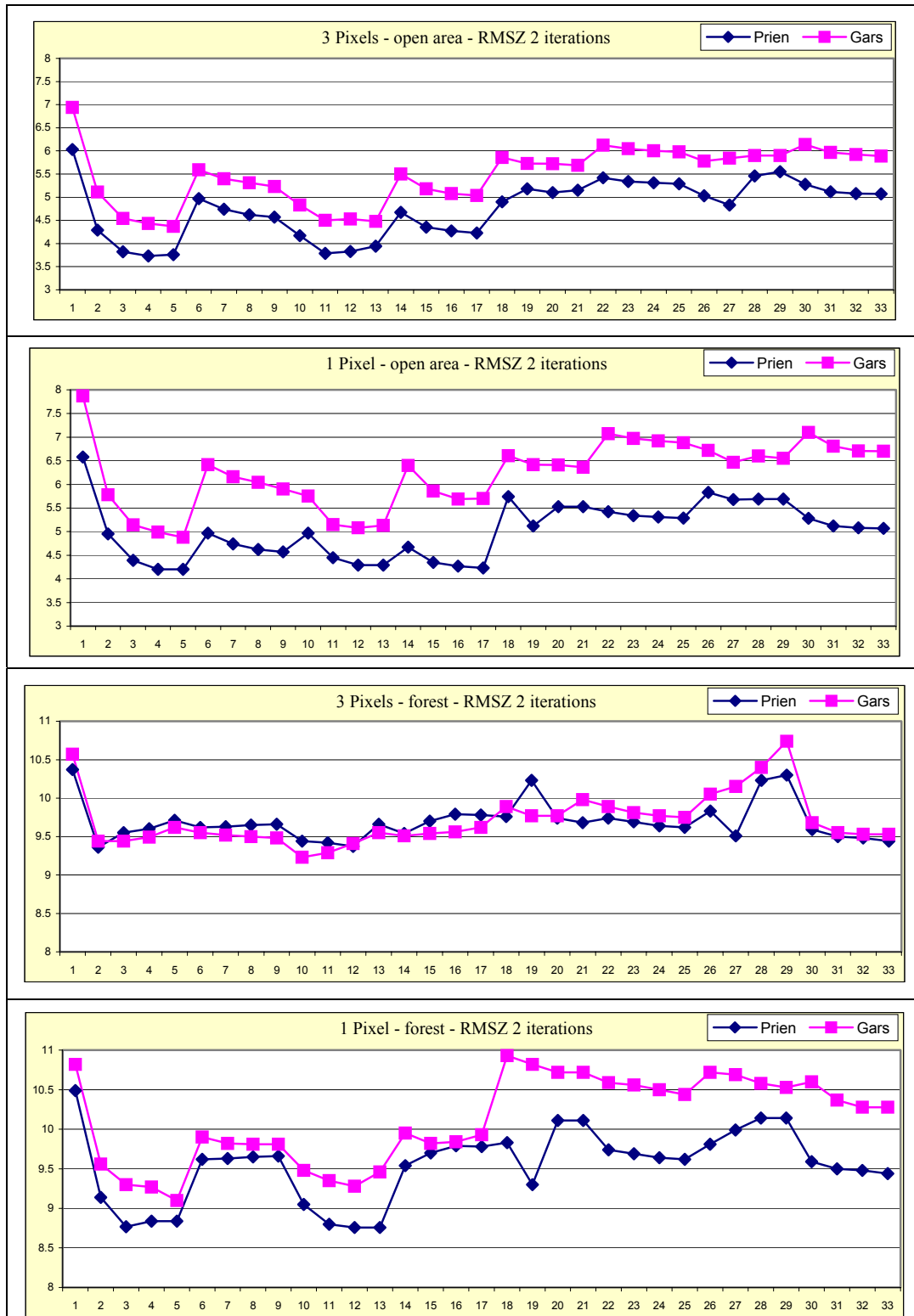
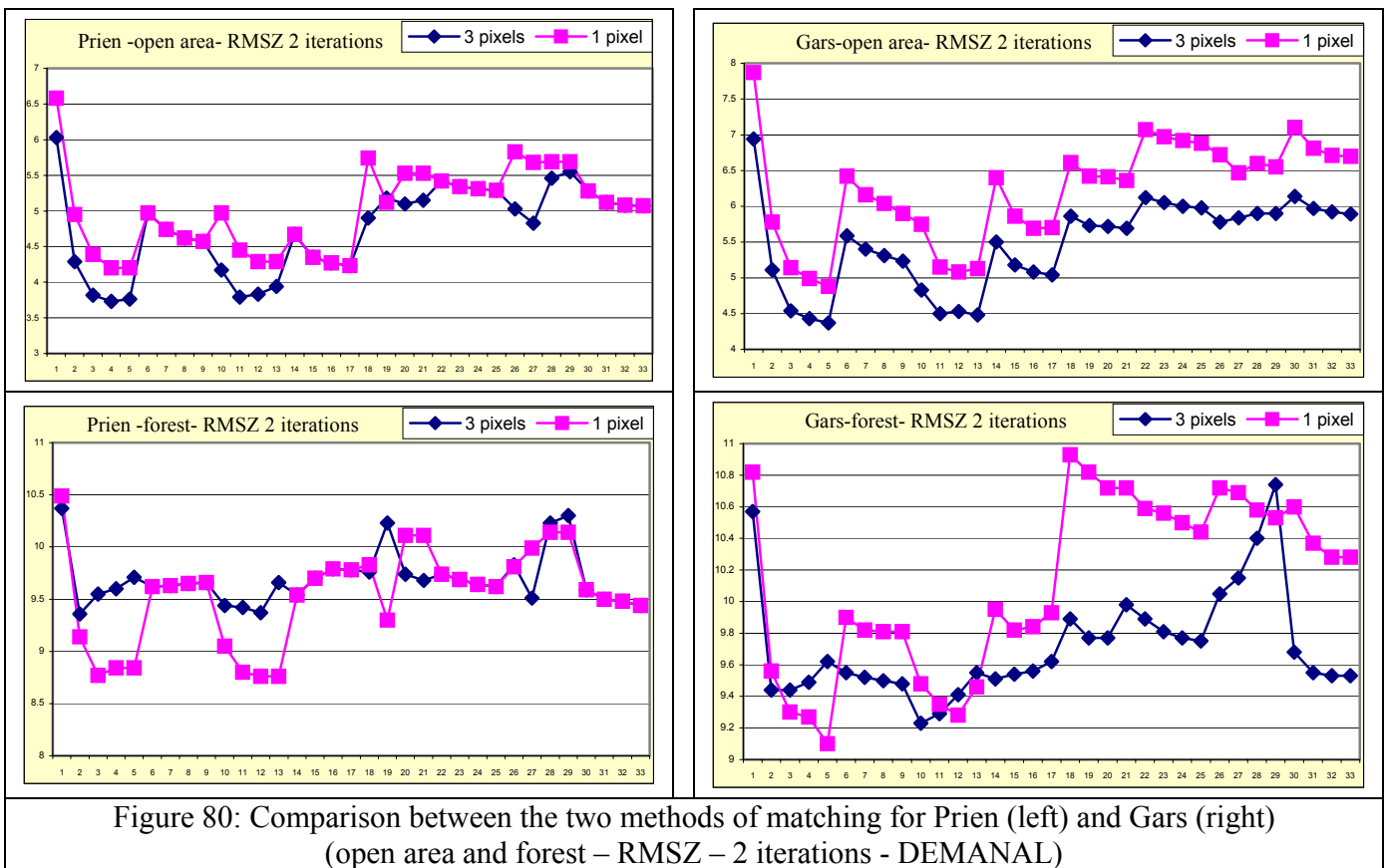


Figure 79: Comparative study: image matching using every third pixel and every pixel (Prien -Gars – open area and forest– 2 iterations - DEMANAL)



The image matching of the SPOT HRS stereo models for every third pixel has similar results even better like the automatic image matching for every pixel. The image matching for every first pixel has the disadvantage that the volume of data is bigger, that means the handling of the data is more difficult and takes more time. The results using this method are no better than in the case of three pixels (figure 75). For test area Prien the results of the analysis are the same in some cases using both methods. In the case of Gars the values for RMSZ are higher using every pixel than every third pixel in most of the case. The conclusion is, the automatic image matching for every pixel does not lead to a better accuracy, the matching is more time consuming and the file size will be enlarged.

### 6.3. Prien

For the generation and analysis of the DEM of the area Prien, data from SPOT HRS and SRTM InSAR had been used. The achieved results are shown in the following table (Table 4). The values of the HRS-DEM from table 4 were achieved considering that the test area has a homogenous flat character, filtering the data by RASCOR using two iterations and interpolating the results by LISA with a grid spacing of 15m. Diagrams for comparison of the results achieved are presented in figure 81. The results acquired in test area Prien using one to four iterations from RASCOR and considering that the area has the same type or varying type of terrain, rolling or flat are presented in figure 82.

Digital Height Model	Test area	RMSZ	MEAN DZ	RMSZ without bias	SZ	Z*
DSM	all points	8.73	0.12	8.73	$7.77 + 6.165 * \tan \alpha$	$-0.76 + 0.00195 * Z$
	open area	6.03	-0.27	6.02	$5.64 + 2.695 * \tan \alpha$	$-2.11 + 0.00351 * Z$
	forest	10.37	0.08	10.37	$9.83 + 1.731 * \tan \alpha$	$-3.74 + 0.00713 * Z$
DEM (HRS)	all points	6.75	-0.70	6.72	$5.74 + 7.144 * \tan \alpha$	$-4.54 + 0.00745 * Z$
	open area	4.83	-1.01	4.72	$4.58 + 1.990 * \tan \alpha$	$-1.09 + 0.00031 * Z$
	forest	9.51	-0.99	9.46	$8.53 + 4.625 * \tan \alpha$	$-3.20 + 0.00464 * Z$
DEM (INSAR)	all points	6.77	1.05	6.69	$6.22 + 3.892 * \tan \alpha$	$-0.64 + 0.00295 * Z$
	open area	4.14	0.34	4.13	$3.55 + 3.061 * \tan \alpha$	$-0.02 + 0.00063 * Z$
	forest	6.96	0.61	6.94	$6.93 - 1.217 * \tan \alpha$	$0.62 - 0.00084 * Z$

Table 4: Results for test area Prien (DSM, DEM-HRS, DEM-INSAR)

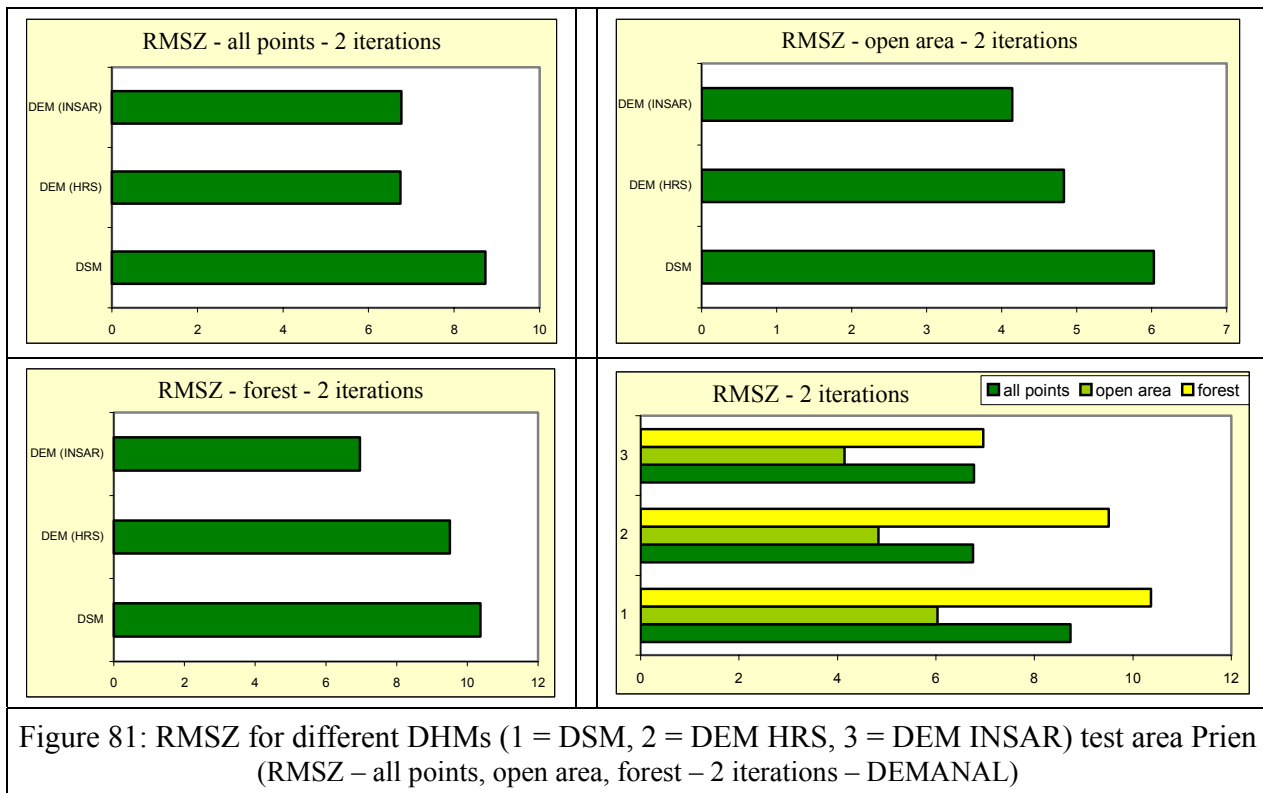


Figure 81: RMSZ for different DHMs (1 = DSM, 2 = DEM HRS, 3 = DEM INSAR) test area Prien (RMSZ – all points, open area, forest – 2 iterations – DEMANAL)

The results achieved by means of INSAR SRTM are better in both cases (open area and forest) than the results obtained using SPOT HRS images. In open area the difference is 0.69m and in forest 2.55m, but nevertheless the spacing of just 3 “ of the SRTM data leads to a loss of details.

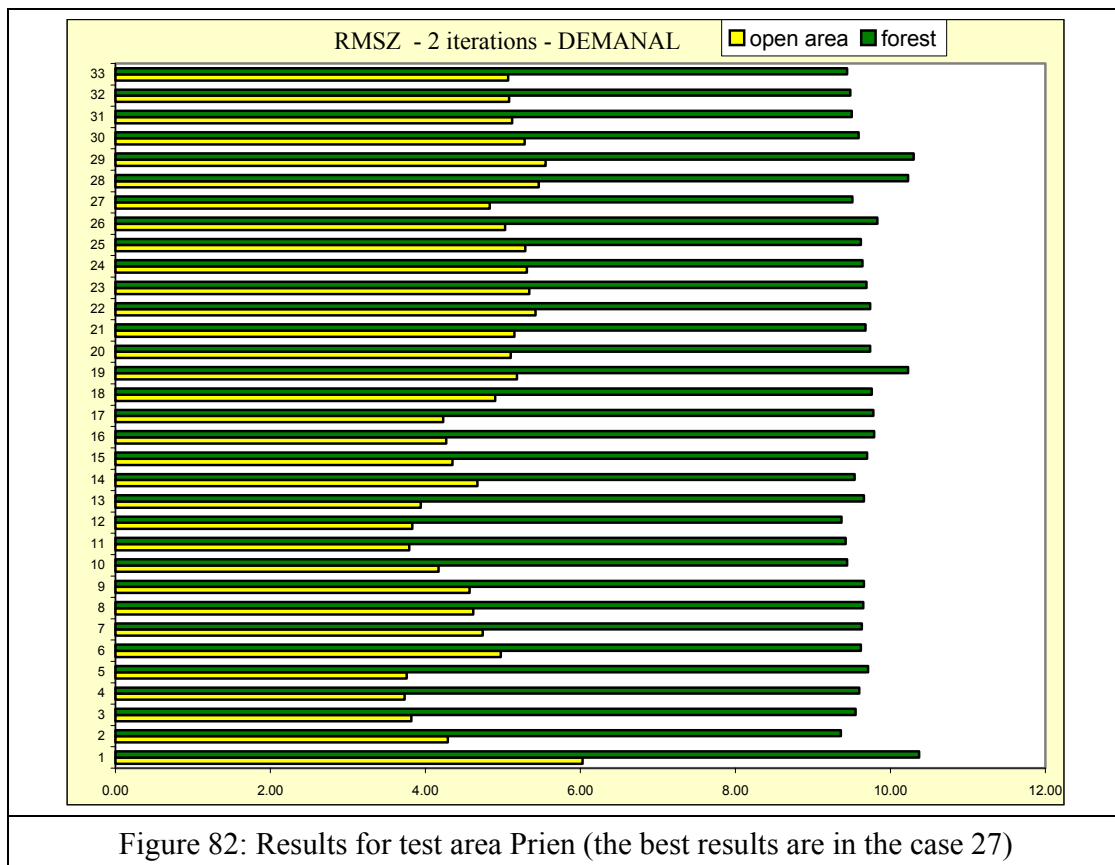
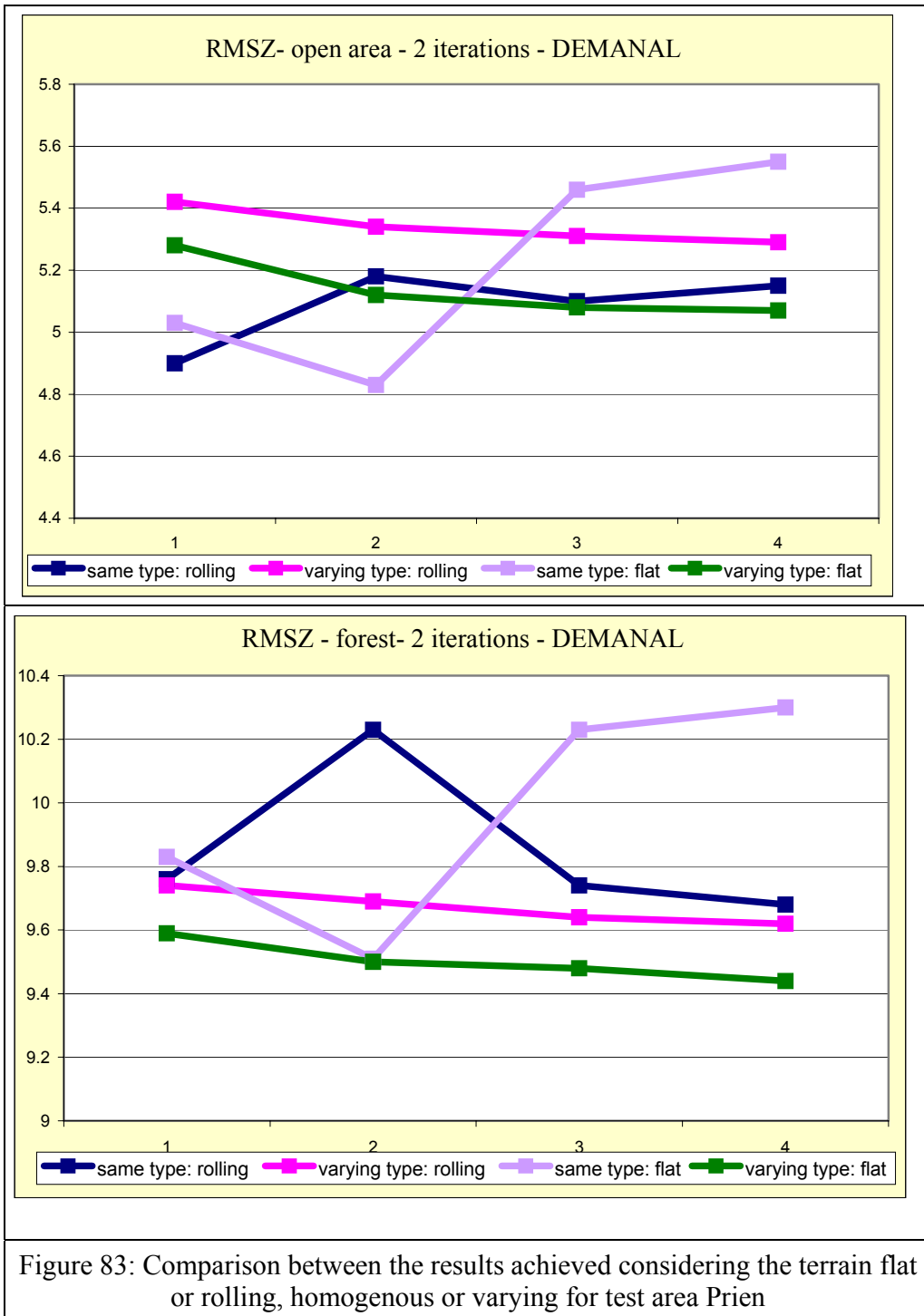
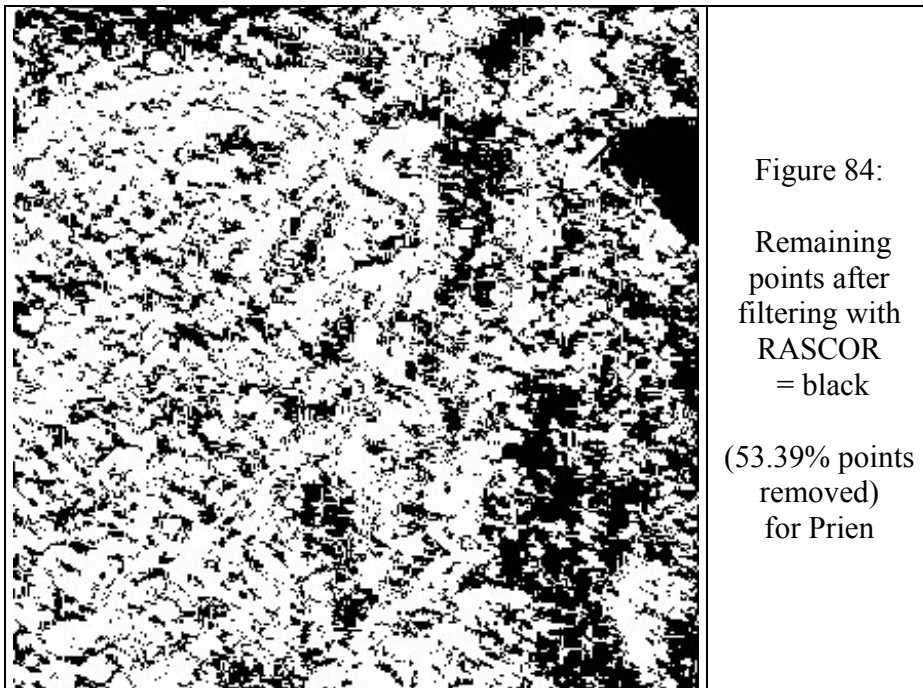


Figure 82: Results for test area Prien (the best results are in the case 27)

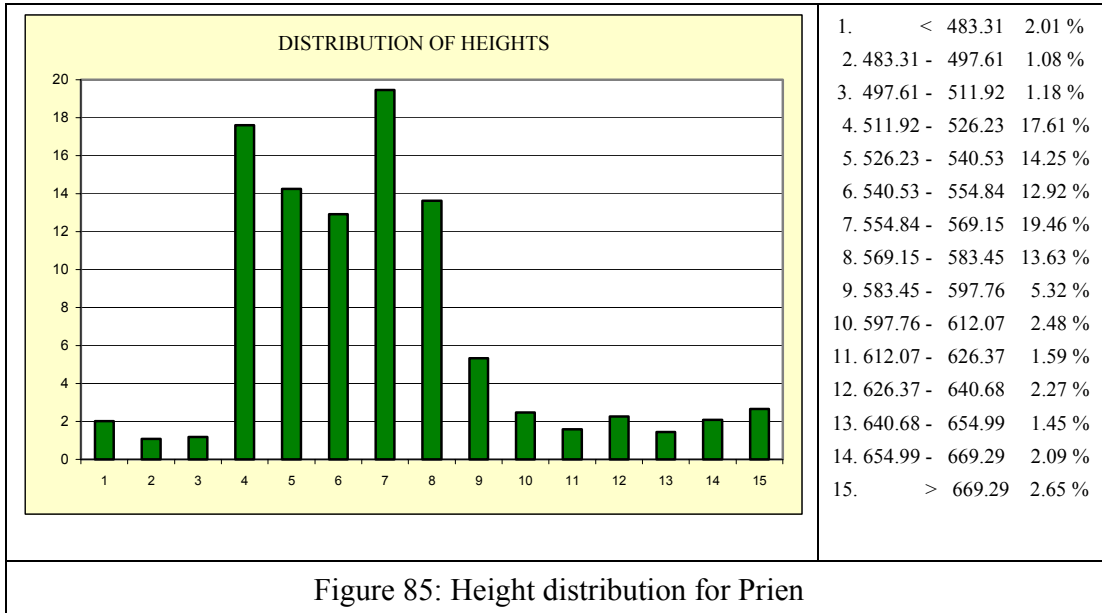
The analysis of the results regarding only the cases that represent interpolated data by LISA reveals the fact that good results can be achieved especially in forest areas if the terrain is considered to have a varying flat character. The results are getting better and better using more and more iterations from RASCOR. The trend in this situation is similar with the one in the case of considering the terrain varying and rolling. But the character of the terrain for test area Prien is flat up to rolling; that means it is mainly flat. The best results were achieved using just two iterations from RASCOR and considering the area has a homogenous flat terrain. Using three or four iterations from RASCOR the results are getting worst. A comparison of the results achieved is shown in figure 83. The X axis represents the number of iterations.

RASCOR removed 22.84% of the points in the first iteration and 53.39% in the second. The situation of the remaining points is shown in figure 84.

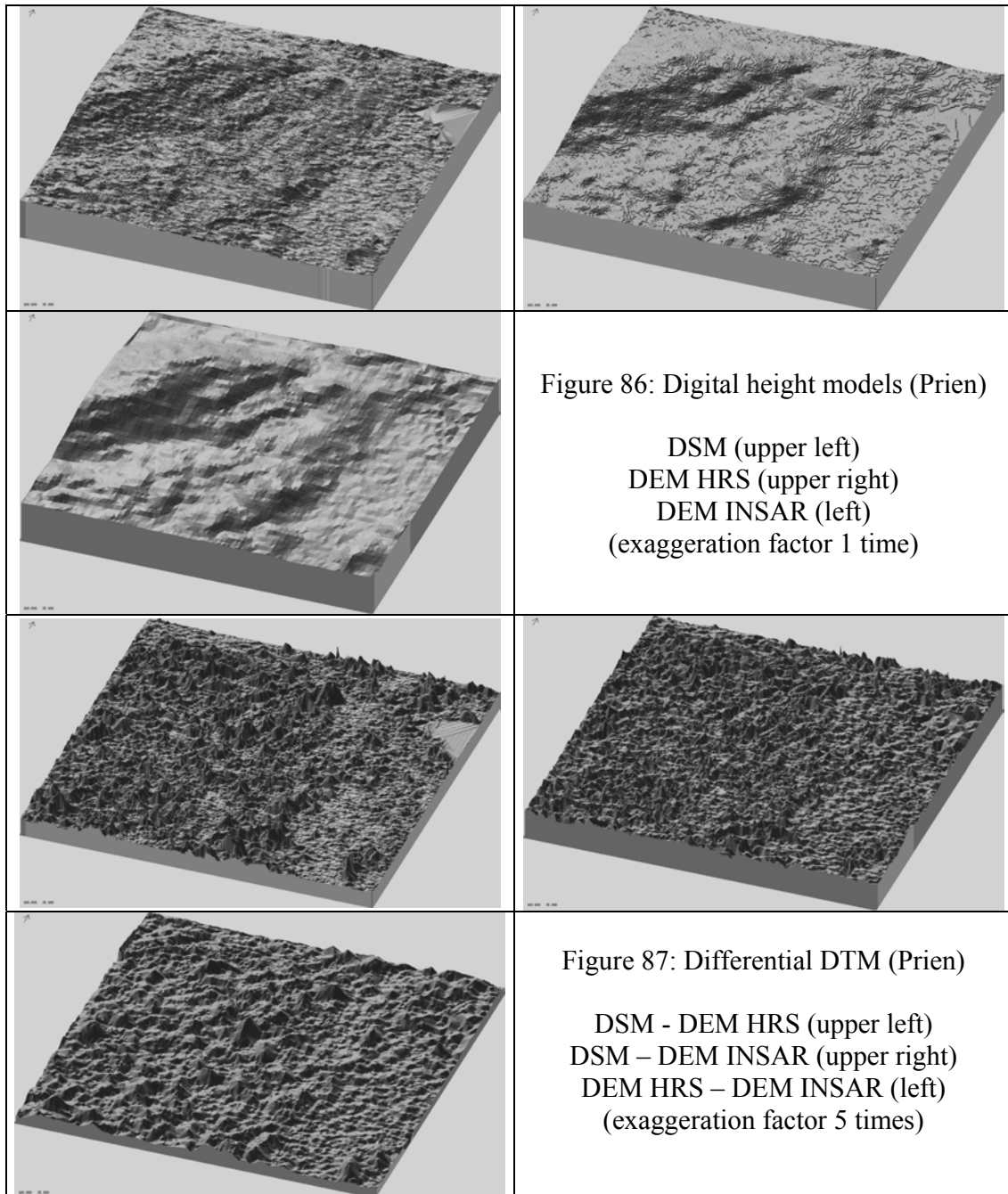




The distribution of heights for Prien, 1001877 points (figure 85):



A view of the three-dimensional shaded presentation of the digital height models (DSM, DEM HRS, DEM INSAR) is presented next (figure 86). The difference between the achieved digital height models is shown in figure 87.



#### 6.4. Gars

The generation and analysis of the DEM for area Gars was made just with SPOT HRS data. The results that have been achieved are presented in Table 5 and the comparison between them in figure 88. In test area Gars the terrain has an homogenous flat character; the results from table 5 represent the filtered DSM using two iterations from RASCOR and

interpolated the results by LISA with a grid with the spacing of 15m. RASCOR removed 23.83% points in the first iteration and 55.91% in the second (figure 89). The results obtained for Gars are presented in figure 90.

Digital Height Model	Test area	RMSZ	MEAN DZ	RMSZ without bias	SZ	Z*
DSM	all points	9.10	-0.72	9.07	$7.81 + 6.780 * \tan \alpha$	$1.04 - 0.00244 * Z$
	open area	6.94	-0.49	6.92	$6.38 + 2.165 * \tan \alpha$	$0.36 - 0.00135 * Z$
	forest	10.57	-0.29	10.57	$9.90 + 2.219 * \tan \alpha$	$-5.72 + 0.01086 * Z$
DEM (HRS)	all points	7.75	-0.59	7.73	$6.61 + 6.630 * \tan \alpha$	$0.35 - 0.00089 * Z$
	open area	5.84	-0.35	5.83	$5.34 + 2.110 * \tan \alpha$	$0.43 - 0.00158 * Z$
	forest	10.15	0.07	10.15	$8.97 + 3.344 * \tan \alpha$	$-1.01 + 0.00227 * Z$

Table 5: Results for test area Gars (DSM, DEM HRS)

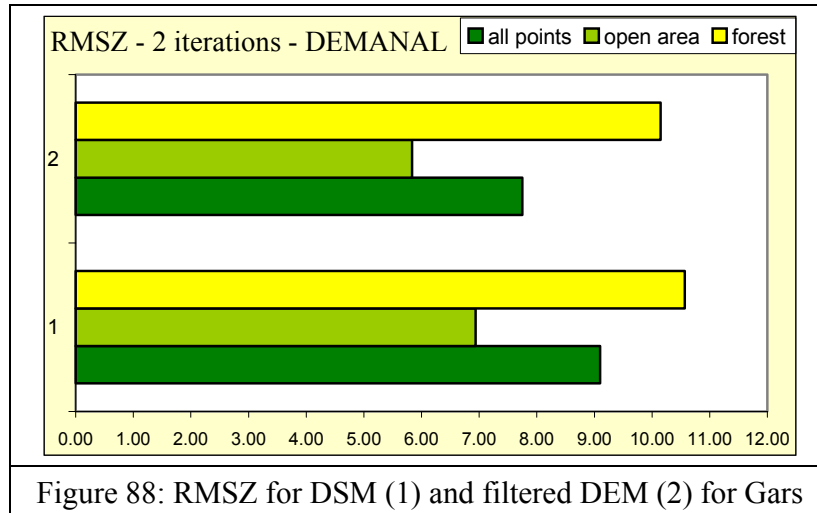
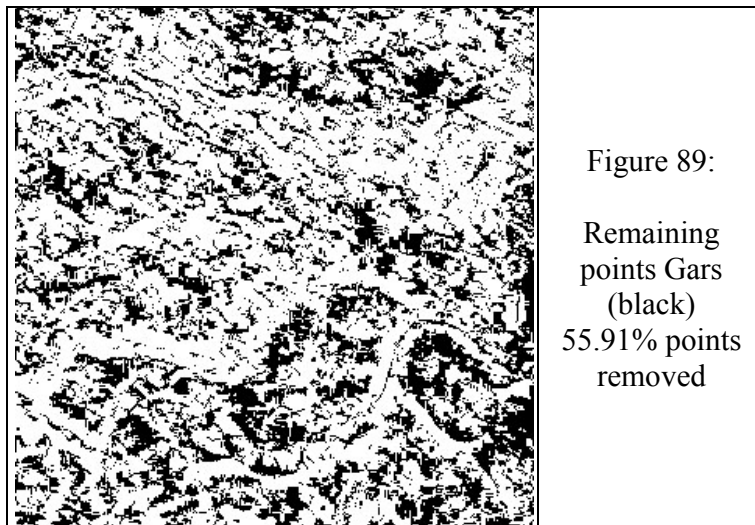


Figure 88: RMSZ for DSM (1) and filtered DEM (2) for Gars



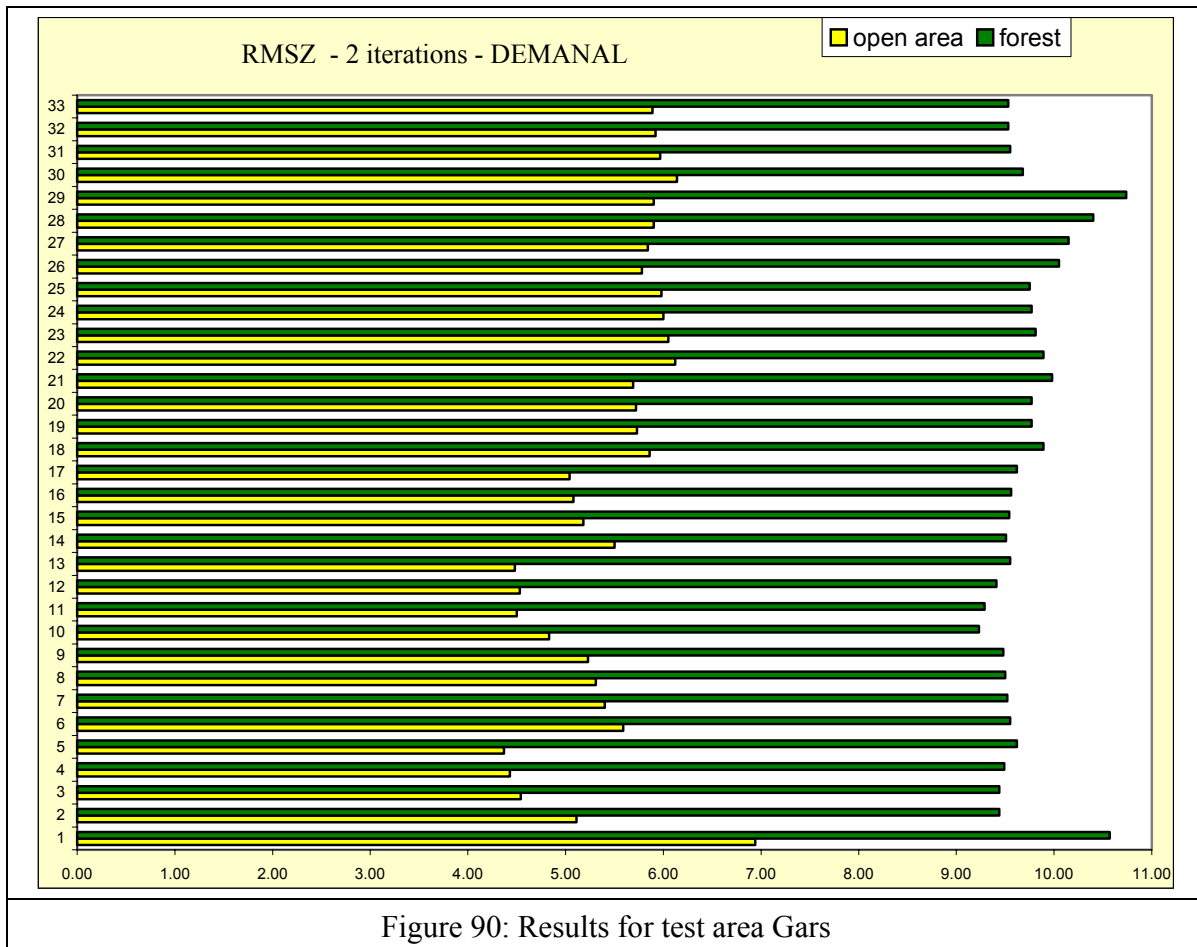
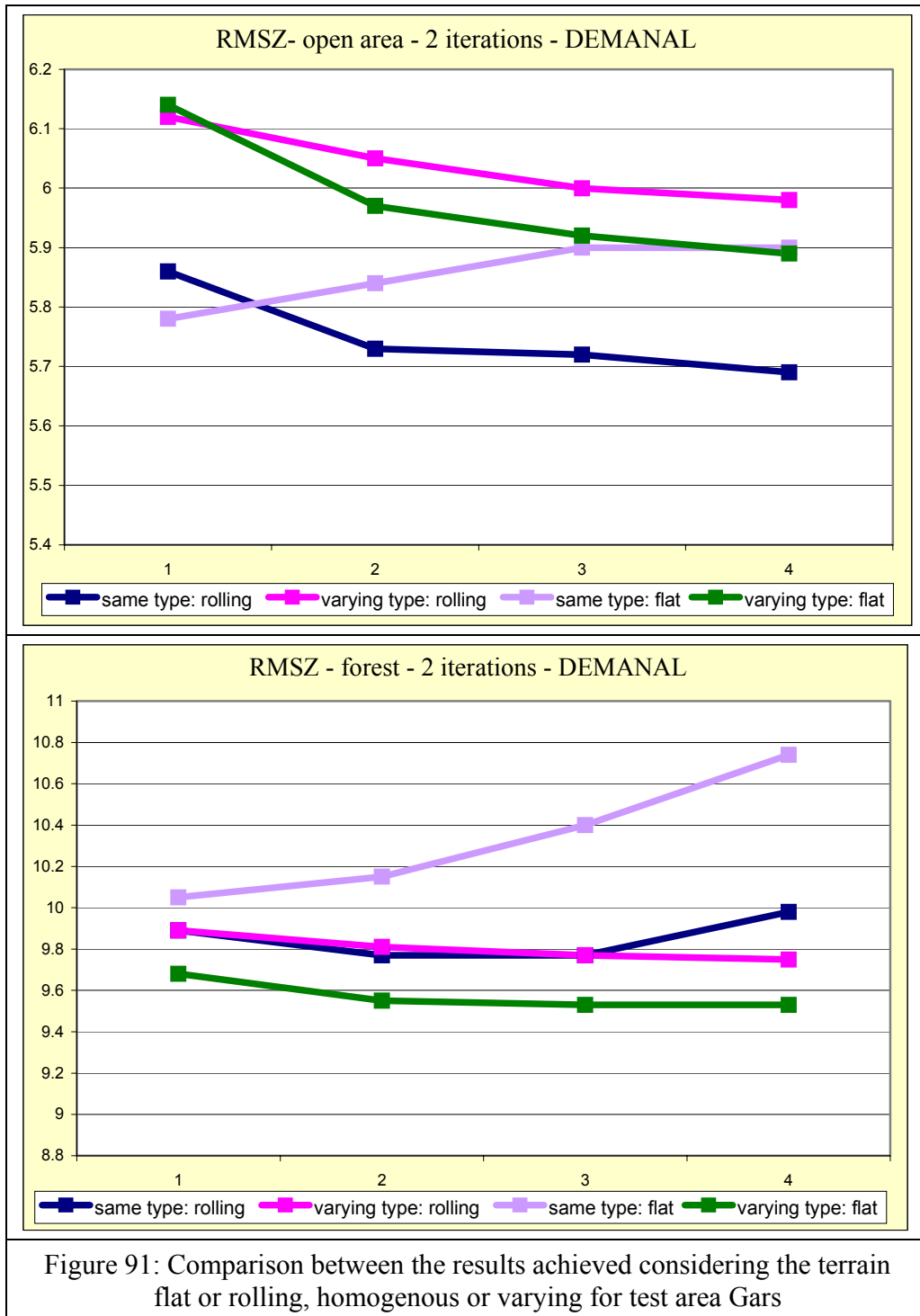
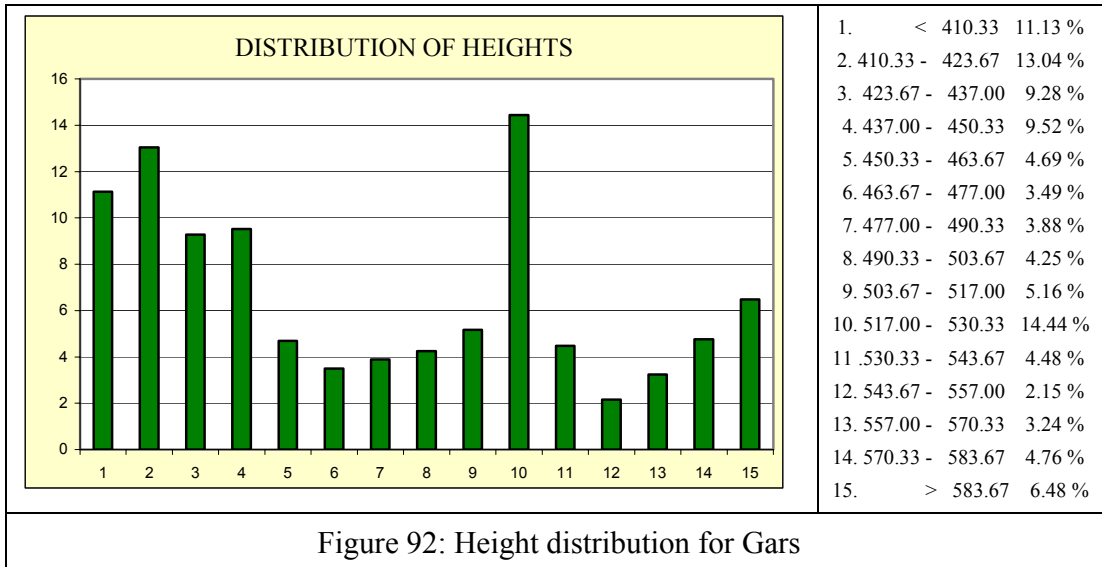


Figure 90: Results for test area Gars

The analysis of the results is regarding only the cases that represent interpolated data by LISA. In open area good results were obtained by considering the area with a homogenous rolling character. But because the area is mainly flat this case shouldn't be taken into consideration. Considering the terrain flat the results show that one iteration is enough in the case of homogenous character nevertheless four iterations can be used if the terrain is considering as varying. For forest the results are good for the case of a flat varying terrain. It can be noticed that there is no significant difference between the second and the third or fourth iteration. The trend is similar with the case of varying rolling type of terrain but the values are smaller. Like in open areas one iteration for homogeneous flat terrain has better results than two, three or four iterations from RASCOR. A comparison of the results achieved is shown in figure 91. The X-axis represents the number of iterations.



The distribution of heights for Gars, 978433 points (figure 92):



A view of the three-dimensional shaded presentation of the digital height models (DSM, DEM HRS) is presented next (figure 93). The difference between the achieved digital height models is presented in figure 94.

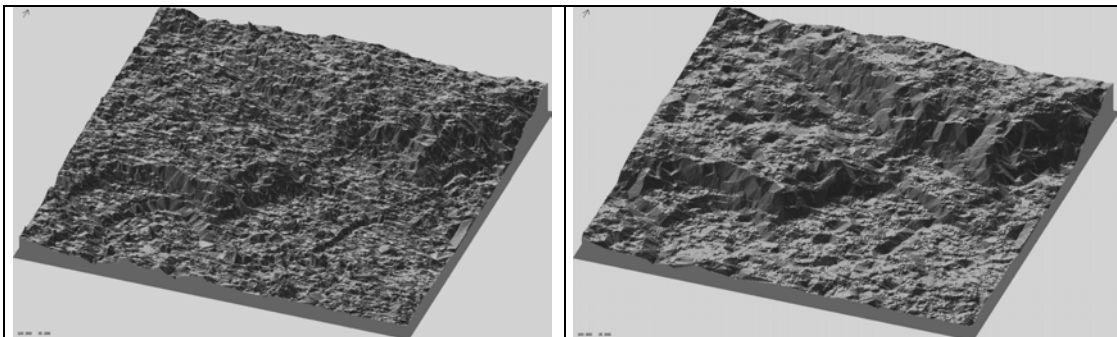


Figure 93: DSM (left) and filtered DSM (DEM) – exaggeration factor 2 times (Gars)

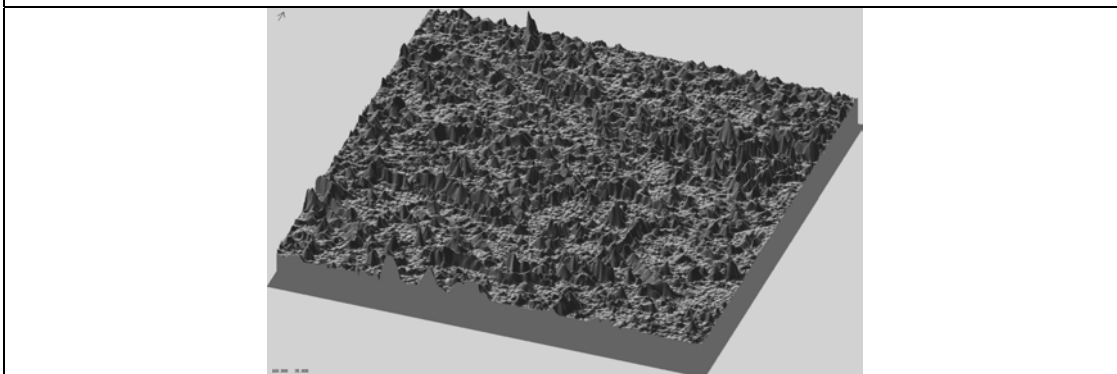


Figure 94: Differential DEM (exaggeration factor 5 times) - Gars

### 6.5. Peterskirchen

Similar like in the case of test area Gars, the generation and analysis of the DEM is made handling data from SPOT HRS. The results obtained are shown in Table 6 were acquired considering that the test area has an homogenous flat character and using in this case the filtering by RASCOR with two or three iterations and interpolating the results with LISA with a grid spacing of 15m. Diagrams for comparison of the results are presented in figure 95. RASCOR removed 25.27% points in the first iteration, 57.64% in the second and 65.34% in the third (figure 96). Figure 97 shows the results for this test area.

Digital Height Model	Test area	RMSZ	MEAN DZ	RMSZ without bias	SZ	Z*
DSM	all points	7.59	-0.34	7.58	$7.25 + 4.614 * \tan \alpha$	$1.11 - 0.00249 * Z$
	open area	5.91	-0.18	5.91	$5.85 - 0.522 * \tan \alpha$	$0.05 - 0.00028 * Z$
	forest	9.18	0.09	9.18	$8.88 + 1.940 * \tan \alpha$	$-10.02 + 0.01970 * Z$
DEM HRS (2 iter.)	all points	5.11	-0.38	5.09	$4.97 + 2.090 * \tan \alpha$	$1.56 - 0.00369 * Z$
	open area	4.31	-0.27	4.30	$4.32 - 1.026 * \tan \alpha$	$0.78 - 0.00209 * Z$
	forest	6.81	-0.37	6.80	$6.81 + 1.136 * \tan \alpha$	$-0.79 + 0.00104 * Z$
DEM HRS (3 iter.)	all points	5.20	-0.40	5.18	$5.07 + 2.029 * \tan \alpha$	$0.89 - 0.00239 * Z$
	open area	4.50	-0.30	4.49	$4.50 - 0.748 * \tan \alpha$	$1.91 - 0.00443 * Z$
	forest	6.71	-0.37	6.70	$6.66 + 1.483 * \tan \alpha$	$2.63 - 0.00577 * Z$

Table 6: Results for test area Peterskirchen (DSM, DEM HRS)



Figure 95: RMSZ for different DHMs (1=DSM, 2,3=DEM HRS 2 and 3 iterations) Petersk. DEMANAL

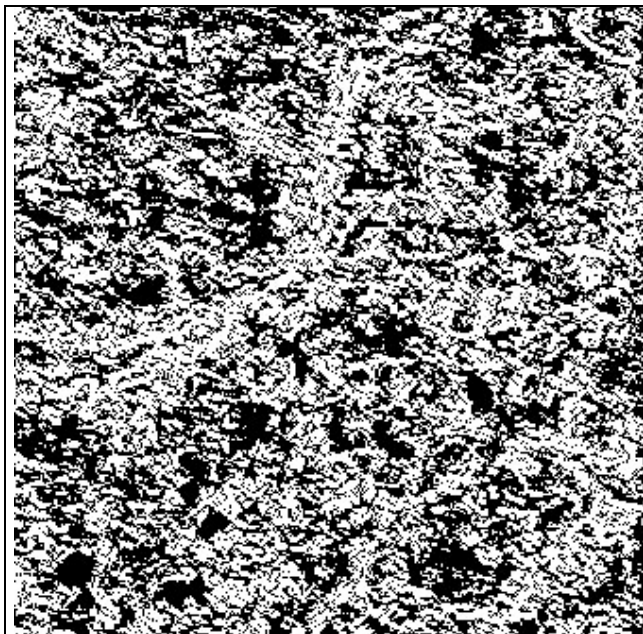


Figure 96: Remaining points (black)  
(57.64% points removed)

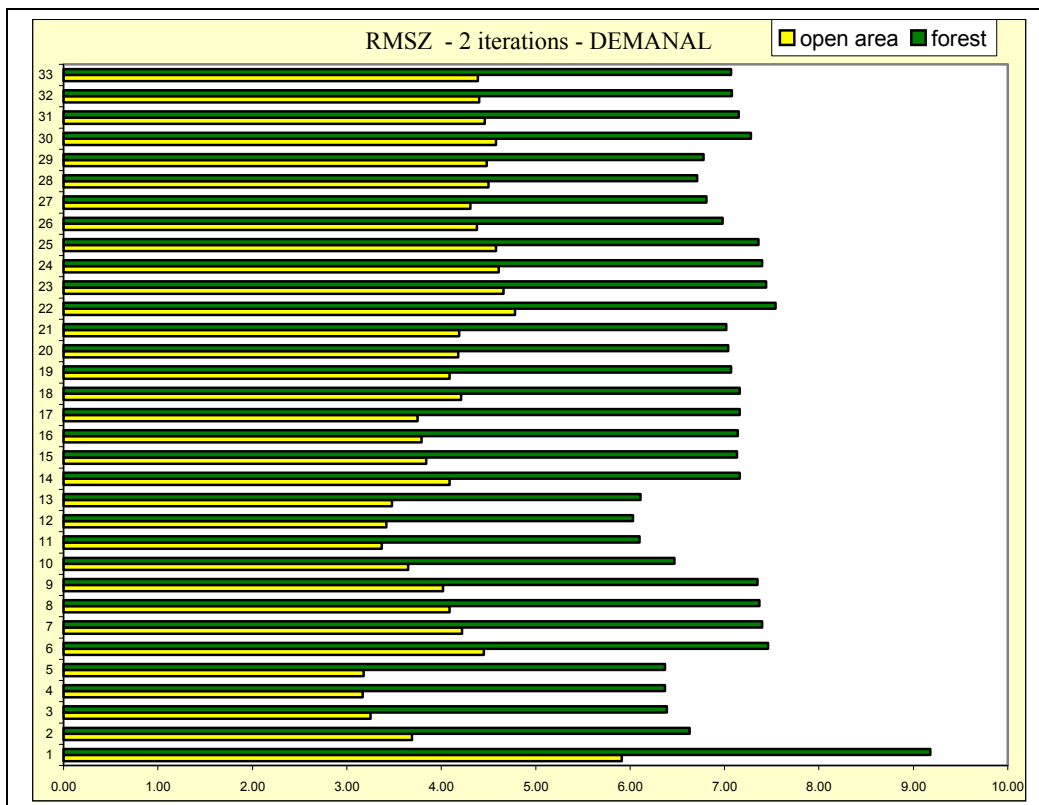
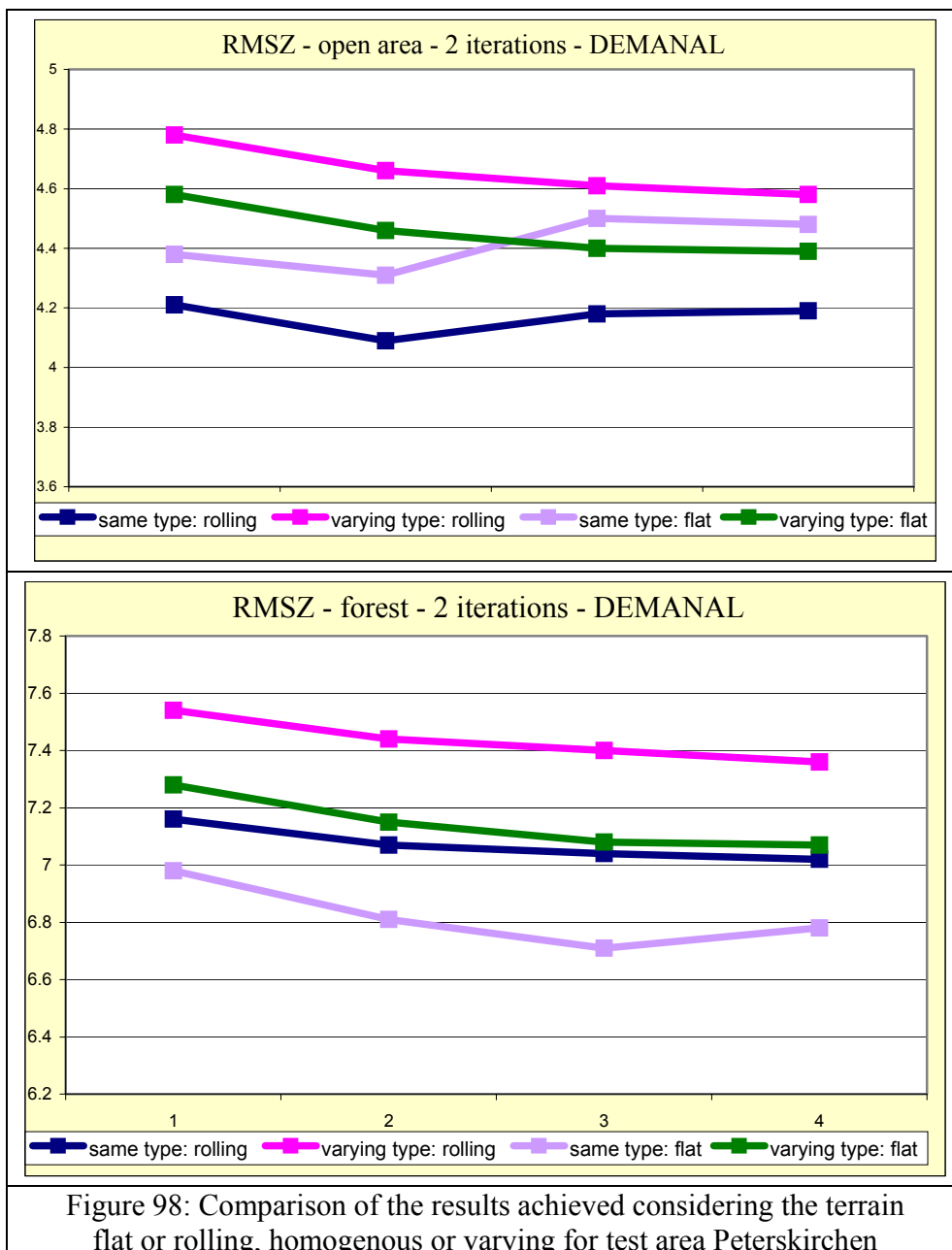
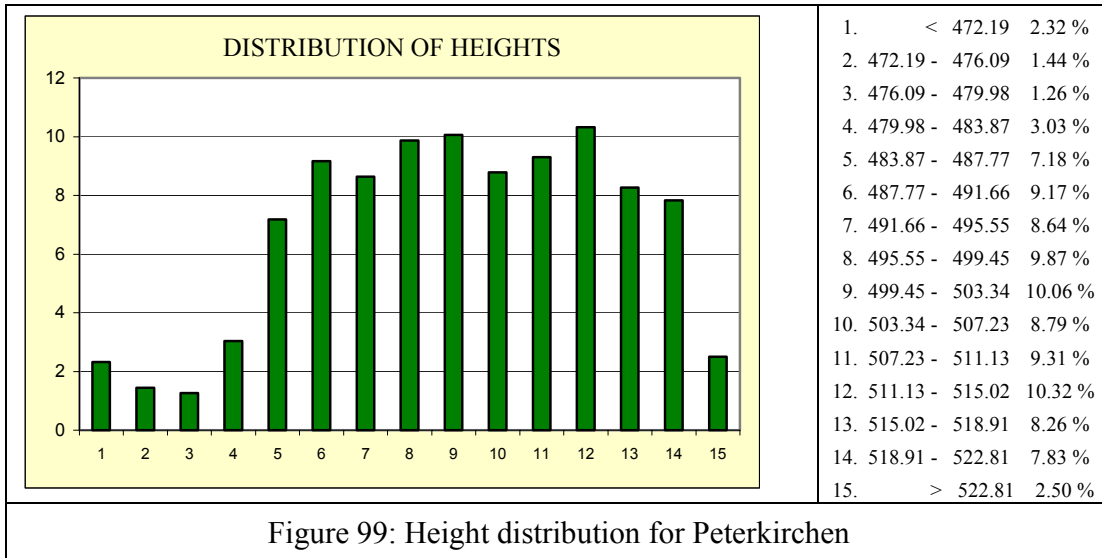


Figure 97: Results for test area Peterskirchen

The comparison study below is made just for interpolated data by LISA. In open area the trend in the case of rolling and varying type of terrain is the same like in the case of flat and varying type. In all the cases the results in the third and fourth iteration have almost the same value. Like in the cases before good results were achieved considering the terrain homogeneous and rolling. But this is not an accurate characterization of the test area so the results in this case are not relevant. The best results were obtained using 2 iterations from RASCOR and characterizing the area as flat and homogeneous. For forest area the best results were acquired using three iterations from RASCOR and considering the terrain flat and having the same characteristics. A comparison of the results achieved is shown in figure 98. The x axis represents the number of iterations.



The distribution of heights for Peterskirchen 1004003 points (figure 99):



A view of the three-dimensional shaded presentation of the digital height models (DSM, DEM) is presented next (figure 100). The difference between the achieved digital height models is presented in figure 101.

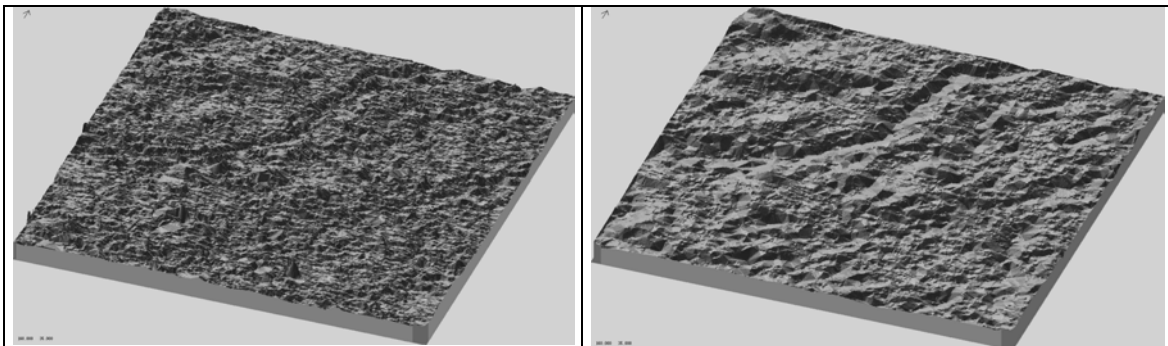


Figure 100: DSM (left) and filtered DSM (DEM) – exaggeration factor 2 times (Petersk.)

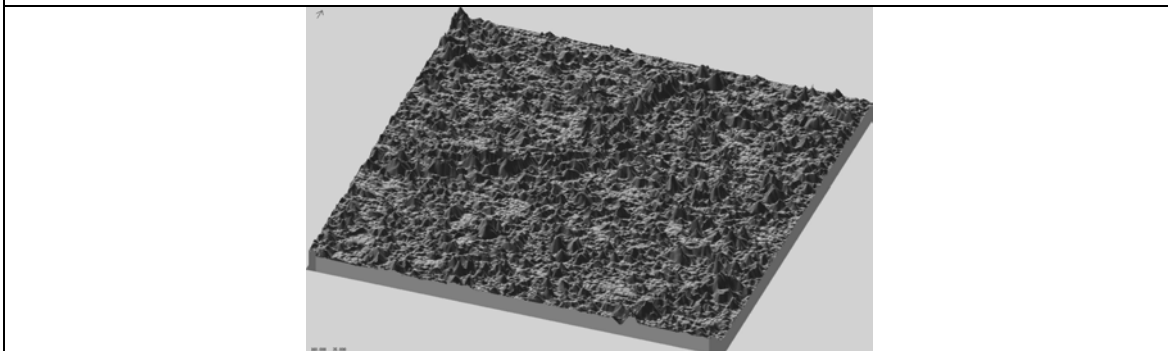


Figure 101: Differential DEM (exaggeration factor 5 times) Peterskirchen

### 6.6. Taching

Test area Taching has the same characteristics like the areas mentioned before. The handling of the data has been made in the same manner. The results of the analysis in this area for the case of interpolated data by LISA with a grid spacing of 15m using two iterations from RASCOR and considering a homogenous flat type of terrain are presented in Table 7 and diagrams for comparison of the results are presented in figure 102. RASCOR removed 23.24% points in the first iteration and 53.31% in the second iteration (figure 103). All the results for test area Taching for open area and forest are shown in figure 104.

Digital Height Model	Test area	RMSZ	MEAN DZ	RMSZ without bias	SZ	Z*
DSM	all points	9.09	0.09	9.09	$8.34 + 5.979 * \tan \alpha$	$-0.43 - 0.00102 * Z$
	open area	5.74	-0.04	5.73	$5.44 + 1.492 * \tan \alpha$	$0.43 - 0.00078 * Z$
	forest	10.42	-0.48	10.41	$9.96 + 3.088 * \tan \alpha$	$4.54 - 0.00928 * Z$
DEM	all points	6.69	0.06	6.69	$6.18 + 4.299 * \tan \alpha$	$-0.36 + 0.00095 * Z$
	open area	4.51	-0.05	4.51	$4.30 + 1.476 * \tan \alpha$	$-0.09 + 0.00000 * Z$
	forest	8.91	-0.09	8.91	$8.27 + 5.153 * \tan \alpha$	$-0.86 + 0.00127 * Z$

Table 7: Results for test area Taching (DSM, DEM)

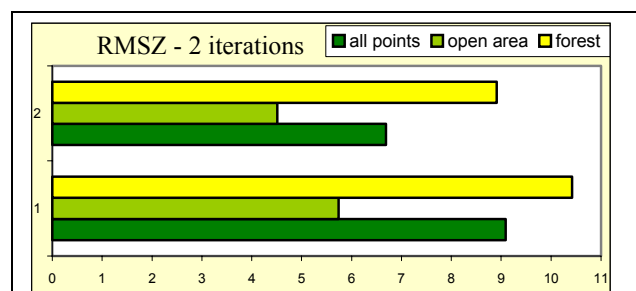
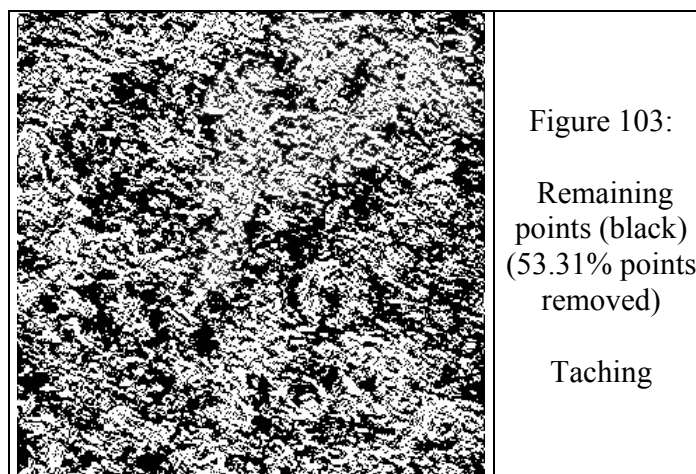


Figure 102: RMSZ for DSM (1) and filtered DEM (2)  
DEMANAL – 2 iterations



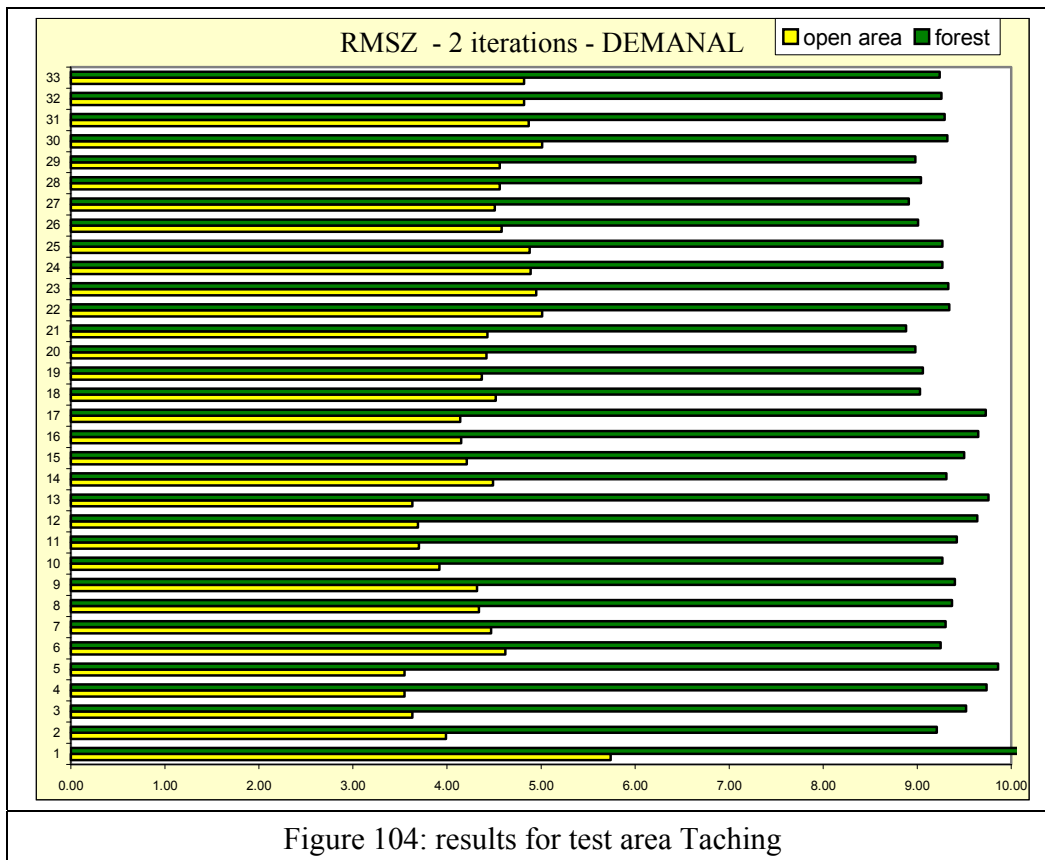
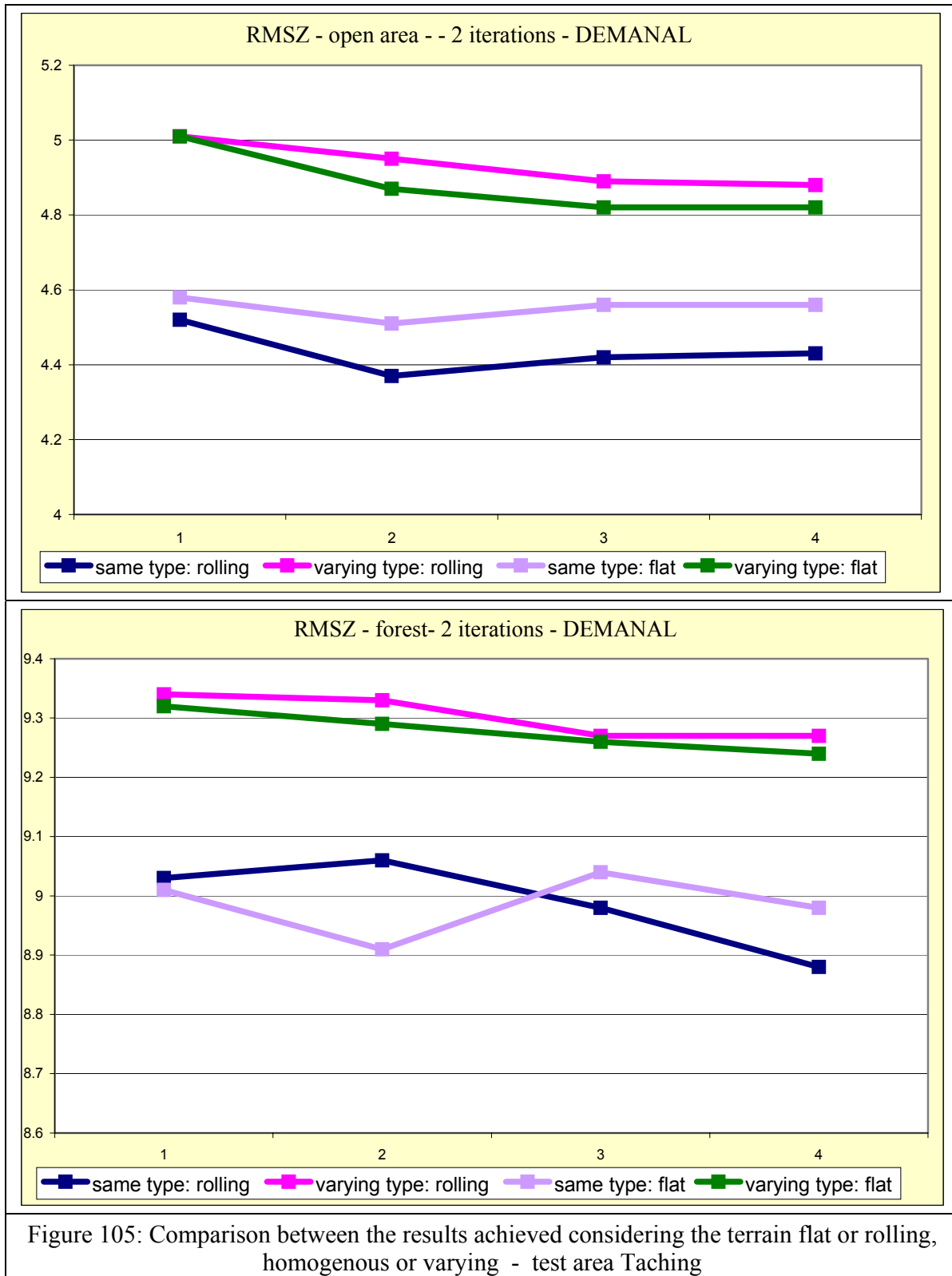
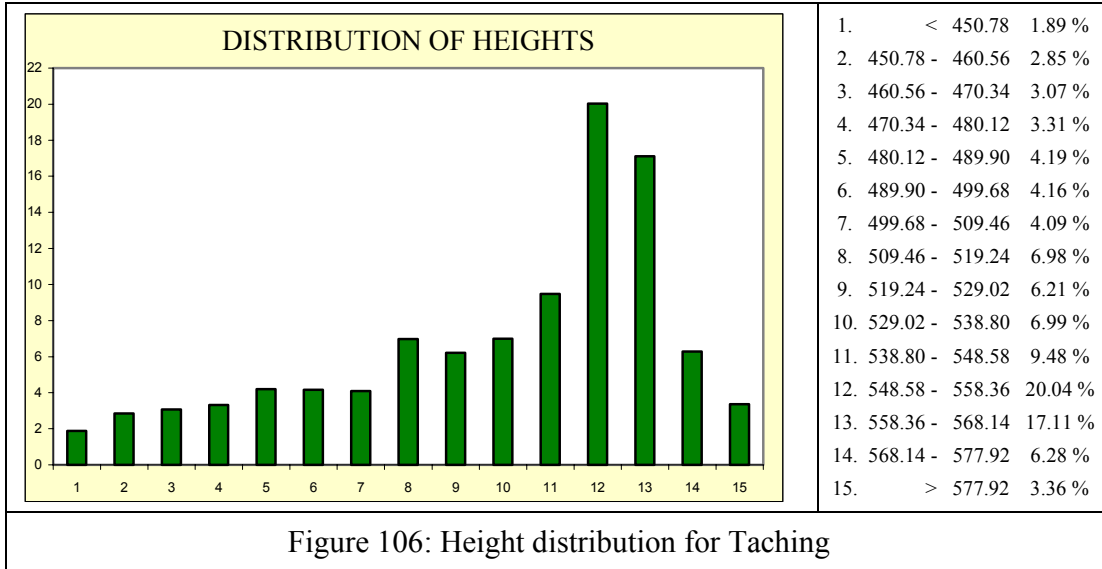


Figure 104: results for test area Taching

The comparison of the results is done for interpolated data by LISA. The results are similar like in the cases before. Considering the terrain as being rolling and with the same characteristics, good results were achieved for open area. But this case is not good to take into account because the terrain is mainly flat. In open area the results considering the area as having varying characteristics rolling or flat are not good. The best results were obtained just like in the cases before using the description of the area as homogenous flat terrain and two iterations from RASCOR. In forest areas the results are similar like in open areas; that means the best results were acquired under same conditions. A comparison of the results achieved is shown in figure 105. The X-axis represents the number of iterations used by handling the program RASCOR.



The distribution of heights for Taching, 1001189 points (figure 106):



A view of the three-dimensional shaded presentation of the digital height models (DSM, DEM) is presented next (figure 107). The difference between the achieved digital height models is shown in figure 108.

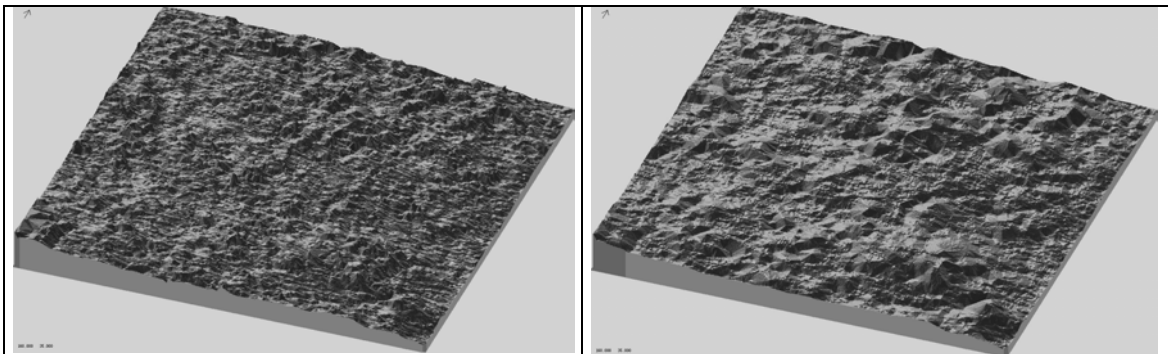


Figure 107: DSM (left) and filtered DSM (DEM) – exaggeration factor 2 times (Taching)

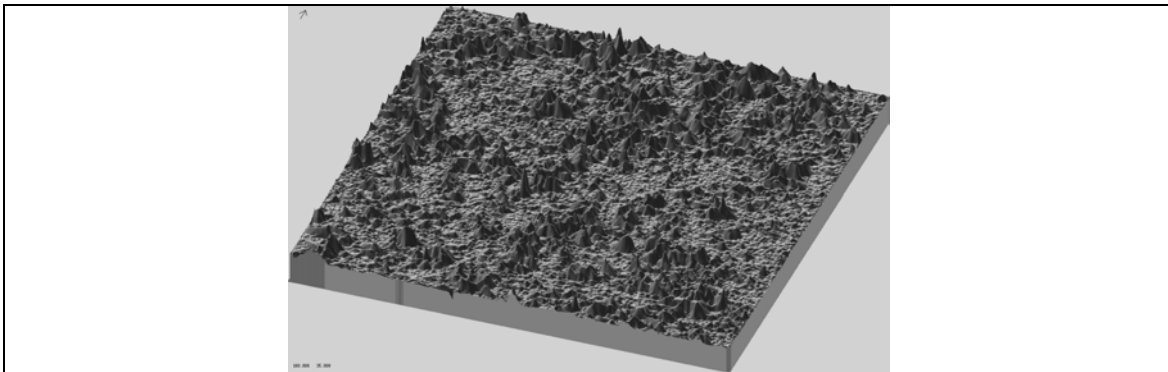


Figure 108: Differential DEM (exaggeration factor 5 times) Taching

### 6.7. Vilsbiburg

Test area Vilsbiburg has the same type of relief like the first four areas: flat up to rolling. The main part of this area is situated in the southern model and just a small part is the northern model. The same procedure was followed in this situation too. The results of the analysis using two iterations from RASCOR and interpolated data with LISA are presented in Table 8 (Vilsbiburg south model) and Table 9 (Vilsbiburg north model). The diagrams for comparison of the results are presented in figure 109. The analysis was made separately for the two models (figure 110 and figure 111).

Digital Height Model	Test area	RMSZ	MEAN DZ	RMSZ without bias	SZ	Z*
DSM	all points	7.20	-0.44	7.18	$6.57 + 3.568 * \tan \alpha$	$-0.09 - 0.00025 * Z$
	open area	6.59	-0.44	6.58	$5.79 + 10.385 * \tan \alpha$	$-0.20 - 0.00017 * Z$
	forest	9.43	-0.15	9.43	$9.33 - 0.096 * \tan \alpha$	$-3.83 - 0.00682 * Z$
DEM	all points	6.80	-0.99	6.73	$6.05 + 11.930 * \tan \alpha$	$-1.95 + 0.00262 * Z$
	open area	6.43	-1.03	6.35	$5.50 + 14.617 * \tan \alpha$	$-1.45 + 0.00125 * Z$
	forest	8.45	-0.44	8.44	$8.45 - 2.342 * \tan \alpha$	$-6.14 + 0.01044 * Z$

Table 8: Results for test area Vilsbiburg southern model

Digital Height Model	Test area	RMSZ	MEAN DZ	RMSZ without bias	SZ	Z*
DSM	all points	9.43	0.61	9.41	$8.61 + 9.855 * \tan \alpha$	$0.08 + 0.00075 * Z$
	open area	8.49	0.36	8.48	$7.58 + 7.813 * \tan \alpha$	$-0.35 + 0.00104 * Z$
	forest	11.36	1.35	11.28	$10.61 - 4.165 * \tan \alpha$	$-0.95 + 0.00422 * Z$
DEM	all points	8.13	-0.25	8.13	$7.48 + 9.134 * \tan \alpha$	$-0.59 + 0.00001 * Z$
	open area	7.53	-0.41	7.52	$6.94 + 7.632 * \tan \alpha$	$-0.94 + 0.00048 * Z$
	forest	10.85	0.42	10.84	$10.52 + 6.563 * \tan \alpha$	$-0.90 + 0.00133 * Z$

Table 9: Results for test area Vilsbiburg northern model

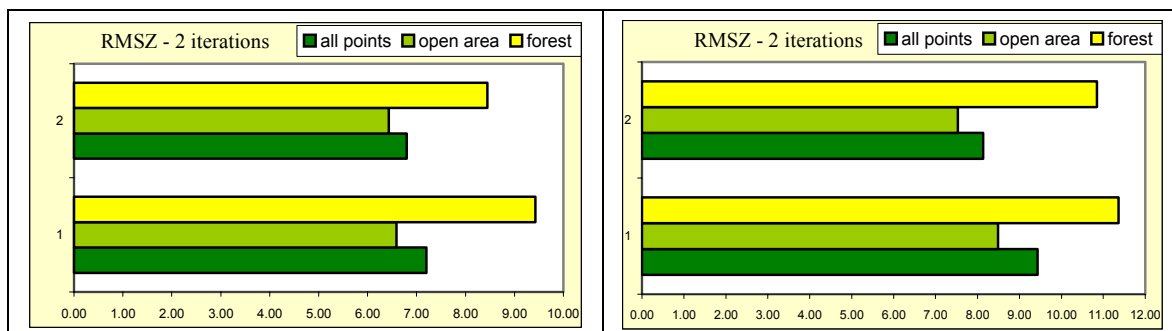


Figure 109: RMSZ for DSM (1) and filtered DEM (2) (left: Vilsbiburg south, right: Vilsbiburg north) RMSZ – 2 iterations - RASCOR

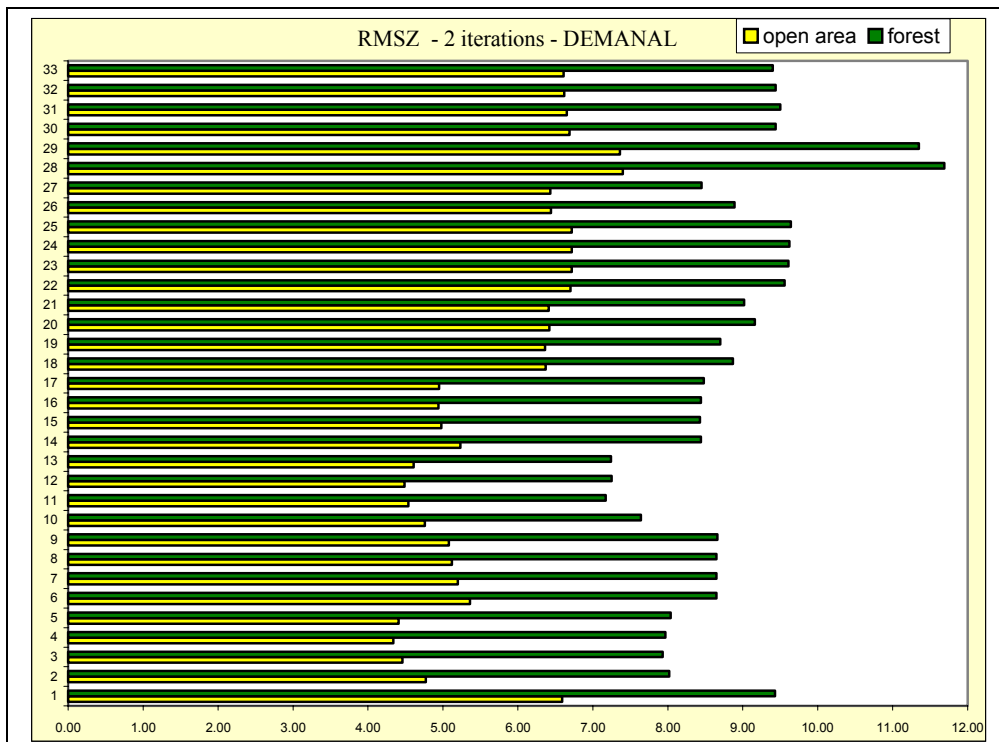


Figure 110: Result for test area Vilsbiburg south

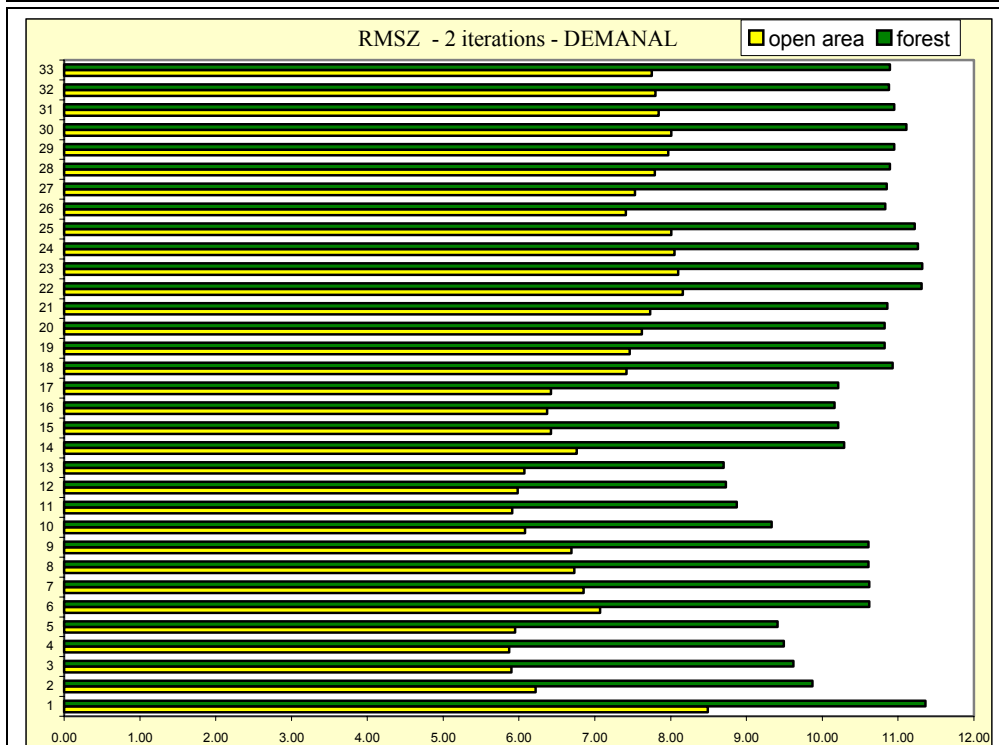


Figure 111: Result for test area Vilsbiburg north

The analysis of the results is made for interpolated data. In open areas using the option varying type of terrain, rolling and flat, when handling the program RASCOR, the results are almost the same. Just like in the areas analyzed before, good results were achieved using the characterization of the terrain as rolling and homogenous, but this case is not an optimal one because of the same reason mentioned in the other analysis. Also the optimal method to handle the data is by considering the terrain flat and with a uniform character and using two iterations from RASCOR. In forest areas the trend is similar like in open areas and the best results were obtained using the same method. A comparison of the results achieved is shown in figure 112. The X-axis represents the number of iterations.

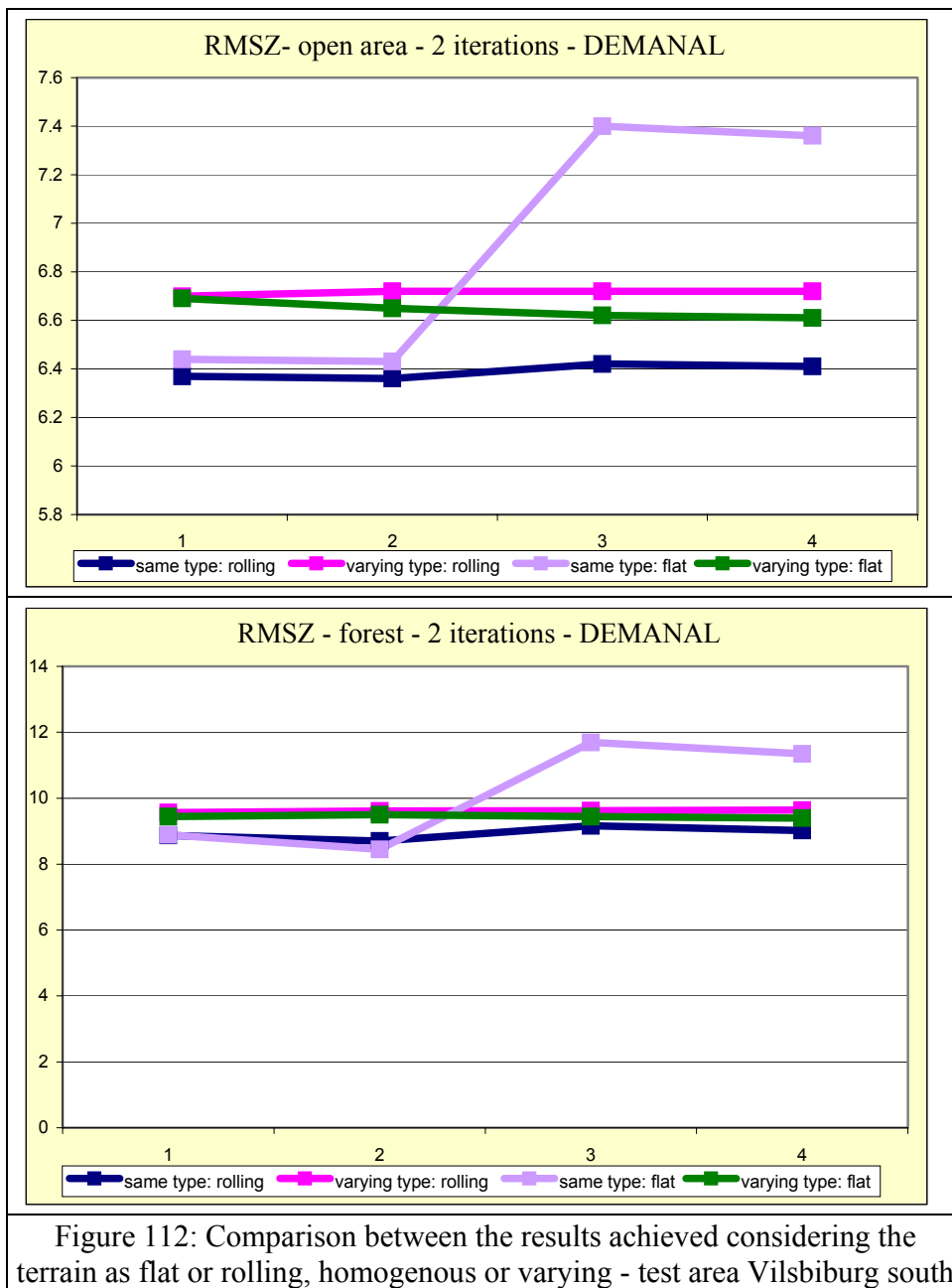


Figure 112: Comparison between the results achieved considering the terrain as flat or rolling, homogenous or varying - test area Vilsbiburg south

The analysis of the results is made for data interpolated by LISA. In open area the trend in the case of rolling and varying type of terrain is very similar like in the case of flat and varying type. Good results were acquired in the case of a homogeneous and rolling type of terrain but this characterization does not describe the test area very accurate. The best results were obtained using two iterations from RASCOR and characterizing the area as flat and homogeneous. The analysis made above for open areas is also valid in the case of forest areas. A comparison of the results achieved is shown in figure 113. The X-axis represents the number of iterations.

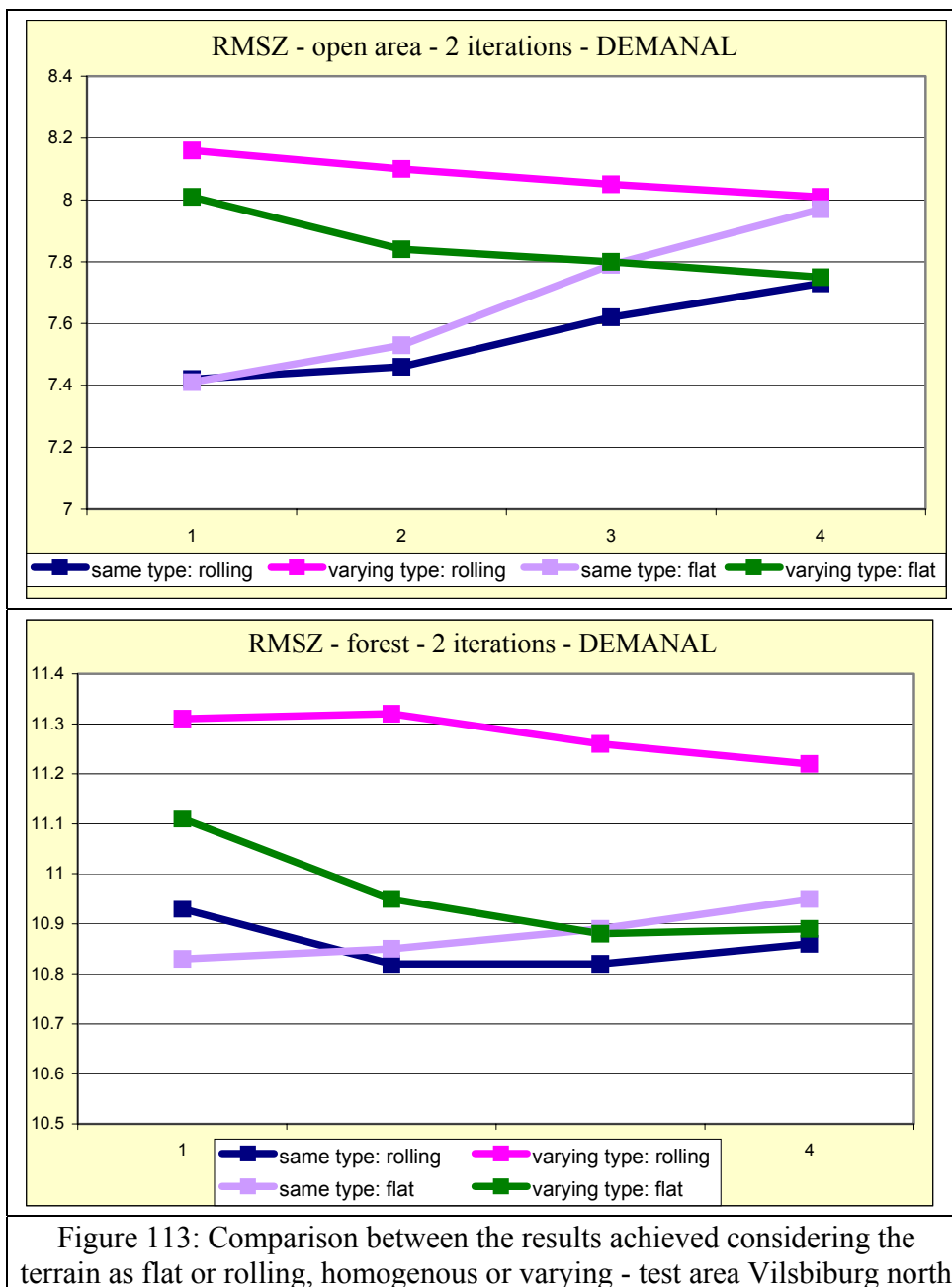
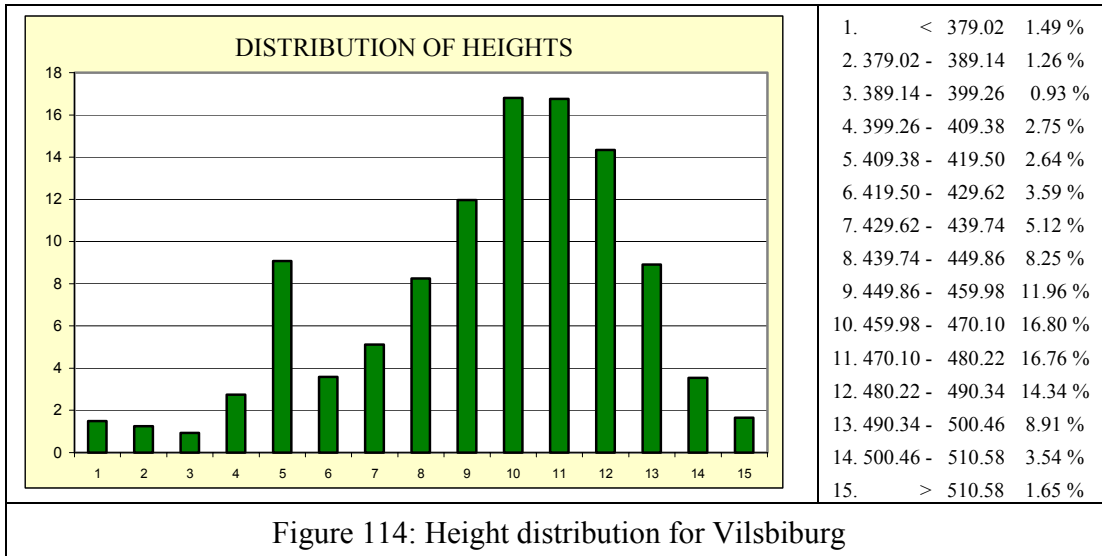


Figure 113: Comparison between the results achieved considering the terrain as flat or rolling, homogenous or varying - test area Vilsbiburg north

The distribution of heights for Vilsbiburg, 601601 points (figure 114):



A three-dimensional shaded presentation of the digital height models (DSM, DEM) is presented below (figure 115 Vilsbiburg southern model and figure 117 Vilsbiburg northern model). The difference between the achieved digital height models is shown in figure 116 for Vilsbiburg southern model and in figure 118 for Vilsbiburg northern model.

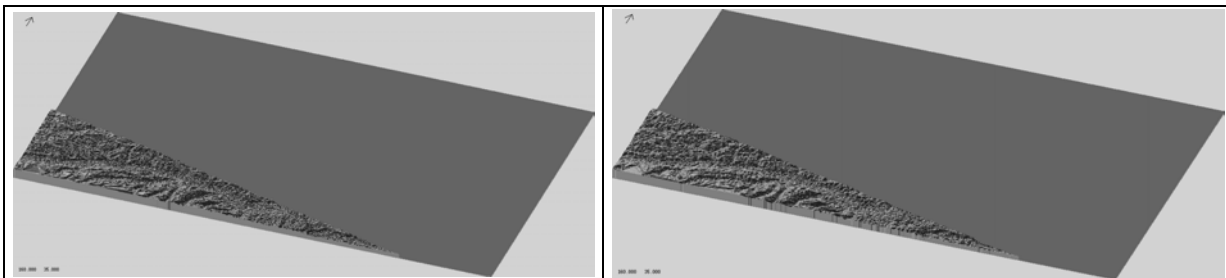


Figure 115: DSM (left) and filtered DEM (right) for south Vilsbiburg (exaggeration factor 5)

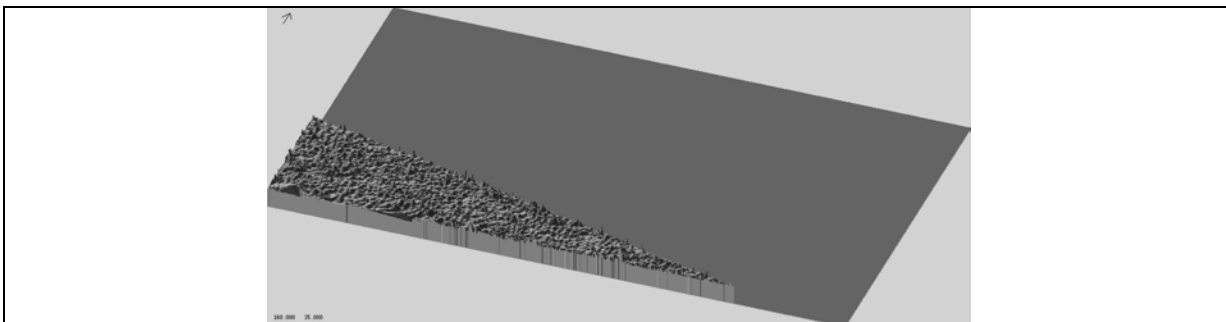


Figure 116: Differential DEM for Vilsbiburg southern model (exaggeration factor 20)

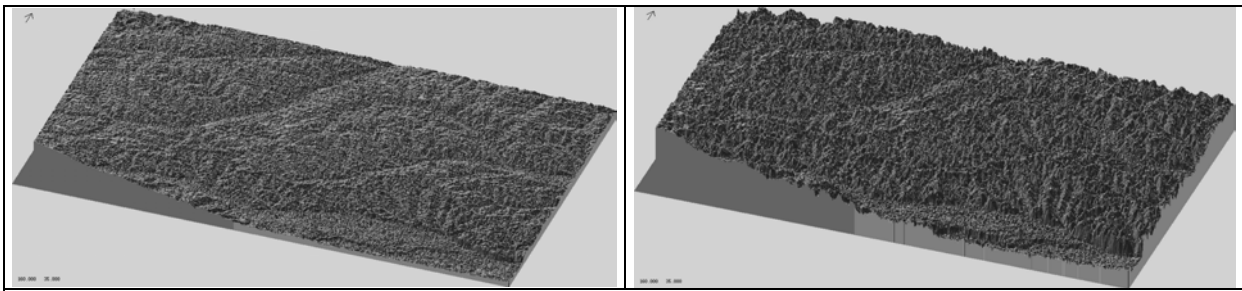


Figure 117: DSM (left) and filtered DEM (right) for north Vilsbiburg (exaggeration factor 5)

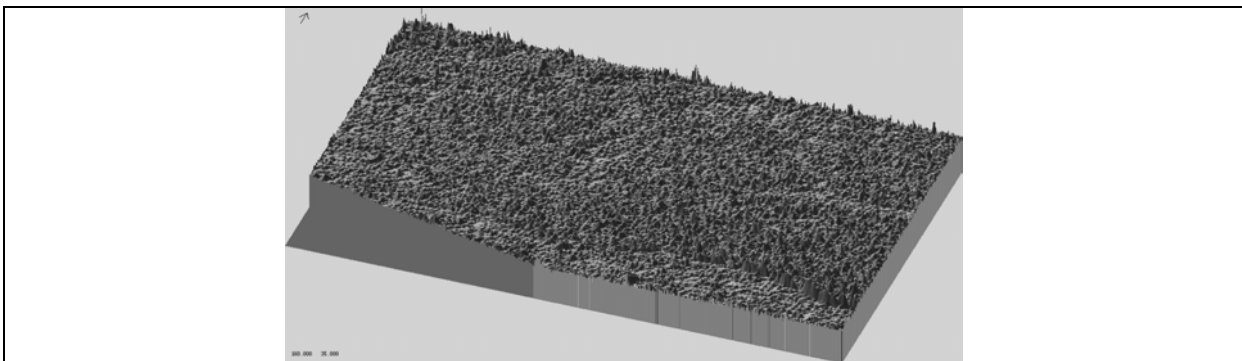


Figure 118: Differential DEM for Vilsbiburg northern model (exaggeration factor 20)

RASCOR eliminated 28.03% points in the first iteration and 55.74% in the second in the second in the southern model and 29.51% in the first iteration and 58.58% in the second iteration in the Vilsbiburg northern model (figure 119).

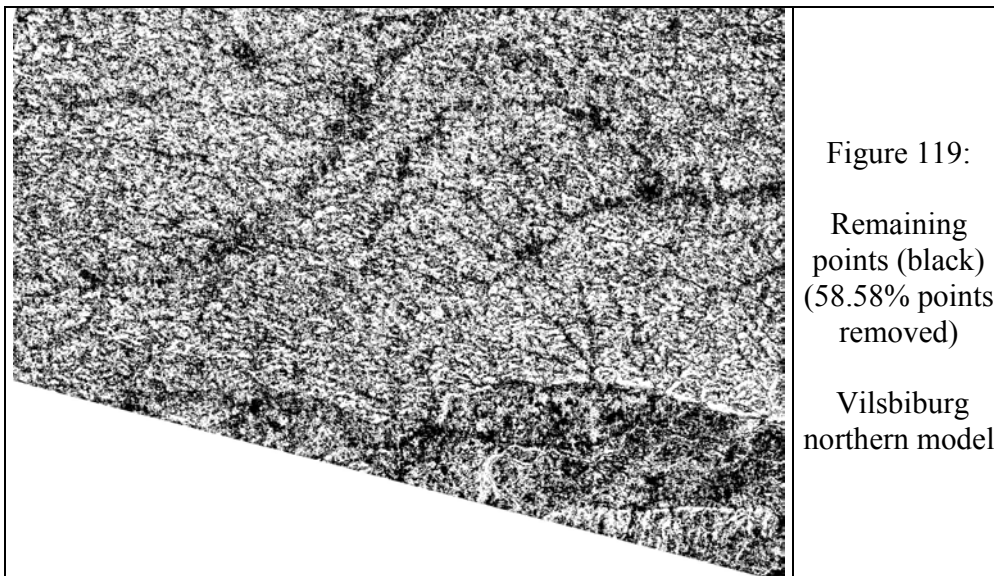


Figure 119:  
 Remaining points (black)  
 (58.58% points removed)  
 Vilsbiburg northern model

## 6.8. Inzell

Like in the case of Prien for the generation and analysis of the DEM of the area Inzell, data from SPOT HRS and SRTM INSAR had been used. The results that have been achieved are shown in table 10. Diagrams for comparison of the results are presented in figure 120. Inzell has a different character comparing to the other areas. The type of terrain is mountainous; the results shown in table 10 are obtained by filtering the data by RASCOR using two iterations and interpolating the results by LISA with grid spacing of 15m. RASCOR removed 23.32% points in the 1st iteration and 49.95% in the 2<sup>nd</sup> (figure 121). The results for RMSZ two iterations are presented in figure 122.

Digital Height Model	Test area	RMSZ	MEAN DZ	RMSZ without bias	SZ	Z*
DSM	all points	15.04	4.10	14.47	$9.95 + 28.982 * \tan \alpha$	$1.79 + 0.00145 * Z$
	open area	9.59	2.62	9.22	$6.69 + 32.814 * \tan \alpha$	$-0.97 + 0.00510 * Z$
	forest	14.45	1.03	14.41	$9.82 + 17.133 * \tan \alpha$	$-1.28 + 0.00141 * Z$
DEM (HRS)	all points	17.27	0.83	17.25	$7.82 + 38.058 * \tan \alpha$	$0.63 - 0.00020 * Z$
	open area	8.62	0.49	8.60	$5.10 + 26.905 * \tan \alpha$	$0.15 + 0.00060 * Z$
	forest	19.54	-0.91	19.52	$8.91 + 34.634 * \tan \alpha$	$-1.68 + 0.00035 * Z$
DEM (INSAR)	all points	10.52	2.54	10.21	$8.12 + 4.294 * \tan \alpha$	$1.83 + 0.00012 * Z$
	open area	8.02	2.45	7.64	$5.66 + 10.531 * \tan \alpha$	$0.36 + 0.00296 * Z$
	forest	9.34	0.25	9.34	$5.45 + 6.013 * \tan \alpha$	$-0.54 + 0.00027 * Z$

Table 10: Results for test area Inzell (DSM, DEM-HRS, DEM-INSAR)

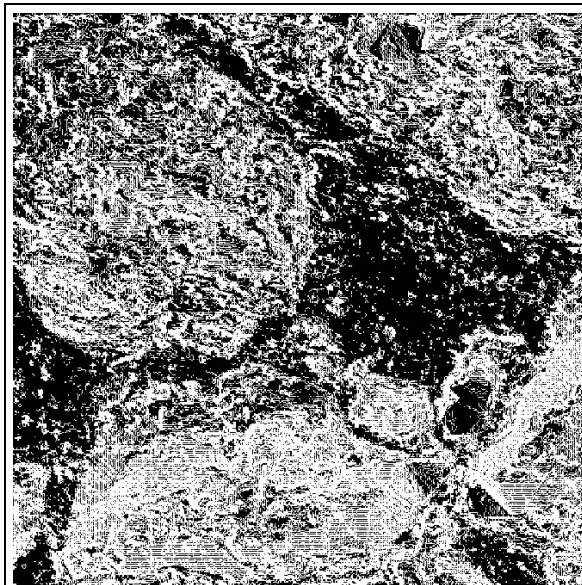


Figure 121: Remaining points (black) (49.95% points removed) - Inzell

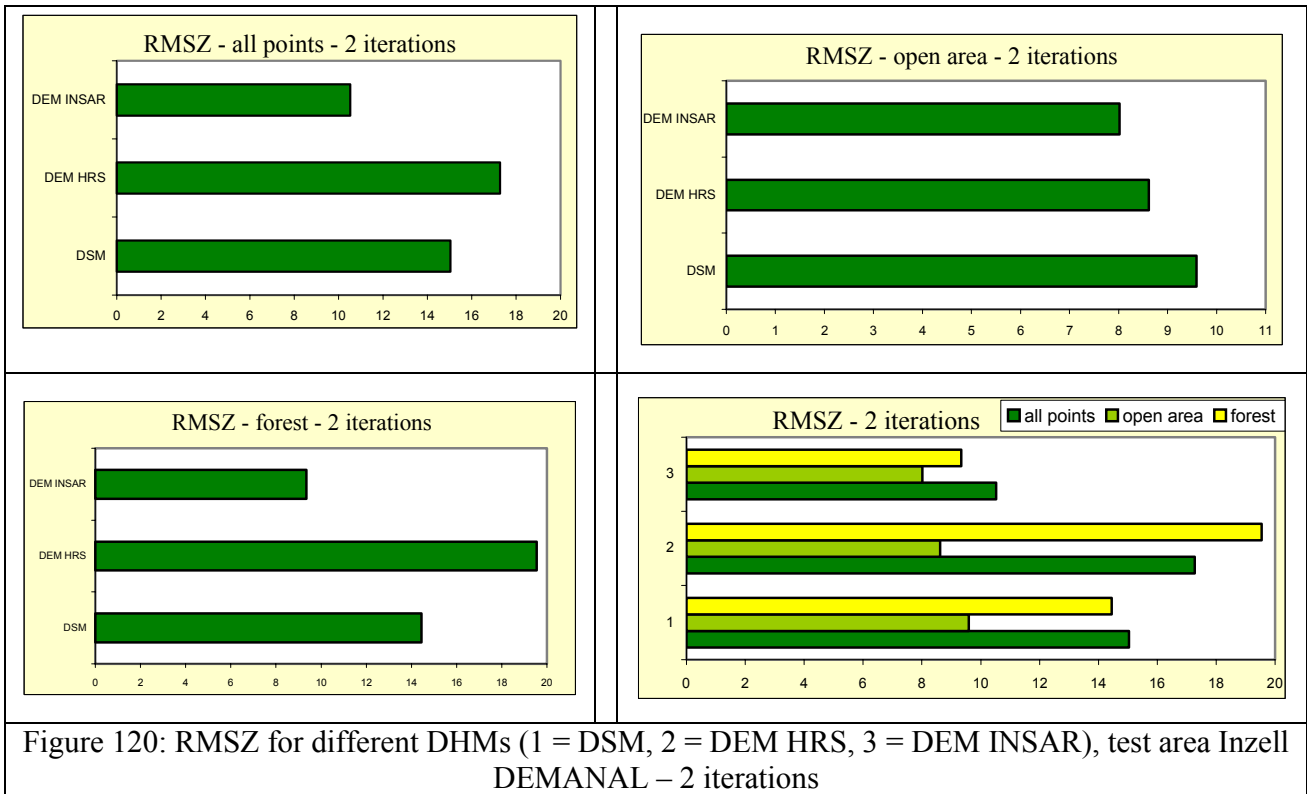


Figure 120: RMSZ for different DHMs (1 = DSM, 2 = DEM HRS, 3 = DEM INSAR), test area Inzell DEMANAL – 2 iterations

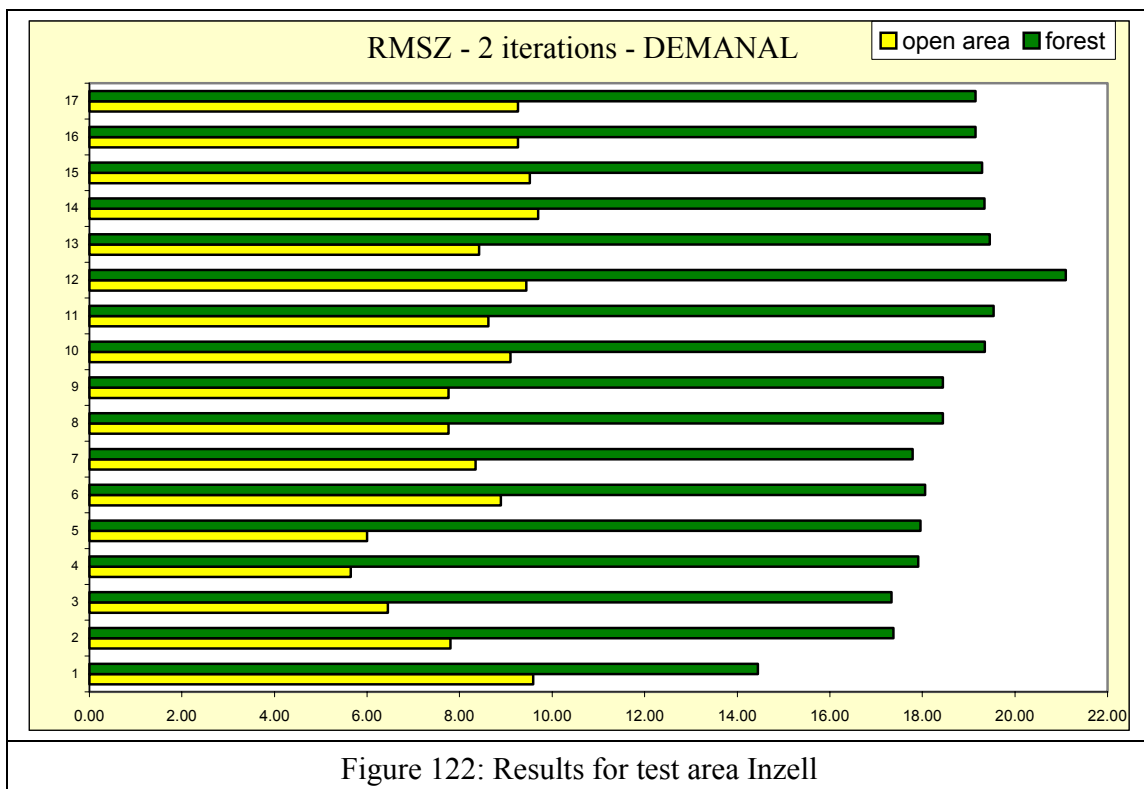


Figure 122: Results for test area Inzell

The analysis of the results for test area Inzell has been done for data interpolated by program LISA. In the case of open areas the results obtained considering the terrain as having a varying and mountainous character are not so good like in the case of a homogenous terrain. The results are good using two iterations from RASCOR. In forest areas the results for the varying case are better than in open areas and also good results were achieved using just two iterations from RASCOR. A comparison of the results achieved is shown in figure 123. The X-axis represents the number of iterations.

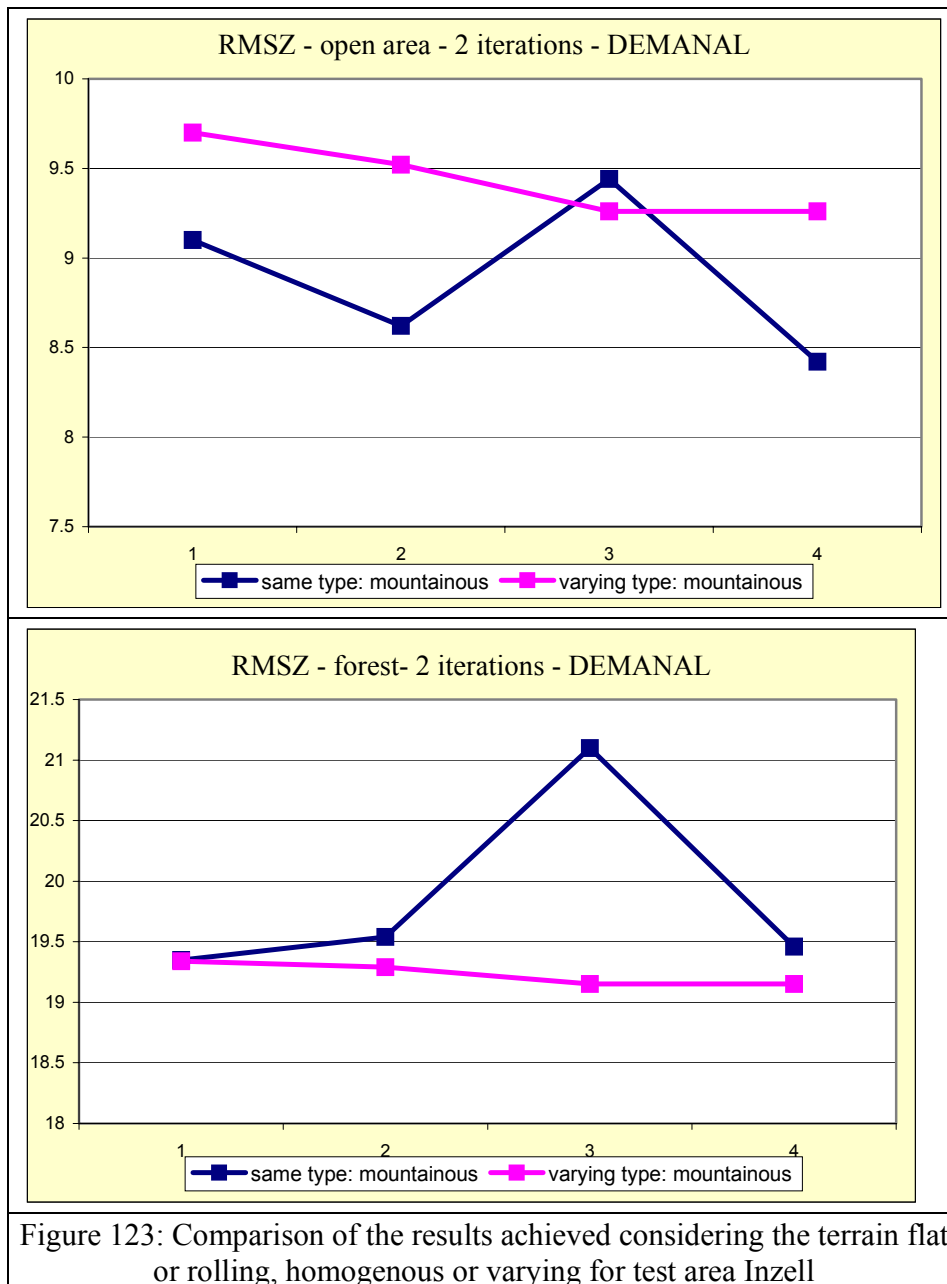
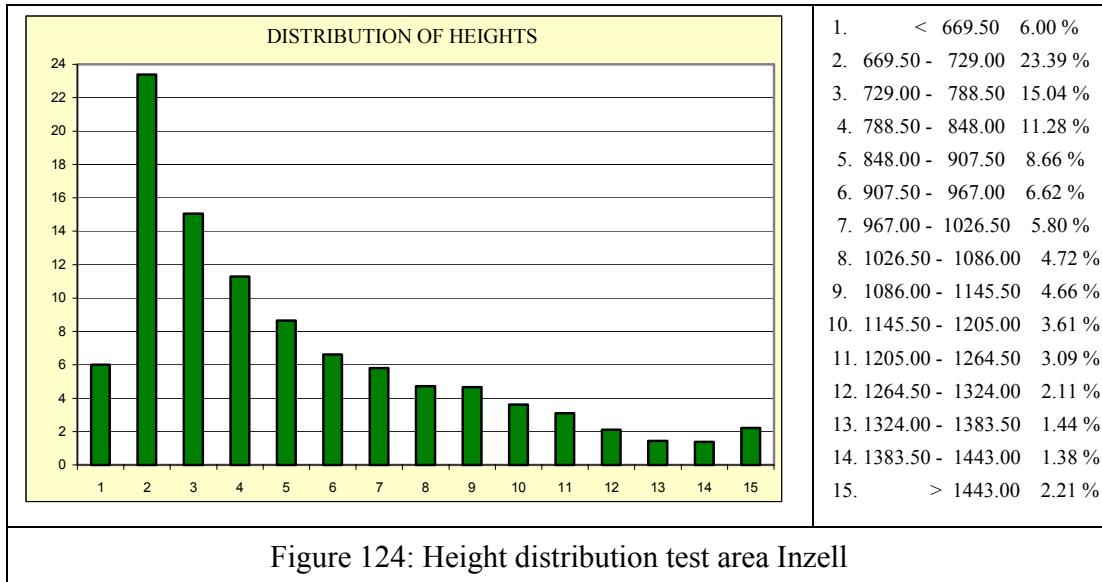
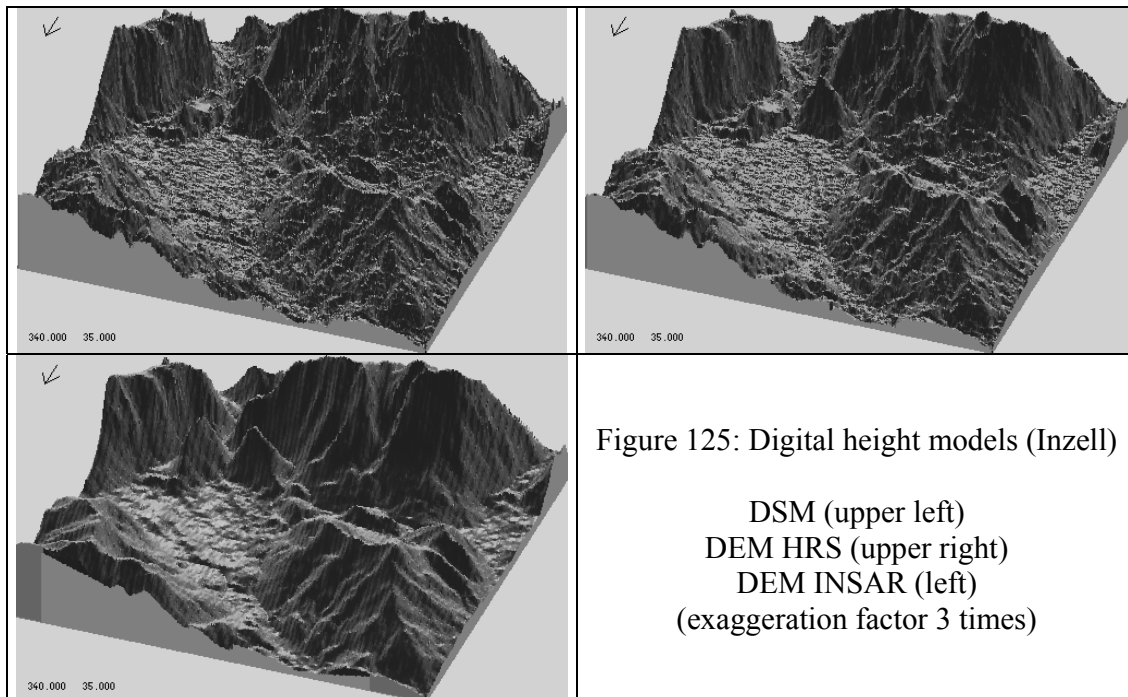


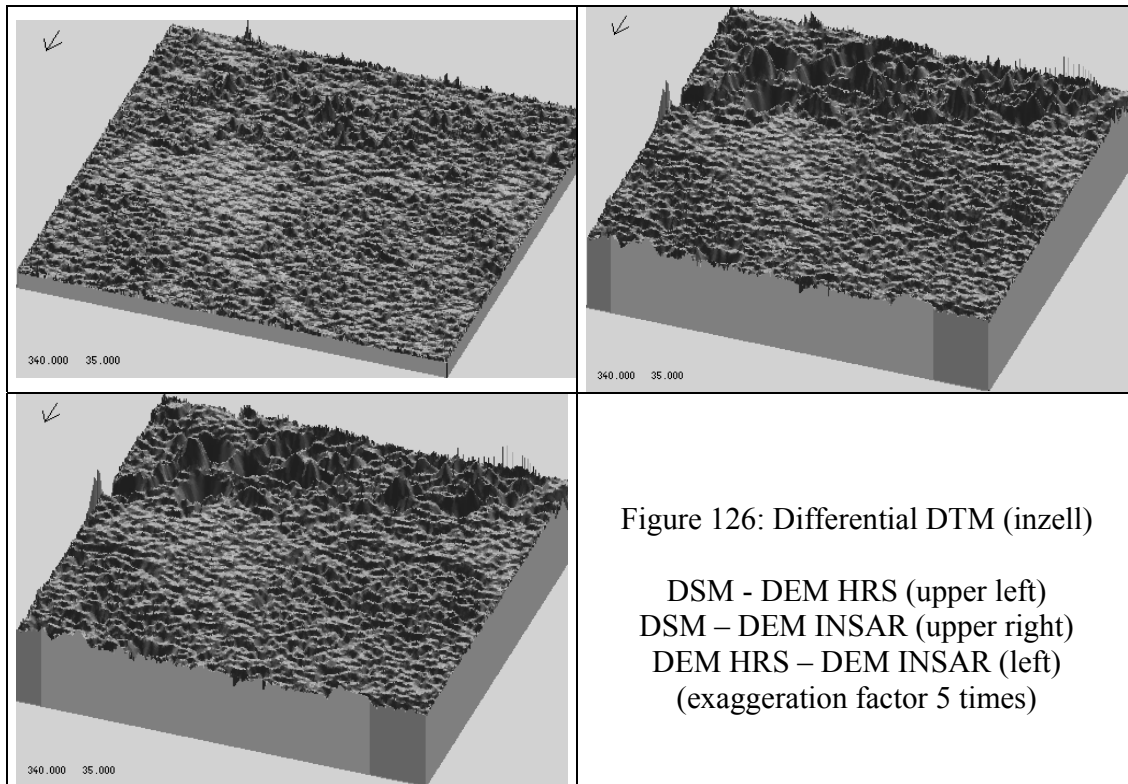
Figure 123: Comparison of the results achieved considering the terrain flat or rolling, homogenous or varying for test area Inzell

The distribution of heights for Inzell (figure 124):



A view of the three-dimensional shaded presentation of the digital height models (DSM, DEM HRS, DEM INSAR) is presented next (figure 125). The difference between the achieved digital height models is shown in figure 126.





### 6.9. Overview of the Results

An overview impression of the results for all the studied areas in the case of data interpolated by program LISA is presented in table 11. A comparison study for the achieved results for all the areas without Inzell in the case of open areas and forest is shown in figure 127. Inzell is not part of this comparison because it has a different type of terrain. On the horizontal axis the first group of four represents results in the of same type of terrain rolling using one to four iterations, the second group represents varying type of terrain rolling, the third same type of terrain flat and the fourth varying type of terrain flat.

Test area	Layer	RMSZ	MEAN DZ	RMSZ without bias	SZ	Z*
Prien	open area	4.83	-1.01	4.72	$4.58 + 1.990 * \tan \alpha$	$-1.09 + 0.00031 * Z$
	forest	9.51	-0.99	9.46	$8.53 + 4.625 * \tan \alpha$	$-3.20 + 0.00464 * Z$
Gars	open area	5.84	-0.35	5.83	$5.34 + 2.110 * \tan \alpha$	$0.43 - 0.00158 * Z$
	forest	10.15	0.07	10.15	$8.97 + 3.344 * \tan \alpha$	$-1.01 + 0.00227 * Z$
Peterskirchen	open area	4.31	-0.27	4.30	$4.32 - 1.026 * \tan \alpha$	$0.78 - 0.00209 * Z$
	forest	6.81	-0.37	6.80	$6.81 + 1.136 * \tan \alpha$	$-0.79 + 0.00104 * Z$
Taching	open area	4.51	-0.05	4.51	$4.30 + 1.476 * \tan \alpha$	$-0.09 + 0.00000 * Z$
	forest	8.91	-0.09	8.91	$8.27 + 5.153 * \tan \alpha$	$-0.86 + 0.00127 * Z$

Vilsbiburg south	open area	6.43	-1.03	6.35	$5.50 + 14.617 * \tan \alpha$	$-1.45 + 0.00125 * Z$
	forest	8.45	-0.44	8.44	$8.45 - 2.342 * \tan \alpha$	$-6.14 + 0.01044 * Z$
Vilsbiburg north	open area	7.53	-0.41	7.52	$6.94 + 7.632 * \tan \alpha$	$-0.94 + 0.00048 * Z$
	forest	10.85	0.42	10.84	$10.52 + 6.563 * \tan \alpha$	$-0.90 + 0.00133 * Z$
Inzell	open area	8.62	0.49	8.60	$5.10 + 26.905 * \tan \alpha$	$0.15 + 0.00060 * Z$
	forest	19.54	-0.91	19.52	$8.91 + 34.634 * \tan \alpha$	$-1.68 + 0.00035 * Z$

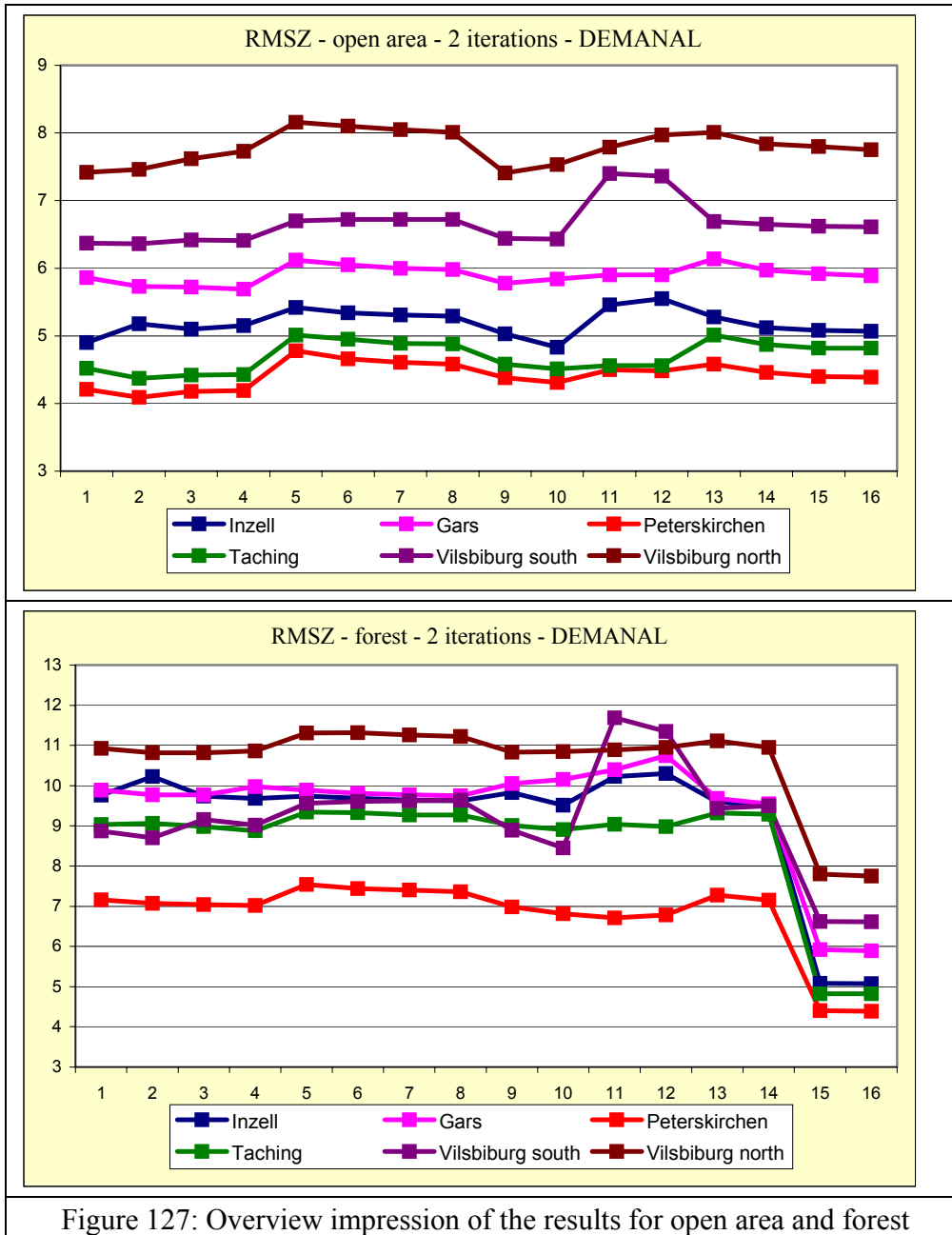


Figure 127: Overview impression of the results for open area and forest

## CONCLUSION

The analysis of the SPOT HRS models in the frame of the SPOT HRS Scientific Assessment Program was made following a sequence of Program System BLUH.

Digital Elevation Models have been generated by automatic image matching using program DPCOR which is based on the least square matching by region growing. For the image matching different spacing have been used. For all the test areas (Prien, Gars, Peterskirchen, Taching, Vilsbiburg and Inzell) the image matching was made for every third pixel with a window size of 10 pixels x 10 pixels and a tolerance limit for the correlation coefficient of 0.6. For two test areas (Prien and Gars) the automatic image matching was made also for every pixel using the same size of the window and the same tolerance limit for the correlation coefficient like in the method described before. The results obtained using these two methods of automatic image matching for test areas Prien and Gars reveal the fact that the automatic image matching for every third pixel has advantages against the other method. Among the benefits of this method are the facts that the image matching operation is consuming less time compared to the image matching for every pixel, the volume of data is smaller that means the computation is done faster and there is no loss of accuracy by a spacing of 3 pixels against one. The results were similar for both areas.

The output of the automatic image matching is a file containing pixel coordinates. The transformation from pixel coordinates to image coordinates was made using the program BLPRE and handling the program COMSPO for the intersection of corresponding rays and the transformation into the national coordinate system.

The data achieved from automatic image matching is not in a regular arrangement and it can also contain gaps in the parts of the image that could not be matched or were matched incorrectly. For creating a regular arrangement of the data set, program LISA was used to interpolate data within a grid with the spacing of 15m. The interpolation was also necessary because program RASCOR accepts only raster form data.

RASCOR was handled for filtering the digital surface model in order to create a digital elevation model. For filtering different characterizations of the terrain were used. The output of this program is a file with the remaining points in a grid arrangement, but with gaps. The data have been interpolated again by LISA using the same grid size. A DEM can be in a random or in a regular arrangement but usually it is presented with a regular point distribution which is a more useful form for many applications. The results for interpolated data are not so good like the results obtained using just RASCOR. The lost of accuracy due to the interpolation is depending upon the terrain roughness, it can go up to 3m.

The analysis of the digital surface models obtained by means of image matching and the analysis of the derived digital elevation models was made by program DEMANAL.

The investigation was made separately for open areas and forest because the areas have completely different characteristics and the accuracy of the digital elevation model is depending upon these aspects. In forest areas the accuracy of the DEM is not so good like in open areas caused by the fact that the matched points are located on top of the vegetation.

A comparison between the accuracy of a DEM achieved by means of SPOT HRS images and the accuracy of a DEM obtained from INSAR SRTM was made for test areas Prien and Inzell. The study showed that the results are better in the case of InSAR-SRTM; especially for forest areas the differences are significant and in open areas also better results were acquired but with small differences between them. But the SRTM data do have the disadvantage of less detailed information caused by the spacing of 3 arc seconds (~90m) in comparison to 15m x 30m for SPOT HRS DEMs.

For the investigated test area Chiemsee (Bavaria) in the frame of HRS SAP the optimal procedure for the absolutely required filtering of the data by RASCOR was the handling as having an homogeneous flat characteristic, using two iterations from RASCOR and interpolate the final results by LISA in order to achieve a digital elevation model with a regular point distribution and without gaps. In some cases using three iterations from RASCOR the results were better but especially in forest areas. Usually in open areas the use of three iterations does not improve the quality of the derived DEM. In forest the best results were obtained following the same procedure but using three iterations from RASCOR and considering the terrain flat with a varying character. Good results were achieved in many cases considering the terrain as rolling but this case should not be taken into account because this is not an accurate characterization of the terrain.

There was a significant difference in accuracy between the forest and the open areas. A dependency of the accuracy from the terrain inclination was very clear.

## **ACKNOWLEDGEMENTS**

I would very much like to thank and acknowledge the help and advice of Dr.-Ing. Karsten Jacobsen from The Institute of Photogrammetry and Geoinformation (IPI), University of Hannover, Germany. I would also like to thank Dr.-Ing. Florea Zavoianu from The Faculty of Geodesy, Technical University of Civil Engineering of Bucharest, Romania and Dipl.-Ing. Hans Neuner from The Institute of Geodesy, University of Hannover, Germany for the support during the project period and all the advice they gave me.

**APPENDIX**

Results for test area Prien (DEMANAL).

- 1 - reference data and matched points
- 2 - reference data and 1 iteration data from Rascor (same type of terrain: rolling)
- 3 - reference data and 2 iterations data from Rascor (same type of terrain: rolling)
- 4 - reference data and 3 iterations data from Rascor (same type of terrain: rolling)
- 5 - reference data and 4 iterations data from Rascor (same type of terrain: rolling)
- 6 - reference data and 1 iteration data from Rascor (varying type of terrain: rolling)
- 7 - reference data and 2 iterations data from Rascor (varying type of terrain: rolling)
- 8 - reference data and 3 iterations data from Rascor (varying type of terrain: rolling)
- 9 - reference data and 4 iterations data from Rascor (varying type of terrain: rolling)
- 10 - reference data and 1 iteration data from Rascor (same type of terrain: flat)
- 11 - reference data and 2 iterations data from Rascor (same type of terrain: flat)
- 12 - reference data and 3 iterations data from Rascor (same type of terrain: flat)
- 13 - reference data and 4 iterations data from Rascor (same type of terrain: flat)
- 14 - reference data and 1 iteration data from Rascor (varying type of terrain: flat)
- 15 - reference data and 2 iterations data from Rascor (varying type of terrain: flat)
- 16 - reference data and 3 iterations data from Rascor (varying type of terrain: flat)
- 17 - reference data and 4 iterations data from Rascor (varying type of terrain: flat)
- 18 - reference data and interpolated data with Lisa using 1 iteration from Rascor (same type of terrain: rolling)
- 19 - reference data and interpolated data with Lisa using 2 iterations from Rascor (same type of terrain: rolling)
- 20 - reference data and interpolated data with Lisa using 3 iterations from Rascor (same type of terrain: rolling)
- 21 - reference data and interpolated data with Lisa using 4 iterations from Rascor (same type of terrain: rolling)
- 22 - reference data and interpolated data with Lisa using 1 iteration from Rascor (varying type of terrain: rolling)
- 23 - reference data and interpolated data with Lisa using 2 iterations from Rascor (varying type of terrain: rolling)
- 24 - reference data and interpolated data with Lisa using 3 iterations from Rascor (varying type of terrain: rolling)
- 25 - reference data and interpolated data with Lisa using 4 iterations from Rascor (varying type of terrain: rolling)
- 26 - reference data and interpolated data with Lisa using 1 iteration from Rascor (same type of terrain: flat)
- 27 - reference data and interpolated data with Lisa using 2 iterations from Rascor (same type of terrain: flat)
- 28 - reference data and interpolated data with Lisa using 3 iterations from Rascor (same type of terrain: flat)
- 29 - reference data and interpolated data with Lisa using 4 iterations from Rascor (same type of terrain: flat)
- 30 - reference data and interpolated data with Lisa using 1 iteration from Rascor (varying type of terrain: flat)
- 31 - reference data and interpolated data with Lisa using 2 iterations from Rascor (varying type of terrain: flat)
- 32 - reference data and interpolated data with Lisa using 3 iterations from Rascor (varying type of terrain: flat)
- 33 - reference data and interpolated data with Lisa using 4 iterations from Rascor (varying type of terrain: flat)

**REFERENCES**

- Jacobsen, K.2003a: DEM Generation from Satellite Data, EARSeL Ghent 2003, Remote Sensing in Transition, Millpress ISBN 90-77017-71-2, pp 273 – 276
- Jacobsen, K. 2004a: DEM Generation by SPOT HRS, ISPRS Istanbul 2004
- Jacobsen, K. 2004b: HRS Scientific Assessment Program, Test Site 9, Bavaria, Germany, Internal report for the HRS Study Team
- Jacobsen, K. 2004c: Analysis of SPOT HRS STEREO Data, Joint Workshop “High Resolution Mapping from Space 2003”, Hannover 2003, on CD and <http://www.ipi.uni-hannover.de/>
- Büyüksalih, G.,  
Jacobsen, K.,2004: Generation and Validation of High Resolution Space Image DEMs, ASPRS annual convention, Denver 2004
- Jacobsen, K.,  
Lohmann, P.,2003: Segmented Filtering of Laser scanner DSMs, ISPRS WG III/3 workshop „3-D reconstruction from airborne laserscanning and InSAR data“, Dresden 2003
- Kocak, G., Büyüksalih,  
G., Jacobsen, K., 2004 Analysis of Digital Elevation Models Determined by High Resolution Space Images, ISPRS Congress, Istanbul 2004
- Baudoin, A.,  
Schroeder, M.,  
Valorge, C., Bernard,  
M., Rudowski, V.,  
2003: The HRS-SAP initiative: A scientific assessment of the High Resolution Stereoscopic instrument on board of SPOT 5 by ISPRS investigators, Joint Workshop “High Resolution Mapping from Space 2003”, Hannover 2003, On CD and <http://www.ipi.uni-hannover.de/html/publikationen/2003/workshop/audoin.pdf>
- Toutin, T. 2004: Stereo High-Resolution DSM from QuickBird Images, Canada Centre for Remote Sensing, Natural Resources Canada, International Journal of Remote Sensing, 2004
- Passini, R., Betzner, D.,  
Jacobsen, K., 2002: Filtering of Digital Elevation Models, ASPRS annual convention, Washington 2002
- <http://www.vterrain.org/Elevation/dem.html>
- [http://www.landinfo.com/products\\_dems.htm](http://www.landinfo.com/products_dems.htm)
- <http://www.geog.ubc.ca/courses/klink/gis.notes/ncgia/u38.html#SEC38.1.1>

- <http://www.geography.wisc.edu/sco/maps/digitalelevation.php>
- <http://www.digital-elevation.com/gallery.htm>
- <http://www.infoterra-global.com/elevation.htm>
- <http://www.basic.org/projects/dtm/dtmdemo.html>
- <http://www.neodc.rl.ac.uk/index.php?option=displaypage&Itemid=58&op=page&SubMenu=-1>
- <http://www.npagroup.co.uk/imagery/satimagery/spot.htm>
- <http://www.spotimage.com.au/home/proser/spot5/documents/S5-filire-va22.pdf>
- [http://spot4.cnes.fr/spot4\\_gb/orbite.htm](http://spot4.cnes.fr/spot4_gb/orbite.htm)
- <http://www.space.edu/projects/book/chapter27.html>
- <http://hosting.soonet.ca/eliris/remotesensing/bl130lec11.html>
- <http://www.ifp.uni-stuttgart.de/publications/phowo95/Baudoin.pdf>
- [http://www.mfb-geo.ch/text\\_e/news\\_old\\_e10.html](http://www.mfb-geo.ch/text_e/news_old_e10.html)
- <http://spot5.cnes.fr/gb/index2.htm>
- [http://www.spotimage.com.au/home/proser/spot5/images/first\\_images.htm](http://www.spotimage.com.au/home/proser/spot5/images/first_images.htm)
- [http://www.cnes.fr/html/\\_112\\_258\\_301\\_.php](http://www.cnes.fr/html/_112_258_301_.php)
- <http://medias.obs-mip.fr/www/Reseau/Lettre/13/en/spot5.pdf>
- <http://www.spotimage.com.au/home/proser/spot5/documents/S5-filire-va22.pdf>
- <http://www.spotimage.com.au/home/proser/spot5/documents/S5-hrs-va22.pdf>
- [http://www.spotimage.fr/html/\\_167\\_171\\_175\\_177\\_.php](http://www.spotimage.fr/html/_167_171_175_177_.php)
- <http://www.spaceref.ca/news/viewpr.html?pid=8191>
- <http://www.ipi.uni-hannover.de/html/publikationen/2003/workshop/jacobs.pdf>
- <http://spot5.cnes.fr/gb/actualites/52.htm>
- <http://www.eranet.gr/ortho/html/apps.html>

<http://www.crisp.nus.edu.sg/~research/tutorial/spot.htm>

<http://www.acsu.buffalo.edu/~lli7/RM/lab2.htm>

[http://directory.eoportal.org/pres\\_SPOT5.html](http://directory.eoportal.org/pres_SPOT5.html)

<http://www.estec.esa.nl/ceos99/papers/p075.pdf>

<http://www.ixl-satinfo.com/english/productsrtm.shtml>

<http://www.estec.esa.nl/ceos99/papers/p165.pdf>

<http://www2.jpl.nasa.gov/srtm/>

## LIST OF FIGURES

Figure 1	An example of a digital elevation model (DEM)	9
Figure 2	Aspect (Santa Margarita)	10
Figure 3	Shaded aspect (Santa Margarita)	10
Figure 4	Digital elevation model (Santa Margarita)	10
Figure 5	Hillshaded digital elevation model (Santa Margarita)	10
Figure 6	Slope (Santa Margarita)	10
Figure 7	Slope draped on DEM (Santa Margarita)	10
Figure 8	Same area viewed from two different direction (stereo condition of optical images)	11
Figure 9	Orthoimage (is generated using just one image and a DEM)	11
Figure 10	Approximate geolocation by means of one image and height level of reference plane	12
Figure 11	World map rendered in cartographic style	13
Figure 12	Sea floor relief of the Chesapeake Bay using Bathymetry DEMs	14
Figure 13	World 1,000 meter resolution land relief merged with world sea relief at 10,000 meter resolution for a map of the Mediterranean Sea, Northern Africa, and Central Europe	15
Figure 14	The map was digitally rendered in a painted look to create terrain images in a soft watercolor style	15
Figure 15	Contour maps with selective elevation banding that may be used to identify elevation ranges for technical, cartographic or scientific purposes.	16
Figure 16	North-Western Afghanistan as grey value coded DEM. The lowest altitudes are black pixels and the highest peaks are white - the elevation is graded into a range of 255 grayscale shades	16
Figure 17	Highly detailed 10 meter resolution DEM of the National Volcanic Park on "Big" island Hawaii. The detail shows extinct volcano craters	17
Figure 18	Satellites of the SPOT series	18
Figure 19	Multispectral image from SPOT (pixel size: 20 x 20m)	19
Figure 20	Panchromatic image from SPOT (pixel size: 10 x 10m)	19
Figure 21	SPOT off-nadir view	20
Figure 22	Nadir viewing	20
Figure 23	Visible light region of the electromagnetic spectrum	21
Figure 24	Across-orbit view	21
Figure 25	SPOT 5 on orbit	22
Figure 26	The first image taken by SPOT 5: Eleusis harbour, Athens, Greece	22
Figure 27	Illustration of SPOT 5 components	23
Figure 28	SPOT HRS camera system	25
Figure 29	In-orbit view	26
Figure 30	DEM generated by SPOT HRS	26
Figure 31	3D view of Mount Vesuvius (Italy)	27
Figure 32	Photo of Shuttle Endeavour lifting off from launch pad	28

Figure 33	The components of the SRTM: the main antennas, the mast and the outboard antennas	29
Figure 34	The components of the main antennas	30
Figure 35	The components of the outboard antenna system	30
Figure 36	SRTM radar beams	36
Figure 37	Interferogram (fringe map)	31
Figure 38	Radar signals being transmitted and received in the SRTM mission	32
Figure 39	The disadvantages of the SAR-images: foreshortening, layover and shadows	32
Figure 40	Location of the test area Chiemsee (Bavaria)	34
Figure 41	Overlapping SPOT HRS-models with the reference areas	35
Figure 42	Overlapping SPOT HRS-models with the reference areas	35
Figure 43	Colour coded DEM generated with the SPOT HRS data	35
Figure 44	Test area: dark part in center = lake other dark parts = mainly forest and smaller lakes	36
Figure 45	3D-view to the DEM generated by HRS images (view direction: south)	36
Figure 46	Anaglyph of the HRS model	37
Figure 47	Topographic map of test area Prien	38
Figure 48	Forest layer of test area Prien	38
Figure 49	3-D view of the reference DEM in test area Prien	38
Figure 50	Topographic map of test area Gars	39
Figure 51	Forest layer of test area Gars	39
Figure 52	3-D view of the reference DEM in test area Gars	39
Figure 53	Topographic map of test area Peterskirchen	40
Figure 54	Forest layer of test area Peterskirchen	40
Figure 55	3-D view of the reference DEM in test area Peterskirchen	40
Figure 56	Topographic map of test area Taching	41
Figure 57	Forest layer of test area Taching	41
Figure 58	3-D view of the reference DEM in test area Taching	41
Figure 59	Topographic map of test area Vilsbiburg	42
Figure 60	Forest layer of test area Vilsbiburg	42
Figure 61	3-D view of the reference DEM in test area Vilsbiburg	43
Figure 62	Topographic map of test area Inzell	43
Figure 63	Forest layer of test area Inzell	43
Figure 64	3-D view of the reference DEM in test area Inzell	44
Figure 65	Distribution of the control points in the southern stereo model (left) and the northern model (right)	47
Figure 66	DPLX – original images (above), overview images (lower right) and zoom window (lower left)	48
Figure 67	Coordinate system used by DPCOR	49
Figure 68	Matching algorithm of DPCOR	50
Figure 69	The test.raw image for test area Prien (the brighter part represents the forest)	52
Figure 70	Colour coded DSM for test area Prien	60
Figure 71	Colour coded DEM for test area Prien	60

Figure 72	Differential DTM for test area Prien (difference between DSM and DEM, exaggeration factor: 3 times)	60
Figure 73	Discrepancies at control points, vertical vectors (red) = DZ (southern model)	63
Figure 74	Discrepancies at control points, vertical vectors = DZ (northern model)	63
Figure 75	Matched points (white) - southern scene	64
Figure 76	Quality map of the test area Prien (correlation coefficient 1.0 = gray value 255, correlation coefficient 0.6 = gray value 51)	65
Figure 77	Comparative study: image matching using every third pixel and every pixel (test area Prien – open area and forest – 2 iterations - DEMANAL)	66
Figure 78	Comparative study: image matching using every third pixel and every pixel (test area Gars – open area and forest – 2 iterations - DEMANAL)	67
Figure 79	Comparative study: image matching using every third pixel and every pixel (Prien -Gars – open area and forest– 2 iterations - DEMANAL)	68
Figure 80	Comparison between the two methods of matching for Prien (left) and Gars (right) – open area and forest – RMSZ- 2 iterations – DEMANAL)	69
Figure 81	RMSZ for different DHMs (1 = DSM, 2 = DEM HRS, 3 = DEM INSAR) test area Prien (RMSZ – all points, open area and forest – 2 iterations –DEMANAL)	70
Figure 82	Results for test area Prien (the best results are in the case 27)	71
Figure 83	Comparison between the results achieved considering the terrain flat or rolling, homogenous or varying for test area Prien	72
Figure 84	Remaining points after filtering with RASCOR = black Prien (53.39% points removed)	73
Figure 85	Height distribution for Prien	73
Figure 86	Digital height models (Prien): DSM (upper left), DEM HRS (upper right), DEM INSAR (left) - (exaggeration factor 1 time)	74
Figure 87	Differential DTM (Prien): DSM - DEM HRS (upper left), DSM – DEM INSAR (upper right), DEM HRS - DEM INSAR (left) (exaggeration factor 5 times)	74
Figure 88	RMSZ for DSM (1) and filtered DEM (2) for Gars	75
Figure 89	Remaining points Gars (black) 55.91% points removed	75
Figure 90	Results for test area Gars	76
Figure 91	Comparison between the results achieved considering the terrain flat or rolling, homogenous or varying for test area Gars	77
Figure 92	Height distribution for Gars	78
Figure 93	DSM (left) and filtered DSM (DEM) – exaggeration factor 2 times (Gars)	78
Figure 94	Differential DEM (exaggeration factor 5 times) - Gars	78
Figure 95	RMSZ for different DHMs (1=DSM, 2,3=DEM HRS 2 and 3 iterations) Petersk. DEMANAL	79

Figure 96	Remaining points for Peterskirchen = black (57.64% points removed)	80
Figure 97	Results for test area Peterskirchen	80
Figure 98	Comparison of the results achieved considering the terrain flat or rolling, homogenous or varying for test area Peterskirchen	81
Figure 99	Height distribution for Peterkirchen	82
Figure 100	DSM (left) and filtered DSM (DEM) – exaggeration factor 2 times (Peterskirchen)	82
Figure 101	Differential DEM (exaggeration factor 5 times) Peterskirchen	82
Figure 102	RMSZ for DSM (1) and filtered DEM (2)	83
Figure 103	Remaining points (black) Taching (53.31% points removed)	83
Figure 104	Results for test area Taching	84
Figure 105	Comparison between the results achieved considering the terrain flat or rolling, homogenous or varying - test area Taching	85
Figure 106	Height distribution for Taching	86
Figure 107	DSM (left) and filtered DSM (DEM) – exaggeration factor 2 times (Taching)	86
Figure 108	Differential DEM (exaggeration factor 5 times) Taching	86
Figure 109	RMSZ for DSM (1) and filtered DEM (2) (left: Vilsbiburg south, right: Vilsbiburg north)	87
Figure 110	Result for test area Vilsbiburg south	88
Figure 111	Result for test area Vilsbiburg north	88
Figure 112	Comparison between the results achieved considering the terrain as flat or rolling, homogenous or varying - test area Vilsbiburg south	89
Figure 113	Comparison between the results achieved considering the terrain as flat or rolling, homogenous or varying - test area Vilsbiburg north	90
Figure 114	Height distribution for Vilsbiburg	91
Figure 115	DSM (left) and filtered DEM (right) for south Vilsbiburg (exaggeration factor 5)	91
Figure 116	Differential DEM for Vilsbiburg southern model (exaggeration factor 20)	91
Figure 117	DSM (left) and filtered DEM (right) for north Vilsbiburg (exaggeration factor 5)	92
Figure 118	Differential DEM for Vilsbiburg northern model (exaggeration factor 20)	92
Figure 119	Remaining points (black) Vilsbiburg northern model (58.58% points removed)	92
Figure 120	Figure 120: RMSZ for different DHMs (1 = DSM, 2 = DEM HRS, 3 = DEM INSAR), test area Inzell	94
Figure 121	Remaining points (black) – Inzell (49.95% points removed)	93
Figure 122	Results for test area Inzell	94
Figure 123	Comparison of the results achieved considering the terrain flat or rolling, homogenous or varying for test area Inzell	95
Figure 124	Height distribution test area Inzell	96
Figure 125	Digital height models (Inzell): DSM (upper left), DEM HRS (upper right), DEM INSAR (left) - (exaggeration factor 3 times)	96

Figure 126	Differential DTM (Inzell): DSM - DEM HRS (upper left), DSM – DEM INSAR (upper right), DEM HRS – DEM INSAR (left) (exaggeration factor 5 times)	97
Figure 127	Overview impression of the results for open area and forest	98

## LIST OF TABLES

Table 1	The characteristics of the bands used by SPOT satellites	21
Table 2	Discrepancies at the control points (southern and northern model)	63
Table 3	Results of height model analysis in the case of test areas Prien and Gars using every third pixel and every pixel for image matching	65
Table 4	Results for test area Prien (DSM, DEM-HRS, DEM-InSAR)	70
Table 5	Results for test area Gars (DSM, DEM HRS)	75
Table 6	Results for test area Peterskirchen (DSM, DEM HRS)	79
Table 7	Results for test area Taching (DSM, DEM)	83
Table 8	Results for test area Vilsbiburg southern model	87
Table 9	Results for test area Vilsbiburg northern model	87
Table 10	Results for test area Inzell (DSM, DEM-HRS, DEM-INSAR)	93
Table 11	Overview impression of the results for open area and forest	97